

Analyses of lipidic bodies from green microalgae

Verushka Pather

A thesis submitted to the University of KwaZulu-Natal, Department of Biochemistry, Westville Campus, Durban, S.A in partial fulfillment of the academic requirements for the degree of Master of Science.

Durban, 2014

Declaration

I hereby declare that the work forming the basis of my thesis is my own and has not been submitted for any degree or examination at any other university.

Signed: -----

V. Pather

at ----- this ----- day of ----- 2014.

Contents

Acknowledgements	i
Abstract	ii
List of figures	iii
List of tables	ix
INTRODUCTION	1
CHAPTER ONE	
LITERATURE REVIEW AND AIM OF THIS STUDY	4
1.1 Selection of algae in this study	4
1.1.1 <i>Chlorella</i> spp.	5
1.1.2 <i>Dunaliella</i> spp.	7
1.2 Lipid metabolism	8
1.2.1 Photosystems associated with lipid metabolism	8
1.2.2 Biosynthesis of fatty acids and lipids	10
1.2.3 Biosynthesis of polyunsaturated fatty acids (PUFAs)	12
1.2.3.1 Genes involved in biosynthesis of PUFAs	13
1.2.4 Oxylipins	14
1.2.5 Factors affecting lipid production in algae	15
1.2.5.1 Nitrogen metabolism	15

1.2.5.2	Phosphate starvation	16
1.2.5.3	Temperature, light intensity and salinity	16
1.3	Lipid - associated proteins	17
1.3.1	Oleosins and caleosins	17
1.3.2	Plastid lipid - associated proteins (PLAPs)	19
1.4	Endoplasmic reticulum (ER) and oil body synthesis	20
1.5	Aim of this study	21
CHAPTER TWO		
MATERIALS AND METHODS		23
2.1	Experimental algae and culture media	23
2.2	Axenic cultivation of <i>C. vulgaris</i> and <i>D. primolecta</i>	23
2.2.1	Starter culture preparation and maintenance	23
2.2.2	Growth culture preparation and maintenance	24
2.3	Analyses of cultures	25
2.3.1	Cell number determination	25
2.3.2	Optical density (OD)	25
2.3.3	pH	26
2.4	Harvesting of microalgae	26
2.4.1	Centrifugation and freeze - drying	26
2.5	Disruption and extraction of cell lysates	26

2.5.1	Hydrocarbon yield	27
2.5.2	Chlorophyll fraction	27
2.5.2	Carotenoid fraction	28
2.6	Analyses of organic extracts	28
2.6.1	Thin layer chromatography (TLC)	28
2.6.2	Spectrophotometry	30
2.6.2.1	Chlorophyll spectrum	30
2.6.2.2	Carotenoid spectrum	30
2.7	Confocal microscopy of algal cells	31
2.7.1	Nile red staining	31
2.7.2	Bodipy staining	31
2.8	Extraction and analyses of protein from microalgal oil	32
2.8.1	Extraction of protein from oil	32
2.8.2	Protein quantification	33
2.8.3	Protein profiling	33
2.9	Derivatization and analyses of fatty acid methyl esters (FAMES)	34
2.9.1	Derivatization of FAMES	34
2.9.2	Analyses of fatty acid methyl esters (FAMES) by gas chromatography	35

CHAPTER THREE	
RESULTS AND DISCUSSION	36
3.1 Growth dynamics of algal cultures	36
3.1.1 Cell density	36
3.1.2 Optical density	40
3.1.3 Biomass determination	44
3.1.4 pH	46
3.2 Algal of the oil - hydrocarbon fraction	48
3.2.1 Determination of oil - hydrocarbon mass	48
3.2.2 Oil - hydrocarbon yield	49
3.3 Thin layer chromatography (TLC) and spectrophotometry	50
4.4 Protein profiling	58
3.4.1 Protein quantification	58
3.4.2 Protein composition of the lipidic body	62
3.5 Analyses of fatty acid methyl esters (FAMES) using gas chromatography (GC)	68
3.6 Detection of lipids and other fluorescent components using confocal microscopy	74
3.6.1 Nile red staining of microalgal cells	74
3.6.2 Bodipy 505/515 staining of microalgal cells	75
4.6.3 Use of DMSO as a dye solvent	76
4.6.4 Autofluorescence	77

3.6.4.1	Autofluorescence detection in algal chloroplasts	77
3.6.5	Lipidic fluorescence detection	92
3.6.5.1	Fluorescence of algal lipidic bodies using Nile red dye stain	92
3.6.5.2	Fluorescence of algal lipidic bodies using Bodipy 505/515 dye stain	109
CONCLUSIONS		119
REFERENCES		122
APPENDIX A: Media and reagents		135
APPENDIX B: Other Technical Information		139

Acknowledgements

I would firstly like to thank my Lord and saviour JESUS CHRIST for making everything possible and always guiding me. I would also like to extend my gratitude to my project supervisors, Professors A.S. Gupthar and F. Bux of the School of Life Sciences, University of KwaZulu - Natal, Westville Campus and Institute for Water and Wastewater Technology, Durban University of Technology, Steve Biko Campus, respectively for their guidance; without which I wouldn't even know where to begin. To my family, thank you for always supporting me in whichever decisions I make.

Abstract

This study presents the analyses of oil body components in microalgae which may be involved in oil droplet assembly including certain triacylglycerol precursors which can be processed to biodiesel, an alternative fuel source. Stress induction of microalgae, *Chlorella vulgaris* CCAP 211/11B and *Dunaliella primolecta* CCAP 11/34 was achieved by exclusion of nitrates in growth media. Contrary to other forms of nitrogen depletion, this condition did not greatly enhance lipid biosynthesis in the microalgae. Confocal microscopy and fluorescent dyes Nile red and Bodipy were employed for the visualization of lipidic body components. The fluorescence hues emitted by neutral lipids and phospholipids were differentiated from those due to autofluorescence and chlorophyll using ZEN software to analyse images from a Zeiss LSM 710 confocal microscope. Oil from both algae, which were subjected to transesterification and gas chromatography, revealed a predominant fatty acid, namely palmitic acid (C16:0). *D. primolecta* produced linoleic acid (C18:2n6t) under growth conditions involving both nitrate supplementation and exclusion; whilst the longest fatty acid, docosanoic acid (C22:0 chain) was produced by the alga *C. vulgaris* only under conditions of nitrate supplementation. Nitrate limitation had minimal effect on the oil hydrocarbon yield which increased only 0.02% and 0.01% for *C. vulgaris* and *D. primolecta*, respectively. The highest biodiesel yield of 26.11 % was recorded from *D. primolecta* when grown under conditions of nitrate exclusion. The protein concentrations extracted from oil of the former alga ranged from 1.87 - 1.95 µg/ml when grown under nitrate supplemented conditions and 1.74 - 1.90 µg/ml when nitrate was excluded from the media. The protein concentrations extracted from oil of *D. primolecta* ranged from 1.91 - 2.23 µg/ml and 1.88 - 1.98 µg/ml, respectively, when the algae were grown in the presence and exclusion of nitrates. In the adaptation of protocols for protein extraction from oil, sunflower and salmon oils were initially used. Sunflower oil extracts produced by 10% (w/v) SDS treatment, yielded protein bands of 198, 96, 70 and 58 KDa on 10% (w/v) polyacrylamide gels while 6M urea treatment yielded a band of 200 KDa. Salmon oil treated with 10% (w/v) SDS and 6 M urea yielded bands of 195 and 27 KDa, and 198 KDa, respectively, as well as common bands of 68 and 64 KDa. In comparison, the extraction of discrete proteins from algal oil proved to be difficult as the extractants SDS and urea could have denatured protein components into subunit structure.

List of figures

Figure 1.1	Image showing spherical cell morphology of <i>Chlorella</i> spp.	5
Figure 1.2	The life cycle of <i>Chlorella</i> spp.	6
Figure 1.3	Image showing Biflagellated cells of <i>Dunaliella</i> spp.	8
Figure 1.4	The life cycle of <i>Dunaliella</i> spp.	8
Figure 1.5	Diagram showing photosystems in algae	9
Figure 1.6	Diagram of an oil body	18
Figure 1.7	Diagram showing the biosynthesis of TAG	21
Figure 3.1	Cell density (cells/ml) of <i>Chlorella vulgaris</i> growth in BG11 test and BG11 nitrate deficient control media over time (days)	39
Figure 3.2	Cell density (cells/ml) of <i>Dunaliella primolecta</i> growth in BG11 test and BG11 nitrate deficient control media over time (days)	39
Figure 3.3	Optical density of <i>Chlorella vulgaris</i> growth in BG11 test and BG11 control media.	41
Figure 3.4	Relationship between OD _{680nm} and algal cell count (cells/ml) of <i>Chlorella vulgaris</i> grown in BG11 test medium	41
Figure 3.5	Relationship between OD _{680nm} and algal cell density (cells/ml) of <i>Chlorella vulgaris</i> grown in BG11 control medium	42
Figure 3.6	Optical density of <i>Dunaliella primolecta</i> grown in BG11 test and BG11 control media.	42
Figure 3.7	Relationship between OD _{680nm} and algal cell count (cells/ml) of <i>Dunaliella primolecta</i> grown in BG11 test medium	43
Figure 3.8	Relationship between OD _{680nm} and algal cell count (cells/ml) of <i>Dunaliella primolecta</i> grown in BG11 control medium	43
Figure 3.9	Changes in pH of <i>Chlorella vulgaris</i> cultivation in BG11 test and BG11 control media.	47
Figure 3.10	Changes in pH of <i>Dunaliella primolecta</i> cultivation in BG11 test and BG11 control media	47

Figure 3.11	TLC image showing separation of lipids. A: Standards 1 - 5 (sunflower oil, olive oil, evening primrose oil, salmon oil, DOPE [R-L]); B: <i>Dunaliella primolecta</i> algal oil in hexane (test); C: <i>Chlorella vulgaris</i> algal oil in hexane (test); D: <i>Dunaliella primolecta</i> algal oil in hexane (control); E: <i>Chlorella vulgaris</i> algal oil in hexane (control)	52
Figure 3.12	TLC image showing, <i>Dunaliella primolecta</i> algal oil (test) extracted in acetone (left) and methanol (right) with corresponding spectra of carotenoid (A) and chlorophyll (B) fractions, respectively	53
Figure 3.13	TLC image showing <i>Chlorella vulgaris</i> algal oil (test) extracted in acetone (left) and methanol (right) with corresponding spectra of carotenoid (A) and chlorophyll (B) fractions, respectively	54
Figure 3.14	TLC image showing <i>Chlorella vulgaris</i> algal oil (control) extracted in acetone (left) and methanol (right) with corresponding spectra of carotenoid (A) and chlorophyll (B) fractions, respectively	55
Figure 3.15	TLC image showing <i>Dunaliella primolecta</i> algal oil (control) extracted in acetone (left) and methanol (right) with corresponding spectra of carotenoid (A) and chlorophyll (B) fractions, respectively	56
Figure 3.16	SDS PAGE gel: A: Bio - Rad protein standards (lane A); B: salmon oil extracted with SDS (lane B); C: salmon oil extracted with urea (lane C); D: sunflower oil extracted with SDS (lane D); E: sunflower oil extracted with urea (lane E).	61
Figure 3.17	SDS PAGE gel: A: Bio - Rad protein standards (lane A); B: <i>C. vulgaris</i> algal oil (test) extracted with urea (lane B); C: <i>D. primolecta</i> algal oil (test) extracted with urea (lane C)	62
Figure 3.18	SDS PAGE gel: A: Bio - Rad protein standards (lane A); B: <i>D. primolecta</i> algal oil (control) extracted with SDS (lane B); C: <i>D. primolecta</i> algal oil (control) extracted with urea (lane C); D: <i>C. vulgaris</i> algal oil (control) extracted with SDS (lane D); E: <i>C. vulgaris</i> algal oil (control) extracted with urea (lane E)	63
Figure 3.19	Gas chromatogram of FAMES derived from oil of unstressed <i>C. vulgaris</i> cultures	67
Figure 3.20	Gas chromatogram of FAMES derived from oil stressed <i>C. vulgaris</i> cultures	67
Figure 3.21	Gas chromatogram of FAMES derived from oil of unstressed <i>D. primolecta</i> cultures	68
Figure 3.22	Gas chromatogram of FAMES derived from oil of stressed <i>D. primolecta</i> cultures	68
Figure 3.23	Chemical structure of Nile red	71

Figure 3.24	Chemical structure of bodipy	72
Figure 3.25	Confocal Micrographs showing (A) Autofluorescence of unstressed cells of <i>C. vulgaris</i> (B) Autofluorescence of stressed cells of <i>C. vulgaris</i>	75
Figure 3.26	Confocal micrographs showing (A) Autofluorescence of unstressed <i>D. primolecta</i> cells (B) Split image of autofluorescence of stressed <i>D. primolecta</i> cells (top left and bottom left) and * DIC image of the chlorophyll (top right)	76
Figure 3.27	Graphical representation of the intensity of autofluorescence (red hue) emitted by unstressed <i>C. vulgaris</i> cells at a range of 420 - 722nm	79
Figure 3.28	Graphical representation of the intensity of autofluorescence (red hue) emitted by stressed <i>C. vulgaris</i> cells at a range of 420 - 722nm	79
Figure 3.29	Graphical representation of the intensity of autofluorescence (red hue) emitted by unstressed <i>D. primolecta</i> cells at a range of 420 - 722nm	80
Figure 3.30	Graphical representation of the intensity of autofluorescence (red hue) emitted by stressed <i>D. primolecta</i> at a range of 420 - 722nm	80
Figure 3.31	Wavelength scanning of the autofluorescence pattern observed in unstressed cells of <i>C. vulgaris</i>	82
Figure 3.32	Wavelength scanning of the autofluorescence pattern observed in stressed cells of <i>C. vulgaris</i>	83
Figure 3.33	Wavelength scanning of the autofluorescence pattern observed in unstressed cells of <i>D. primolecta</i>	85
Figure 3.34	Wavelength scanning of the autofluorescence pattern observed in stressed cells of <i>D. primolecta</i>	86
Figure 3.35	Split fluorescence image of unstressed <i>C. vulgaris</i> cells using Nile red dye stain visualizing the phospholipids (top left), chlorophyll (bottom left), neutral lipids (top right) and a composite image of all the fluorescence patterns (bottom right)	90
Figure 3.36	Split fluorescence image of stressed <i>C. vulgaris</i> cells using Nile red dye stain visualizing the phospholipids (top left), chlorophyll (top right), neutral lipids (bottom left) and a composite image of all the fluorescence patterns (bottom right)	91
Figure 3.37	Split fluorescence image of unstressed <i>D. primolecta</i> cells using Nile red dye stain visualizing the phospholipids (top left), chlorophyll (top right), neutral lipids (bottom left) and a composite image of all the fluorescence patterns (bottom right)	92

Figure 3.38	Split fluorescence image of stressed <i>D. primolecta</i> cells using Nile red dye stain visualizing the phospholipids (extreme top left), chlorophyll (top centre), neutral lipids (extreme top left), DIC image on bottom left and composite image of all the fluorescence patterns (centre right)	93
Figure 3.39	Graphical representation of the intensity of fluorescence emitted by unstressed <i>C. vulgaris</i> cells using Nile red dye at a range of 420 - 722nm showing neutral lipids, phospholipids and chlorophyll	95
Figure 3.40	Graphical representation of the intensity of fluorescence emitted by stressed <i>C. vulgaris</i> cells using Nile red dye at a range of 420 - 722nm showing neutral lipids, phospholipids and chlorophyll	96
Figure 3.41	Graphical representation of the intensity of fluorescence emitted by unstressed <i>D. primolecta</i> cells using Nile red dye at a range of 420 - 722nm showing neutral lipids, phospholipids and chlorophyll	97
Figure 3.42	Graphical representation of the intensity of fluorescence emitted by stressed <i>D. primolecta</i> cells using Nile red dye at a range of 420 - 722nm showing neutral lipids, phospholipids and chlorophyll	98
Figure 3.43	Wavelength scanning of fluorescence pattern observed in unstressed <i>C. vulgaris</i> cells subject to Nile red staining indicating fluorescent components neutral lipids, phospholipids and chlorophyll at 546, 585 and 673 nm, respectively	99
Figure 3.44	Wavelength scanning of fluorescence pattern observed in stressed <i>C. vulgaris</i> cells subject to Nile red staining indicating fluorescent component chlorophyll at 683 nm	100
Figure 3.45	Wavelength scanning of fluorescence pattern observed in unstressed <i>D. primolecta</i> cells subject to Nile red staining indicating fluorescent components neutral lipids, phospholipids and chlorophyll at 546, 595 and 663 nm, respectively	102
Figure 3.46	Wavelength scanning of fluorescence pattern observed in stressed <i>D. primolecta</i> cells subject to Nile red staining indicating fluorescent components neutral lipids, phospholipids and chlorophyll at 527, 595 and 663 nm, respectively	103
Figure 3.47	Micrograph showing (A) Fluorescence image of unstressed <i>C. vulgaris</i> cells using Bodipy 505/515 dye stain (B) Fluorescence image of stressed <i>C. vulgaris</i> cells using Bodipy 505/515 dye stain (C) Split fluorescence image of stressed <i>C. vulgaris</i> cells using Bodipy 505/515 dye stain visualizing the lipid bodies (top left) and chlorophyll (top right) and a composite image of all the fluorescence patterns	106

Figure 3.48	Confocal micrograph showing (A) Fluorescence image of unstressed <i>D. primolecta</i> using bodipy 505/515 dye stain (B) Split fluorescence image of stressed <i>D. primolecta</i> using bodipy 505/515 dye stain visualizing the lipid bodies (top left) and chlorophyll (top right), DIC image (bottom left) and a composite image of all the fluorescence patterns (bottom right)	107
Figure 3.49	Graphical representation of the intensity of fluorescence emitted by unstressed <i>C. vulgaris</i> cells in the range of 420 - 722nm	109
Figure 3.50	Graphical representation of the intensity of fluorescence emitted by stressed <i>C. vulgaris</i> cells in the range of 420 - 722nm	110
Figure 3.51	Graphical representation of the intensity of fluorescence emitted by unstressed <i>D. primolecta</i> cells in the range of 420 - 722nm	111
Figure 3.52	Graphical representation of the intensity of fluorescence emitted by stressed <i>D. primolecta</i> cells in the range of 420 - 722nm	112
Figure 3.53	Wavelength scanning of fluorescence pattern observed in unstressed <i>C. vulgaris</i> cells subject to bodipy staining indicating chlorophyll fluorescence at 673 nm	113
Figure 3.54	Wavelength scanning of fluorescence pattern observed in stressed <i>C. vulgaris</i> cells subject to bodipy staining indicating lipidic and chlorophyll fluorescence at 517 and 663 nm, respectively	114
Figure 3.55	Wavelength scanning of fluorescence pattern observed in unstressed <i>D. primolecta</i> cells subject to bodipy staining indicating lipidic and chlorophyll fluorescence at 517 and 673 nm, respectively	116
Figure 3.56	Wavelength scanning of fluorescence pattern observed in stressed <i>D. primolecta</i> cells subject to bodipy staining indicating lipidic and chlorophyll fluorescence at 517 and 617 nm, respectively	117
Figure B1	Diagram of a hemacytometer chamber	140
Figure B2	Standard curve of BSA versus absorbance using the Bio - Rad RC - DC kit	141
Figure B3	Standard curve of SDS treated BSA and standards versus absorbance using the Bio - Rad RC - DC kit	142
Figure B4	Standard curve of urea treated BSA versus absorbance using the Bio - Rad RC - DC kit	142
Figure B5	Standard curve of SDS and urea treated BSA versus absorbance using the Bio - Rad RC DC kit	143

Figure B6

Standard curve of log of the molecular weight of the broad range protein standards versus the relative mobility

143

List of tables

Table 3.1	Biomass yield recorded from test and control cultures of <i>C. vulgaris</i>	45
Table 3.2	Biomass yield recorded from test and control cultures of <i>D. primolecta</i>	45
Table 3.3	Oil - hydrocarbon yield of <i>C. vulgaris</i> test and control cultures	49
Table 3.4	Oil - hydrocarbon yield of <i>D. primolecta</i> test and control cultures	50
Table 3.5	Protein concentration of extracted algal oil samples	57
Table 3.6	Protein concentration of extracted oil standards	57
Table 3.7	Nomenclature of FAMES extracted from algal oils	69
Table 3.8	Percentage composition of individual fatty acids relative to an internal standard	69
Table 3.9	FAME content in % of algal cultures	69
Table 3.10	Confocal parameters used for autofluorescence detection in <i>C. vulgaris</i>	84
Table 3.11	Confocal parameters used for autofluorescence detection in <i>D. primolecta</i>	87
Table 3.12	Confocal parameters for lipid detection in Nile red stained <i>C. vulgaris</i> cells	101
Table 3.13	Confocal parameters of lipid detection in <i>D. primolecta</i> subject to Nile red staining	104
Table 3.14	Confocal parameters of lipid detection in <i>C. vulgaris</i>	115
Table 3.15	Confocal parameters of lipid detection in <i>D. primolecta</i>	118

INTRODUCTION

Since the 1970s, microalgae have become the focus of intensive research due to their potential to serve as renewable resources for biodiesel (Chisti, 2007; Dermibas, 2008). In contrast to energy availability and safety from non-renewable resources, this alternative to fossil fuels is neither hindered by limitation, such as availability, nor does it impose as much of a threat to the environment. Approximately 98% of carbon emissions result from fossil fuel combustion; hence there is an increasing trend towards use of algae-based technologies for the reduction of greenhouse gas emissions as less harmful substances are released into the atmosphere. In addition, many algae act as a source of production of supplements and biomaterials in the pharmaceutical industry (Rubio - Rodriguez *et al.*, 2010; Singh and Gu, 2010).

Much research has also been devoted to the study of lipid-associated protein complexes known as oleosins which are found in eubacteria, mammalian organisms and plants. This recently discovered assembly comprises structural proteins with no discernable enzymatic motifs. They are thought to be involved in the stabilization of the oil body and contain a characteristic "hair-pin" - like hydrophobic domain which is inserted randomly inside the triacylglyceride (TAG) component, whilst their hydrophilic regions are exposed outside the oil body (Hsieh and Huang, 2004). During recent years, several additional classes of lipid-associated proteins have been described including and plastid-lipid associated proteins (PLAPs) (Murphy, 2004) and caleosins, which are found in a wide range of plant grain such as maize, barley, rice, sesame seed and soya bean (Hsieh and Huang, 2004). Caleosins are thought to be involved in signalling, assembly and mobilization of oil bodies (OBs), as a result of their constituent calcium binding ability, protein kinase domains and their single membrane spanning region (Chapter 1; 1.4). Initially these proteins were suggested to be involved in abscisic acid (ABA) - mediated responses because rice caleosin (OsCLO), is induced by ABA (Frandsen *et al.*, 2001) and both calcium and protein phosphorylation are involved in ABA signalling. Oleosin expression is also responsive to ABA, as are some enzymes involved in oil body formation. Caleosins are probably more directly involved in membrane and oil body fusion. The microsomal caleosins, found in young plant embryos and tissues such as roots and leaves, may possibly be involved in membrane-fission and/or fusion events which relate to

trafficking between the endoplasmic reticulum (ER) and transport or storage vesicles. This is brought about as the caleosin co-localizes in an ER subdomain with a protein storage vacuole and/or autophagic vacuole marker, known as α -TIP. This subdomain may be associated with both oil body formation and vacuolar biogenesis. Newly synthesized oil bodies, with caleosin, are released as immature oil bodies into the cytosol where they may fuse under the influence of calcium to form mature oil bodies. In some cells, oil bodies are taken up by vacuoles with tonoplast α -TIP which forms by budding off or maturation of the ER subdomain containing caleosin (Frandsen *et al.*, 2001).

Unlike the aforementioned proteins, PLAPs are located exclusively in specialized plastids, known as chromoplasts which are present in non-green pigmented tissues like coloured flower petals or fruit. These proteins have various roles including storage and stabilisation of lipid-derived pigments in chromoplasts (Murphy, 2004). Exposure to high light intensities and nitrate deprivation induces β -carotene production in globules within the inter-thylakoid spaces of the halotolerant green alga, *Dunaliella bardawil*. Studies conducted by Ben-Amotz *et al.* (1989; 1999) demonstrated that under these conditions, the β -carotene containing globules from *D. bardawil* were shown to consist predominantly of this pigment, neutral lipids and a minute quantity of protein known as carotene globule protein (Cpg). Although the function of these proteins is not yet known, their involvement in the structural stabilization of the β -carotene containing globules has been suggested (Katz *et al.*, 1995). This is due to the peripheral localization and improved aggregation of the globules subsequent to cleavage by trypsin. This stability could possibly be brought about as a result of the hydrophilic layer which covers the hydrophobic pigment core in Cpg. A similar structure has been postulated to contribute to the stability of triacylglycerol-type oil bodies in seeds (Hsieh and Huang, 2004; 1.3.2) (2.4.1) although it has not yet been fully established if Cpg is structurally related to oleosins (Katz *et al.*, 1995).

Whether or not oleosins are present in algae is not known (Hsieh and Huang, 2004) as they are typically found in true plants (Murphy, 2004). However, a caleosin-like sequence has been identified in the genome of the single-celled alga, *Auxenochlorella protothecoides*, which suggests that caleosins are probably ubiquitous in plants but prevalent in some algae (Murphy, 2004). The biochemical content of microalgae can be influenced by varying growth conditions

and thus significantly promoting oil yields. Nitrogen starvation is known to bring about an increase in microalgal oil production (Lv *et al.*, 2010).

In spite of microalgae serving as efficient solar energy converters (Singh and Gu, 2010) there still remain challenges towards the development of large scale biofuel plants. Prior to commencing with large scale cultivation, several factors require consideration such as economical supply and storage barriers (Chisti, 2007; 2008). A thorough understanding of the biology of the algal species proves to be essential and their ability to produce copious amounts of useful oil is vital. It is therefore imperative that the utilization of microalgae be further researched as the benefits far outweigh the disadvantages or impediments.

In the current study, two conditions of algal growth are examined; namely, nutrient - rich growth in BG 11 medium (Appendix A) and restricted growth in BG 11 medium deficient in nitrates (Appendix A). The analyses of algal oil from the freshwater alga *Chlorella vulgaris* and marine alga *Dunaliella primolecta* were undertaken in an attempt to correlate oil yields and growth conditions. Constituent oil - associated components, typical of those found in oil body assemblies, were analyzed by confocal microscopy, thin layer chromatography, polyacrylamide gel electrophoresis and gas chromatography.

CHAPTER ONE

LITERATURE REVIEW AND AIM OF THIS STUDY

1.1 Selection of algae in this study

Microalgae can be divided into two categories which relate to lipid production and biomass generation, namely, (i) high lipid content but low cell growth and (ii) low lipid content but high cell growth (Lv *et al.*, 2010). *Chlorella vulgaris*, a freshwater alga, has received attention as a promising candidate for commercial lipid production due to their ease of cultivation and rapid growth rates. Griffiths and Harrison (2009) reported *C. vulgaris* exhibited a relatively short doubling time of 19 hours whilst only increasing in lipid content to 20% thus, classifying this alga as one of low lipid content and high cell growth. *Dunaliella primolecta* Butcher (1959) is a marine Chlorophyceae that is tolerant of concentrations of ammonia, purines and nitrates within its medium (Uriarte *et al.*, 1993). Little is known about the classification of *D. primolecta* with respect to cell growth and lipid content. Uriarte and co-workers (1993) reported findings confirming the potential for significant variability in composition of this marine microalga, both in its natural habitat and following experimental manipulation. Closely related to *D. primolecta* is *Dunaliella salina*, a halophilic microalga that was initially reported to produce lipids between 45 - 55% of its total weight (Tornabene *et al.*, 1980). Further research by Weldy and Huesemann (2007), showed *D. salina* to produce a relatively high lipid content ranging from 16 - 44% (wt) as a result of high biomass growth and thus classifying this alga as one of high cell growth and high lipid content, and thereby placing this alga in a third category. Green algae are amongst the most taxonomically diverse and plentiful of the Chlorococcalean genera with almost 1200 infraspecific taxa being identified (Kim *et al.*, 2007). These "green algae" contain chlorophyll, an essential component for photosynthesis which is responsible for capturing CO₂ and solar energy to generate the metabolic flux for both cell growth and lipid accumulation. Lv *et al.* (2010) reported the high lipid content but low cell growth of the alga, *Botryococcus braunii*

based on earlier studies conducted by Dayananda *et al.* (2007b) which revealed a lipid content of 50% and low biomass productivity of 28 mg//d.

1.1.1 *Chlorella* spp.

The name *Chlorella* given to the unicellular green algae, belonging to the phylum Chlorophyta, is appropriate, as the Greek word *chloros* meaning green and the Latin word *ella* meaning small, correctly describes this genus. These algae are non - motile, ranging from 2 to 10 μm in diameter and they assume a spherical morphology (Figure 1.1). As they contain chlorophyll a and b in their chloroplasts, photosynthesis is the main process which promotes the proliferation of this organism, and requires essentially carbon dioxide, water, sunlight and a small amount of minerals.

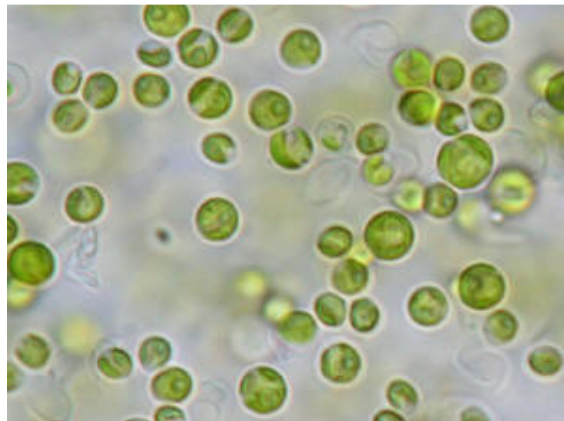


Figure 1.1. Image showing spherical cell morphology of *Chlorella* spp. (http://botany.natur.cuni.cz/algo/images/CAUP/H1998_1).

Chlorella are of pharmaceutical importance and they produce carotenoids, namely, canthaxanthin and astaxanthin (Arad - Malis *et al.*, 1993; Chinnasamy *et al.*, 2009). Initially it was believed that algae were susceptible to high levels of carbon dioxide. Yet it has now been reported that some microalgae grow at rapid rates under very high levels of this trace gas,

which is about 1000 times higher than the ambient level of 0.036%. Carotenoids are produced by *Chlorella* at an elevated rate under high levels of carbon dioxide therefore rendering this species economically important. Under these conditions, not only were the levels of carotenoids elevated but so were the levels of protein, carbohydrates and biomass of the microalgae (Chinnasamy *et al.*, 2009). The value of *Chlorella* is not only limited to the pharmaceutical industry but also the food industry. At one point in time, these green algae were relatively inexpensive, yet after their value was realized, this has quickly changed. It is believed that *Chlorella* can be used as a source of food as on a dry weight basis, the algal composition is 45% protein, 20% fat, 20% carbohydrate, 5% fibre and 10% mineral and vitamins (<http://www.wikipedia.org/wiki/Chlorella>).

Cell cycle processes, such as new cell wall formation, vary amongst the diverse algal species. The overall duration of the cell cycle depends on the time required for doubling of the biomass, which in turn depends upon the uptake of sufficient nutrients such carbon, phosphorous and nitrogen. The cell cycle for *Chlorella* is relatively minimal in duration, lasting for approximately 6 hours (Sigeo, 2005) and shows haplontic features (Figure 1.2). The alternation of generations found in this species involves isomorphic haploid zoospores which act as gametes that form a zygote which differentiates with diploid vegetative cells. The haplontic phase involves the generation of zoospores from the diploid vegetative cells via meiosis (Figure 1.2).

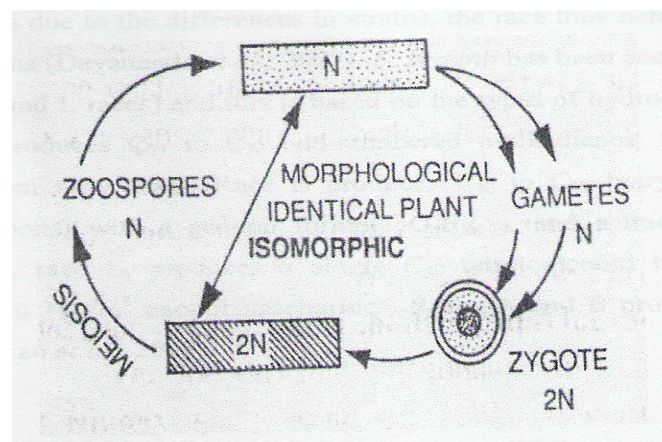


Figure 1.2. The life cycle of *Chlorella* spp. (Panday, 1994).

Under certain growth conditions, *Chlorella* yields oils which are high in polyunsaturated fats. For example, *Chlorella minutissima* has yielded eicosapentaenoic acid (EPA) (20:5 ω 3) comprising 39.9% of total lipids. It is for this reason that the growth conditions ought to be optimized for culturing of this alga in order to obtain high lipid or oil yields. *Chlorella vulgaris* has shown its growth to be optimal in BG 11 medium (Appendix A) in the temperature range of 30 - 39 °C and at a pH of 8 as reported by Ra (2010).

1.1.2 *Dunaliella* spp.

Belonging to the class of *Chlorophyceae*, *Dunaliella* spp. are eukaryotic, motile, unicellular, biflagellated (Figure 1.3) and show a haplo diplontic life cycle (Figure 1.4). Known to tolerate vast variations of in concentrations of ammonia, nitrates and purines within its environment (Uriarte *et al.*, 1993), these algae generally encompass a high protein content of approximately 35 - 48 w/w% (Gibbs and Duffus, 1976). This species does not contain a rigid cell wall but does possess a glycoprotein - cellulosic cell coat that is formed by 25 - 200 nm long fibrils. The halotolerant green alga *Dunaliella bardawil* accumulates massive amounts of β - carotene when exposed to high light intensities, nutrient deprivation and other stress conditions. It has been stated that cells with elevated levels of β - carotene globules are resistant to photodamage at very high light intensities, suggesting that β - carotene protects the cells from such damage (Katz *et al.*, 1995). Hence, this type of algal species can be mass cultured in saline lagoons in order to stimulate the production of β - carotene for commercial purposes (Ben - Amotz, 1999; Garcia - Gonzalez *et al.*, 2000).

Recently, a new category of *Dunaliella* species was discovered in the Atacama Desert. It has been hypothesized that the algal species is maintained via the condensation of water vapour through hanging spider - webs (Azúa - Bustos *et al.*, 2010). Literature published on this novel species is relatively limited.

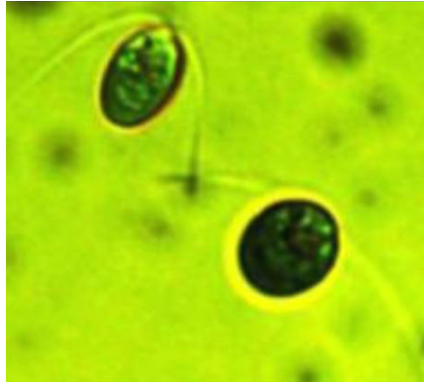


Figure 1.3. Image showing Biflagellated cells of *Dunaliella* spp. (<http://www.dunaliella.org/dccbc/picturegallery.php>).

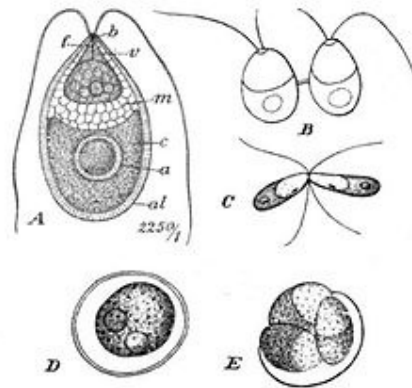


Figure 1.4. The life cycle of *Dunaliella* spp. indicating (A) a diploid vegetative cell which forms (B) zoospores through meiosis. The zoospores act as mating gametes (C) forming (D) a diploid zygospore that germinates (E) into vegetative cells (A). (<http://en.wikipedia.org/wiki/Dunaliella>).

1.2 Lipid metabolism

1.2.1 Photosystems associated with lipid metabolism

Algae contain complex regulatory and metabolic networks that alter the amount and type of photosynthetic proteins in response to changes in oxygen and sunlight (Johnson and Schmidt -

Dannert, 2008). This makes them capable of light - driven processes (Johnson and Schmidt - Dannert, 2008). The resident photosystems are responsible for more sophisticated methods of capturing light energy, therefore making light - independent reactions possible. Essentially, two photosystems (PSI and PSII) work in tandem to transfer electrons from water to ferredoxin, which is the source of low potential electrons, for subsequent reactions of the Calvin cycle in which CO₂ is converted into organic matter (Johnson and Schmidt - Dannert, 2008).

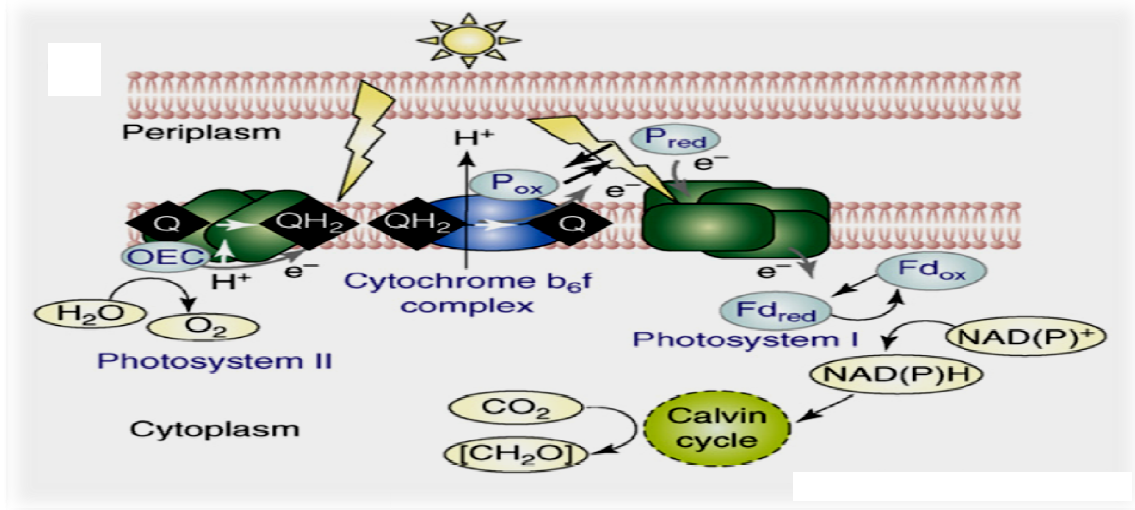


Figure 1.5. Diagram showing photosystems in algae. Q: ubiquinone, QH₂: ubiquinol, OEC: oxygen - evolving complex, Fd: ferredoxin, P: plastocyanin. (Johnson and Schmidt - Dannert, 2008).

The photosystems are light - driven ferredoxin (PSI) and quinone (PSII) reductases (Figure 1.5) which initiate a series of electron transfer reactions that generate NAD(P)H or a proton gradient used to drive the biosynthesis of ATP. PSI is excited by absorption of light at 675 - 700 nm by chlorophyll *a*. Generally, photosystems contain pigment - protein complexes known as the photosynthetic reaction centre (RC) that catalyze the initial transfer reactions and “light harvesting antenna complexes” (LH1 and LH2) (Johnson and Schmidt - Dannert, 2008) which influence the amount of light available to the reaction centre complexes, respectively. Photosystems are composed of several polypeptides and excitation of PSII leads to the reduction of ubiquinone to ubiquinol, which is then oxidized by the cytochrome b₆f complex. The oxygen - evolving complex oxidizes water and reduces the primary donor of PSII to regenerate

the system for further ubiquinone reduction (Johnson and Schmidt - Dannert, 2008). The cytochrome complex is the intermediary electron transfer complex between PSI and PSII. In this complex, the electrons are transferred from ubiquinol to plastocyanin and thereby resulting in a reduction of plastocyanin and subsequent oxidation of ubiquinol. The reaction centre of PSI becomes excited and produces two reduced molecules of ferredoxin for every two oxidized molecules of plastocyanin. Excitation of PS1 drives the reduction of ferredoxin which then reduces NAD(P)⁺ to NAD(P)H for further use in the Calvin cycle (Johnson and Schmidt - Dannert, 2008). With the procession of photosynthesis, the release and absorption of protons (H⁺) from the stroma to the thylakoid increases which consequently results in a pH change of 7 to 8 in the stroma. Along with the transmembrane transport of the protons, an accumulation of Mg²⁺ occurs in the stroma and upon the interaction between chlorophyll and light; electrons are transported through the electron transport chain and to thioredoxin and NADPH. It is therefore evident that the processes occurring in algae are highly complex and can be influenced by a variety of factors thereby affecting the ambient conditions of the stroma and the quantity of chlorophyll, consequently altering lipid metabolism (Lv *et al.*, 2010).

1.2.2 Biosynthesis of fatty acids and lipids

Fatty acid biosynthesis occurs in the plastid and is mediated by the enzyme complex fatty acid synthase (FAS). A two step reaction involving acetyl - CoA carboxylase (ACC) generates the formation of the substrate malonyl - CoA. According to Lv *et al.* (2010), the quantity and activity of ACCase plays an important role in the synthesis of fatty acids. It was shown that lipid synthesis in *Chlorella vulgaris* was highly complex. The quantity of chlorophyll and the ambient conditions of the stroma were susceptible to influence by any factor, thus suggesting that the activity and quantity of ACCase might have an effect on lipid accumulation. In green algae, two types of ACCase were identified, namely, a plastidial prokaryotic - type multisubunit enzyme and a multifunctional homomeric enzyme resident to the cytosol (Khozin - Goldberg and Cohen, 2010).

The malonyl - CoA substrate is transferred to an acyl carrier protein (ACP), this occurs prior to the decarboxylation of the malonyl moiety and condensation of C1 of an acetate and C2 of the malonyl group on ACP. A sequence reaction involving reduction and dehydration results in the formation of palmitic acid (16:0) and stearic acid (18:0) with the introduction of the first double bond into 16:0 - ACP and 18:0 - ACP, thus generating either 16:1 - ACP or 18:1 - ACP in a reaction catalyzed by stearoyl - ACP - desaturase. The aforementioned fatty acids are then used in either the synthesis of plastidial glycerolipids or released into the cytoplasm where they become activated to CoA esters for reactions such as elongation. Fatty acids, produced via the prokaryotic pathway, are transferred to the *sn* - 1 and *sn* - 2 position of glyceraldehyde - 3 - phosphate (G3P) which is converted into phosphatidic acid (PA). A reaction involving acyl - ACP : glycerol - 3 - phosphate acyltransferase (GPAT) then leads to the formation of lysophosphatidic acid (LPA) which, when catalyzed by lysophosphatidic acid acyltransferase (LPAT), forms more PA. This PA can be further metabolized to the lipids responsible for glycolipid synthesis, namely, diacylglycerol (DAG) and phosphatidylglycerol (PG). Outside the plastid are acyl - CoA - esters which can be incorporated into lipids in reactions making up the eukaryotic biosynthetic pathway. PA and DAG syntheses occur in a similar manner to that of the prokaryotic pathway (within the plastid) but in contrast to acyl - ACPs, acyl - CoAs function as substrates for LPAT and GPAT. DAG is further converted into phospholipids phosphatidylcholine (PC) and phosphatidylethanolamine (PE). The production of glycolipids involves the formation of PA in the plastids and at the endoplasmic reticula (ER). The distribution of FAs at the glycerol backbone is commonly associated with green microalgae. Lastly, the synthesis of TAG occurs at the ER membrane with the precursor DAG; to which a third acyl residue is bound at the *sn* - 3 position. This transfer reaction is either catalyzed by phospholipid diacylglycerol acyltransferase (PDAT) or by diacylglycerol acyltransferase (DGAT), depending on the substrate. Levels of DGAT may present a bottleneck with regard to TAG biosynthesis as the transferase shows the lowest activity amongst the enzymes of the Kennedy pathway (Khozin - Goldberg and Cohen, 2010).

1.2.3 Biosynthesis of polyunsaturated fatty acids (PUFAs)

The introduction of double bonds into the acyl chains is catalyzed by desaturases which demonstrate substrate specificity. The acyl - ACP - desaturase which is localized in the plastid acts on acyl chains bound to ACP. As mentioned above, the stearoyl - ACP Δ^9 - desaturase introduces a double bond into stearic acid resulting in 18:1 Δ^9 - ACP. With the exception of the soluble acyl - ACP desaturase family, all other desaturases are integral membrane proteins with either acyl - CoA or acyl - lipid substrates. The initial substrate in this pathway is oleic acid (18:1 Δ^9) subsequent to its incorporation into PC. A Δ^{12} - desaturase then introduces the second double bond forming linoleic acid (LA), which may be further desaturated by a Δ^{15} - desaturase to α - linolenic acid (ALA) (Lang, 2007). These modified FAs are then exchanged by other 18:1 acyl residues and can be released as acyl - CoA derivatives into the cytoplasm. With this release, they can be extended to longer acyl chains by specific membrane - bound elongase complexes (Lang, 2007). According to Khozin - Goldberg and Cohen (2010) microalgal PUFA elongases are similar in structure to the fatty acid elongase enzyme (ELO) family which are responsible for catalyzing the condensation step of fatty acid elongation in animals and fungi. These elongases differ from higher plant condensing enzymes which are responsible for microsomal elongation of monounsaturated and saturated fatty acids. With regard to substrate specificity, PUFA elongases were characterized from long - chain polyunsaturated fatty acid (LC - PUFA) producing microalgae. Amongst these are C18 Δ^6 - PUFA - specific elongases, shown to participate in the elongation of C18 PUFA, α - linolenic acid (ALA, 18:3 ω 6), where ω 6 represents the fatty acid belonging to the omega - 6 family (Bigogno *et al.*, 2002). These elongases are also involved in the production of arachidonic acid (ARA) and eicosapentaenoic acid (EPA) (Khozin - Goldberg and Cohen, 2010). C20 Δ^5 - PUFA - specific elongases are involved in the elongation of EPA in the docosahexaenoic acid (DHA) biosynthesis pathway (Khozin - Goldberg and Cohen, 2010).

1.2.3.1 Genes involved in biosynthesis of PUFAs

According to studies conducted by Guschina and Harwood (2006), it has been reported that two cDNA clones corresponding to $\Delta 12$ and ω -3 fatty acid desaturase (FAD) genes (designated as CvFad2 and CvFad3, respectively) have been isolated from *Chlorella vulgaris* C - 27. These clones were isolated based on sequence information from genes encoding for plant $\Delta 12$ and ω -3 FADs which desaturate oleate to linoleate and linoleate to α - linolenate, respectively. The deduced amino acid sequence of Cvfad2 displayed approximately 66% similarity to those of higher plant microsomal $\Delta 12$ encoded FADs and approximately 35% similarity to plastidial $\Delta 12$ FADs. When Cvfad2 was expressed in *Saccharomyces cerevisiae*, linoleic acid (C18:2) accumulated. The predicted protein of Cvfad3 showed approximately 60% similarity to the plastidial and microsomal ω -3 FADs and lower similarity to $\Delta 12$ FAD. Based on the features of the amino acid sequences of the C - and N - terminal regions, Cvfad3 seemed to encode a microsomal ω -3 FAD rather than a plastidial one; however based on results, the authors could not conclude the exact localization of the protein in *C. vulgaris*. In addition to this, these genes (for the ω -3 and $\Delta 12$ FADs) proved to be upregulated by low temperature. The level of the transcript of Cvfad2 increased gradually during exposure to low temperatures and, after 24 hours had reached 3.2 times the initial level. In contrast the level of the transcript of Cvfad3, after only three hours of cold exposure, increased to 5.4 times the initial level but then decreased gradually. This suggests that the two desaturase genes may possibly be involved in the development of low temperature freezing tolerance in *C. vulgaris* (Guschina and Harwood, 2006). Wang *et al.* (2009) reported the accumulation of abundant cytoplasmic lipid bodies (LBs) and starch in the alga, *Chlamydomonas reinhardtii* when exposed to nitrogen deficient conditions. When starch biosynthesis was blocked in the *sta6* mutant, the LB content was shown to increase 30 - fold thus, demonstrating genetic manipulation as a tool for the enhancement of lipid production.

1.2.4 Oxylipins

Recently, the topic of oxylipins has received much attention in the field of lipid metabolism (Guschina and Harwood, 2006). Lipid peroxidation is a crucial process in the aforementioned process. Essentially lipid peroxides are collectively termed oxylipins and serve as precursors for the synthesis of signal molecules. This entails the role of hydroxyl fatty acids and oxygenated derivatives of fatty acids, known as oxylipins (Guschina and Harwood, 2006). Initially the term "oxylipin" was proposed to encompass polyunsaturated fatty acid metabolites formed by reaction (s) involving one or more steps of mono - or di - oxygenase catalyzed oxygenation, thus including metabolites of different chain length and eicosanoids (Bernart *et al.*, 1993). Generation of these oxylipins follow the major biosynthetic pathway known as the lipoxygenase pathway (LOX). Formation of a family of non - heme iron containing fatty acid dioxygenases which catalyze the regio - and stereospecific insertion of molecular oxygen into PUFA's ultimately leads to the generation of fatty acid hydroperoxides (Blee', 2002; Lang, 2007).

Generally, green algae metabolize C18 acids at C - 9 and C - 13 positions, principally using lipoxygenases with an *n* - 6 specificity (Guschina and Harwood, 2006). The terrestrial acidophile, *Dunaliella acidophila*, was described to contain methyl (12R) - hydroxyl - (9Z, 13E, 15Z) - octadecatrienoate, methyl (9S) - hydroxyl - (10E, 12Z, 15Z) - octadecatrienoate and methyl ricinoleate [methyl (12R) - hydroxyl - (9Z) - octadecenoate) subsequent to methylation of the acidic lipid mixture. Two LOX - derived hydroperoxides were detected from the chlorophyte *Ulva conglobata* (Lang, 2007), namely, (9R, 10E, 12Z) - 9 - hydroperoxy - 10,12 - octadecadienoic acid ((9R) - HPODE) and (9R, 10E, 12Z, 15Z) - 9 - hydroperoxy-10,12,15 - octadecadienoic acid ((9R) - HPOTE), as well as other compounds such as (8Z) - 8 - heptadecenal and (8Z, 11Z, 14Z) - 8, 11, 14 - heptadecatrienal. As a result, these oxylipins lead to the hypothesis that PUFA's such as α - linolenic acid (ALA) and linolenic acid (LA) were converted to 2 -, 9 - and 13 - hydroperoxides which were then subsequently converted into C - 17, C - 9 and C - 6 aldehydes (Lang, 2007). Furthermore, the freshwater green alga *Chlorella pyrenoidosa* is known as a source of 9 - and 13 - HPODE isomers which are present in an equal ratio and hydroperoxide lyase activity (Lang, 2007). In spite of the growing interest in oxylipins, little is known about the role of oxylipin metabolism. However, an increase in

sequence information from genome sequencing projects allow for the use of biochemical and molecular tools for the characterization of new LOX pathways and related enzymes.

1.2.5 Factors affecting lipid production in algae

1.2.5.1 Nitrogen metabolism

Lipids have served as bioindicators of the physiological state and origin of organic material in a body of water. Total lipid content of *Dunaliella viridis* remains relatively unaffected when exposed to nitrogen deficiency, yet the lipid class composition of the micro - organism does change. This is, however, coupled to a specific level of carbon dioxide supply. It is observed that at a level of 1% CO₂, rather than the conventional atmospheric level, the main lipid reserve, triacylglycerides, accumulated in high amounts. Studies by Gordillo *et al.*, (1998) showed an increase from 1 to 22% of triacylglycerides when *D. viridis* was exposed to 1% CO₂ under nitrogen deficiency. Atmospheric levels of CO₂ slightly decreased the amount of total lipid content. These findings also state that lipid class composition may vary for cell cultures in exponential growth as opposed to those in the stationery phase. Nitrogen starvation caused the opposite result in the content of fatty acids. High levels of CO₂ promoted an elevated amount of fatty acids to be produced and in contrast, atmospheric levels of CO₂ decreased the production of fatty acids. Both of the aforementioned conditions promoted the syntheses of hydrocarbons, wax esters and sterols. Hydrocarbons are suggested to be end products of the fatty acid cycle metabolism and their presence reflect an extreme physiological case when they are not used as substrates to provide metabolic energy in the form of ATP. Under these CO₂ conditions, a lipidic synthesis pathway would be taken as a carbon sink as carbon incorporation is forced and because of nitrogen deficiency, carbon skeletons are not incorporated into proteins to allow the cell to grow (Gordillo *et al.*, 1998).

1.2.5.2 Phosphate starvation

Studies by Khozin - Goldberg and Cohen (2006) reveal that under phosphate deprivation, cells of the freshwater eustigmatophyte, *Monodus subterraneus*, increase in diacylglyceroltrimethylhomoserine (DGTS) and digalactosyldiacylglycerol (DGDG). Under phosphate limitation, cell division and chlorophyll synthesis were greatly retarded. However, when the micro - organism was grown in phosphate - free medium, the cell number doubled after 4 days of cultivation. This indicates that the intracellular phosphate was sufficient for at least one cell division. In the phosphate - deprived cells, the phospholipid content decreased drastically whilst the content of triacylglycerols increased. This phenomenon observed is similar to that induced by nitrogen starvation (Khozin - Goldberg and Cohen, 2006).

1.2.5.3 Temperature, light intensity and salinity

The effect of temperature on lipid metabolism by different algal species would differ. For *Botryococcus braunii*, the optimal growth temperature is approximately 23°C and at temperature higher than optimal, lipid content decreases. Varying photoperiods have been reported to affect fatty acid production in marine microalgae. Vladislav and Jaromir (1994) reported that photoperiod could be one of the factors that trigger hydrocarbon production. Studies on photoperiod conducted by Qin (2005) have shown no significant difference in algal growth or lipid production. However, they did show that light intensity does affect the production of hydrocarbons. Chirac *et al.*, (1985) reported that low illumination reduced hydrocarbon synthesis. *B. braunii* has a narrow range of light intensity for growth. At very low illumination (30 W/m²), growth was inhibited and at light intensities above 100 W/m², photoinhibition had also occurred thus, decreasing lipid content.

B. braunii not only survives in freshwater environments, but also adapts to salinity variations. Qin (2005) showed that a moderate increase in salinity (< 0.25 M NaCl) influenced lipid content. Approximately 0.5 M NaCl inhibited algal growth, whereas high mortality occurred upon

exposure to 0.7 M NaCl. A study by Va`zquez - Duhalt and Arredondo - Vega (1990) reported that the lipid composition could be altered by salinity. This provides a tool to influence algal biomass and lipid composition.

1.3 Lipid - associated proteins

1.3.1 Oleosins and caleosins

Oleosins are alkaline proteins associated with the oil bodies which range from 15 to 30 kDa in size. Originally, oleosins were identified by immunocytochemistry and characterized in terms of size by subcellular fractionation (Frandsen *et al.*, 2001). Studies have shown that approximately 5% of the oleosin is associated with endoplasmic reticulum segments which lie in close proximity to the oil bodies (Frandsen *et al.*, 2001). A novel feature of oleosins is the central hydrophobic stretch of 72 uninterrupted residues. This allows for the formation of a hairpin structure that penetrates the surface phospholipid monolayer of the oil body and into the matrix. Found amongst this stretch are three proline residues and one serine residue which form the exclusive feature known as the "pro knot" (Hsieh and Huang, 2004; Murphy, 2004). Two oleosins isoforms, which are known to be immunologically distinct from each other, are found in diverse angiosperms whilst only one oleosin is found in gymnosperms (Frandsen *et al.*, 2001).

These proteins are suggested to be involved in the stability of the lipid body, in their metabolism and synthesis. They shield the phospholipids and in doing so thereby prevent contact between the phospholipid surfaces of adjacent oil bodies. Coalescence and aggregation of the oil bodies in the cytosol are alleviated due to their negatively charged surfaces which are influenced by the oleosin (Frandsen *et al.*, 2001). Hence, oil body stability is thus due to steric hindrance and electrical repulsion. The complexity of the oil body coat is not fully understood as initially the oleosins were the only well - characterized proteins associated with the oil body. However, this was until the recent discovery, by immune - labelling, of three minor proteins in sesame seed oil bodies differentiated as Sop1, Sop2 and Sop3 (Frandsen *et al.*, 2001). Sesame Sop1 was

sequenced and shown to be homologous to a rice protein with a calcium - binding domain, hence these minor proteins are tentatively named “caleosins” (Frandsen *et al.*, 2001). Caleosins lack an N - terminal signal peptide, however they do possess a central hydrophobic region with the potential to form a transmembrane helix and amphipathic β - sheets. They contain a proline - rich region with the potential to form a hairpin - knot - like that of the oleosin motif involved in lipid body targeting (Hsieh and Huang, 2004; Frandsen *et al.*, 2001; Murphy, 2004) . In addition to this, they also possess an amphipathic α - helical domain, which functions in the binding to lipid bodies and bilayer membranes (Murphy, 2004). Since caleosins contain a single putative membrane - spanning domain, as well as calcium binding domains and a C - terminal domain with protein kinase phosphorylation sites; they may function in signalling and mobilisation of the oil bodies (Murphy, 2004). Although not much is known about these proteins in algae; the complete structure and function of the oleosins are not fully elucidated.

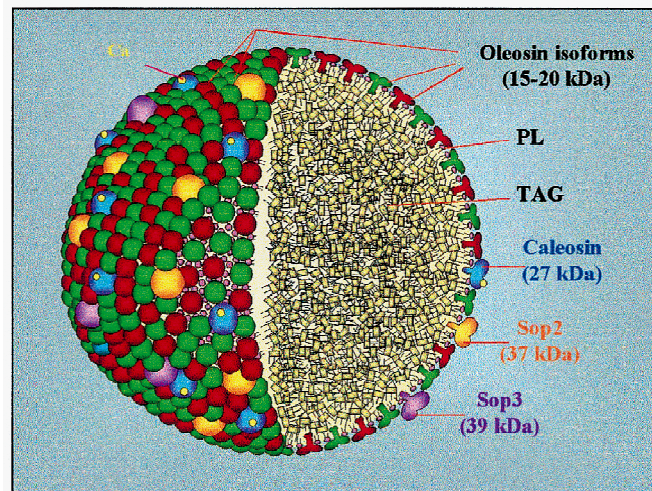


Figure 1.6. Diagram of an oil body (Frandsen *et al.*, 2001). PL: phospholipid, TAG: triacylglycerol, Sop 2 and 3: sesame seed oil minor proteins.

Lacking a cleavable signal sequence, oleosins probably attain a conformation or contain sequences that target them to oil bodies. Mutated oleosins lacking the central domain displayed reduced oil body targeting, whilst removal of the N - or C - terminal showed little or no affect

(Frandsen *et al.*, 2001). Site - directed mutagenesis of three proline residues to leucine confirmed the paramount role of the “proline knot“ in accumulation of oil bodies. Originally believed to be involved in the insertion into the endoplasmic reticulum (ER), the central hydrophobic domain of the “pro knot“ is now known to serve as a targeting signal instead.

1.3.2 Plastid lipid - associated proteins (PLAPs)

Originally thought to be functional in the storage and stabilization of lipidic pigments in chromoplasts, these proteins which are exclusive inhabitants of plastids are now regarded as being far more useful. The alga, *Dunaliella bardawil*, was shown to contain similar lipid associated proteins in the triacylglycerol / carotenoid globules. As in the case with oleosins in seeds, trypsinized cleavage of the protein localised on the plastoglobuli led to the coalescence of the globules hence implicating PLAPs in the role of stabilization of plastid lipidic bodies (Murphy, 2004). Apart from being the predominant component in the triacylglycerol / carotenoid - rich fibrils and globules in chromoplasts, these minor proteins are also found in chloroplasts and elaioplasts (Murphy, 2004). Whilst there is no obvious homology between the conserved regions of PLAPs and other lipid - associated proteins, such as oleosins and caleosins, there are several interesting motifs that may be significant in their lipid - binding properties. For example, localised in the middle of the protein are two non - polar regions of 16 and 22 residues, respectively, each of which is flanked by relatively polar regions. Structurally this reveals the potential to form integrating transbilayer or monolayer - associated domains. In consideration of their lower abundance, PLAPs are less likely to be involved in structural roles but rather in other aspects of lipid - body function or possibly in intra - plastidial lipid trafficking (Murphy, 2004).

1.4 Endoplasmic reticulum (ER) and oil body synthesis

Synthesis of oil bodies and their constituent phospholipids, triacylglycerides and oleosins occurs in the endoplasmic reticulum (ER). Continuous accumulation of TAG at a region of the ER allows for the budding of an oil body enclosed by a monolayer of phospholipid (Figure 1.7). This budded oil body is stabilized by the inclusion of oleosins onto its surface. Via the signal - recognition particle (SRP) pathway (Hsieh and Huang, 2004), the ribosome - mRNA with the nascent oleosin peptide is guided to the ER. Translation of this oleosin mRNA in an *in vitro* system is enhanced with the addition of microsomes, whilst inclusion of SRP consequently retards the aforementioned action (Hsieh and Huang, 2004). When transformed with an oleosin gene, *Saccharomyces cerevisiae* (yeast) synthesizes and targets the oleosin similar to yeast oil bodies (Hsieh and Huang, 2004). When the transformed yeast strains are defective in SRP components, the oleosin is not targeted to the oil bodies and are subsequently proteolyzed. The nascent oleosin polypeptide synthesised or being synthesised assumes a topology on the basis of its hydrophobic or hydrophilic interaction with the phospholipid bilayer, whilst the central hydrophobic stretch buries itself in the hydrophobic acyl portion of the bilayer. Oleosins ought to be on the cytosolic side of the ER to be able to diffuse to the budding oil bodies. An N - terminal ER targeting peptide from a non - oleosin protein attached to the N - terminus of an oleosin, produced via gene cloning, can pull the N - terminal portion of the oleosin but not the hydrophobic stretch (with or without the C - terminal portion) into the ER lumen. This is probably due to the interaction between the hydrophobic stretch and the acyl moieties of the phospholipid bilayer which proves to be too strong to allow for the insertion of the oleosin into the lumen (Hsieh and Huang, 2004). This modified oleosin can be incorporated into the ER but will not be inserted into the oil bodies. As the newly synthesised oleosins and TAGs on the ER diffuse to and converge at the budding oil bodies, a gradient of enrichment of the aforementioned components exists. This concentration gradient exists from the point of synthesis to the budding oil body, and explains the immunocytochemical observation that more oleosins are present in the ER near the budding oil bodies (Hsieh and Huang, 2004).

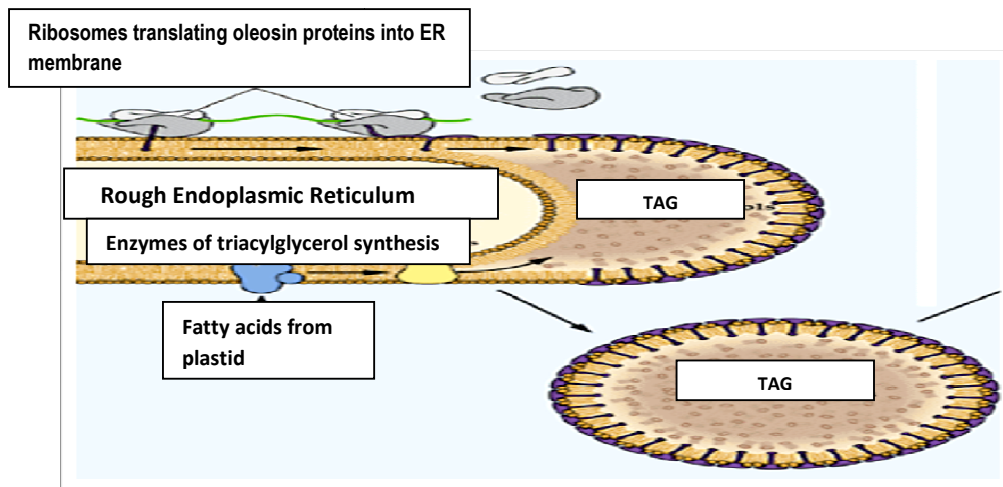


Figure 1.7. Diagram showing the biosynthesis of TAG.
 (http://www.uky.edu/~dhild/biochem/20/fig10_20.png).

1.5 Aim of this study

The objective of the current study focuses on the analyses of algal oil body components, based on the postulate that triacylglycerols form the central domain or matrix of the oil droplet while phospholipids and integrated protein make up the periphery of such droplets (Wang *et al.*, 2009; Moellering and Benning, 2010; Davidi and Pick, 2012).

Two green microalga, namely, a freshwater strain of *Chlorella vulgaris* and a marine biflagellate strain of *Dunaliella primolecta*, were propagated under conditions where nitrogen availability is defined by supplementation of a mineral salts medium with nitrate salts NaNO_3 and $\text{Co}(\text{NO}_3)_2 \cdot 6\text{H}_2\text{O}$. Their exclusion from the same medium is used for stress induction. Oil yields and growth - related parameters were compared under these varied growth conditions as nitrogen limitation may correlate with enhanced lipid biosynthesis in algae (Weldy and Huesemann, 2007; Wang *et al.*, 2009). In addition, this study aimed to investigate specific constituents of the oil which are analyzed as follows:

- i. Fluorescence differentiation using laser scanning confocal microscopy and fluorescent dyes Nile red and Bodipy 505/515.

- ii. Spectrophotometry of oil - associated pigment extracts, thin layer chromatography of hexane - oil extracts and profiling of fatty acid methyl esters using gas chromatography.
- iii. Polyacrylamide gel - electrophoresis and quantification of protein extracted from oil.

CHAPTER TWO

MATERIALS AND METHODS

2.1 Experimental algae and culture media

The green microalgae *Chlorella vulgaris* CCAP 211/11B and *Dunaliella primolecta* CCAP 11/34 of the Culture Collection of Algae and Protozoa (UK), were provided by Professor Faizal Bux, Durban University of Technology, Durban, SA. *C. vulgaris* CCAP 211/11 B was isolated by Beijerinck in 1890 from freshwater in Delft, Holland (http://www.ccap.ac.uk/strain_info.php?Strain_No=211/11B). *D. primolecta* CCAP 11/34 is of marine origin, isolated by F. Gross in 1936 off the coast of Plymouth, Devon, UK (http://www.ccap.ac.uk/strain_info.php?Strain_No=11/34). The seed cultures were axenically cultivated (2.2) and maintained routinely in autotrophic BG11 medium (pH 7.1) or BG11 control medium excluding nitrates to bring about a culture growth impediment or induction of stress (Appendix A). BG 11 medium was devised from the American Type Culture Collection (ATCC) '616 Medium' (Chinnasamy *et al.*, 2009) and is subsequently referred to as test medium while the variant lacking nitrates is referred to as control medium. All experiments conducted herein were done in triplicate. Cultures that were harvested, and not used immediately, were freeze-dried and stored in a freezer at -20 °C.

2.2 Axenic cultivation of *C. vulgaris* and *D. primolecta*

2.2.1 Starter culture preparation and maintenance

C. vulgaris and *D. primolecta* growth was activated by inoculating 50 ml batches of BG11 medium and BG11 control medium excluding nitrates (2.1) in 250 ml Erlenmeyer flasks with 3 ml of respective seed. The seed cultures were grown for 7 days at 28 °C in a temperature controlled laboratory. A 16 : 8 h dark - light photoperiod was considered to be the optimum light regime to sustain algal growth

(<http://www.marine.csiro.au/microalgae/methods/Light%20Physical%20Units.html>).

Triplicate seed cultures were prepared by inoculating 50 ml of BG11 and BG11 medium excluding nitrates with 5 ml of culture in 250 ml Erlenmeyer flasks. The light intensity of 5400 lux was measured using a Major Tech light meter, Model MT 940, (Major Tech); this assisted in the correct positioning of the lights to ensure the specified intensity of approximately 86 $\mu\text{mol photons m}^{-2} \text{sec}^{-1}$ was achieved. This was established with the use of two 18 watt Phillips cool white tubes and two Phillips Genie energy saver bulbs of 11 and 14 watts. In addition to the use of the electric lights, the culture samples received natural sunlight from a north facing window to aid their growth. illuminance conversion of “1 foot candle = 10.8 lux” and “1000 lux = 16 $\mu\text{mol photons m}^{-2} \text{sec}^{-1}$ ” was taken from the website of the Australian National Algae Culture Collection - Methods

(<http://www.marine.csiro.au/microalgae/methods/Light%20Physical%20Units.html>).

2.2.2 Growth culture preparation and maintenance

Approximately 3 to 5 ml of the 50 ml starter culture (2.2.1) was added to 300 ml water batches to achieve an inoculum size of 10^7 cells/ml, this was done by means of cell counting using a haemocytometer. Once the appropriate volume of the inocula were established, culture of the

same volume was added to 300 ml of BG11 and BG11 control media in separate 500 ml Erlenmeyer flasks. At this time of inoculation (T_0), and subsequently every 3 or 4 days, 4 ml medium of each flask was removed and analysed (2.3).

2.3 Analyses of cultures

From the growth culture media, 4 ml aliquots were removed at T_0 (2.2.2) and every 3 or 4 days to routinely analyse the growth of *C. vulgaris* and *D. primolecta* in the stressed and unstressed media (Appendix A). This was done until the stationary period had been attained. Following the removal of the inocula, fresh medium of the same volume and type was used to replenish the withdrawn aliquot as to accommodate for the headspace created by removing the media. The addition of the fresh media was to accommodate for the headspace created by the withdrawal samples, thereby maintaining consistency in the air volume above the medium. This certainly resembles a fed batch system and was adopted in both test and control media devoid of nitrates. The maintenance of headspace is critical in standardizing CO₂ and oxygen requirements in the light-dark growth cycle. Culture growth was analysed in terms of cell number, pH and OD_{680 nm} measurements.

2.3.1 Cell number determination

In accordance with the technique established by Rao *et al.* (2007), cell counts per ml of sample were achieved using a haemocytometer (Neubauer Improved Bright Line, Superior) at 40X magnification. A dilution of 10^{-1} was employed in cases where high cell numbers made counting cumbersome. Microsoft Excel 2007 (Microsoft) was used to generate a plot of cell number/ml versus time using average data values. Further analyses were done by generating a plot showing the relationship between algal number and optical density (OD_{680nm}). The % dead cells was estimated using 10 μ l of sample plus 10 μ l of 0.01 % w/v Loeffler's methylene blue (Gurr,

BDH Ltd., Poole, UK) stain. The mixture was left standing for 10 minutes and followed by an estimation of dead cells which had taken up the dye to stain blue.

2.3.2 Optical density (OD)

Algal growth was monitored , every 3 or 4 days, by optical density measurements at 680 nm (Lee *et al.*, 1998). Uninoculated BG11 medium (pH 7.4) was used as a blank sample against the withdrawn aliquots. Optical density values versus time were plotted using Microsoft Excel 2007 (Microsoft).

2.3.3 pH

Centrifugation at 10000 rpm (Appendix B: G force) for 10 minutes in an Eppendorf centrifuge 5424 (Eppendorf) yielded cell - free supernatants which were subjected to pH measurement using a Hanna pH meter (Hanna, USA), calibrated with standards of pH 4, 7 and 9 (Merck) at 25 °C. This was routinely every 3 or 4 days until the stationary phase was attained.

2.4 Harvesting of microalgae

2.4.1 Centrifugation and freeze - drying

At the onset of stationary phase, which was established by a decline in the cell count, algal samples (those used in the routine analyses) were harvested to prevent a further decline in cell numbers. Triplicate cultures were decanted into three separate sterile 500 ml centrifuge bottles

and pelleted at 5000 rpm (Appendix B: G force) for 15 minutes at 4 °C using a Beckman Coulter Avanti J-2 XPJ centrifuge (Beckman) fitted with a JA-10 rotor. Subsequently, the supernatants were discarded and the pellets were re - suspended in vials with 20 ml of distilled water with a further addition of 10 ml to transfer any residue. These vials were pre - weighed using a bench - top Pioneer Ohaus fine balance. They were then subjected to liquid nitrogen freezing for 5 minutes prior to being placed in a Virtis Benchtop K freeze - dryer which was operated for 48 hours at - 70 °C to dry the cell pellet. Weights of the algal samples were determined gravimetrically.

2.5 Disruption and extraction of cell lysates

2.5.1 Hydrocarbon yield

Extraction of the algal cells was achieved by disrupting the algal biomass with a mortar and pestle, using *n* - hexane (Merck) as an extraction solvent (Miao and Wu, 2006; Halim *et al.*, 2013). The extraction procedure was selected on the basis that it was applied successfully to a species of *Chlorella*. Cells (in pellet form) were ground to a paste at random intervals which required addition of 2 ml *n* - hexane before being transferred to a 2 ml Eppendorf tube and centrifuged at 5000 rpm (G force reference: Appendix B) for 5 minutes. Supernatants were transferred to glass test tubes, each fitted with a metal cap. The pellets were re - suspended in 2 ml *n* - hexane using a Genie 2 vortex (Genie) prior to being ground further. This process was repeated several times until the residue converted from light green to grey and assumed a clay - like texture. The hexane - oil supernatants were then transferred to pre - weighed conical flasks and subjected to rotary evaporation using a Buchi rotary evaporator (Buchi). The mass was then determined gravimetrically. The determination of the % yield of algal oil - hydrocarbon mixture was as follows:

$$\% \text{ yield} = \text{oil - hydrocarbon mass} / \text{dry algal biomass} \times 100$$

2.5.2 Chlorophyll fraction

To approximately 1 ml of algal oil, 1.5 ml of 99.5 % (v/v) methanol (Merck) was added to re-suspended the hydrocarbons (Rao *et al.*, 2007). This was centrifuged at 5000 rpm (G force: Appendix B) for 1 minute. The suspension was then analyzed by thin layer chromatography (2.6.1) and spectrophotometry (2.6.2).

2.5.3 Carotenoid fraction

Approximately 1.5 ml of acetone was added to 1 ml of algal oil to extract the carotenoids (Rao *et al.*, 2007). This suspension was centrifuged at 5000 rpm (G force: Appendix B) for 1 minute prior to being analyzed by thin layer chromatography (2.6.1) and spectrophotometry (2.6.2).

2.6 Analyses of organic extracts

2.6.1 Thin layer chromatography (TLC)

TLC experiments were performed on aluminium silica gel 60 plates (20 x 20 cm) (Merck) which were prepared by etching nine spots 4 cm from the bottom of the plate. Each sample lane was separated by a spacer approximately 1.5 cm wide to avoid samples mixing with each other in the event of expansion of the sample spot diameter during chromatography. The liquid samples that were applied to the individual lanes were:

1. Sunflower oil (Flora, SA) [20 μ l in 100 μ l chloroform]
2. Olive oil (Santagata, SA) [20 μ l in 100 μ l chloroform]
3. Evening primrose oil (Vital capsule, Vital, SA) [20 μ l in 100 μ l chloroform]
4. Norwegian salmon oil (Vital capsule, Vital, SA) [20 μ l in 100 μ l chloroform]
5. L - α - dioleoylphosphatidylethanolamine (DOPE) (Sigma Chemicals Co.) [10 μ g/ μ l]
6. *D. primolecta* algal oil from culture of test medium [approx. 5 μ g in 300 μ l chloroform]
7. *C. vulgaris* algal oil from culture of test medium [approx. 5 μ g in 300 μ l chloroform]
8. *D. primolecta* algal oil from culture of control medium [approx. 5 μ g in 300 μ l chloroform]
9. *C. vulgaris* algal oil from culture of control medium [approx. 5 μ g in 300 μ l chloroform]

Algal oil samples (6 - 9 above) were extracted using hexane (2.5.1), dried by rotary evaporation and taken up in 300 ml of chloroform. Similarly, carotenoid and chlorophyll fractions (2.5.2; 2.5.3) were analyzed by applying the following liquid samples in individual lanes;

1. *D. primolecta* algal oil (test medium) extracted in acetone
2. *D. primolecta* algal oil (test medium) extracted in methanol
3. *C. vulgaris* algal oil (test medium) extracted in acetone
4. *C. vulgaris* algal oil (test medium) extracted in methanol
5. *D. primolecta* algal oil (control medium) extracted in acetone
6. *D. primolecta* algal oil (control medium) extracted in methanol
7. *C. vulgaris* algal oil (control medium) extracted in acetone
8. *C. vulgaris* algal oil (control medium) extracted in methanol

Plates were air - dried and exposed to a running solvent containing 50.5 ml of hexane - diethyl ether - acetic acid (35:15:0.5 v/v/v) (Gurr and James, 1980). Plates were immediately placed into a pre - equilibrated elution tank and the solvent was allowed to travel within 4 cm from the top. Thereafter, the plates were air dried and exposed in an iodine chamber followed by spraying with 50 % (v/v) H₂SO₄ for visualization of the migrated components. The plates were developed by heating gently on a flat hotplate in a fume hood.

2.6.2 Spectrophotometry

2.6.2.1 Chlorophyll spectrum

From the 99.5 % (v/v) methanol and oil supernatant mixture (2.5.2), 0.5 ml was removed and dissolved in twice its volume of 99.5 % methanol in one of a pair of matched glass microcuvettes (QS 1000). The absorbance spectrum of pooled extracts was measured between 400 - 700 nm using a Shimadzu spectrophotometer Model UV - 160A (Shimadzu) using 1.5 ml 99.5 % methanol as a blank.

2.6.2.2 Carotenoid spectrum

Approximately 0.5 ml of acetone was added to the oil supernatant and acetone mixture (2.5.3) and dissolved in twice its volume of acetone in one of two matched glass cuvettes (QS 1000). The absorbance spectrum of the pooled extracts was measured between 400 - 700 nm (2.6.2.1) using 1.5 ml of pure acetone to zero the spectrophotometer.

2.7 Confocal microscopy of algal cells

2.7.1 Nile red staining

Stationary phase algal cells of both test and control media were stained with Nile red (Sigma Chemicals Co.) at a final concentration of 1.6 mg/ml, from a stock of 4 mg/2.5 ml DMSO (Merck, FRG) (Chen *et al.*, 2009). An aliquot of 7 μ l was placed onto a clean glass slide, over which a coverslip was sealed in a central position with cosmetic nail varnish. Images were acquired using a Zeiss LSM 710 Axio observer Z1 microscope (Zeiss) and a 63X oil immersion lens objective with a numerical aperture setting of 1.4. Slides were viewed immediately to avoid fading of the dye from exposure to light. For neutral lipid - specific detection of Nile red fluorescence, the 488 nm argon excitation laser was used in combination with a 516 to 547 nm band pass filter. The Nile red signal for phospholipids was captured using a laser excitation wavelength of 514 nm and the emission was captured between 580 - 615 nm (Fowler and Greenspan, 1985). Chlorophyll fluorescence was captured using a helium - neon 633 nm laser excitation line and the emission was recorded between 639 - 721 nm. Micrographs were merged and individual fluorescent components pseudo - coloured using Zen 2008 software (Carl Zeiss). Individual wavelength scanning and the use of the lambda stack facility allowed for addition of individual fluorescent components in each frame. This data was correlated with fluorescent intensity and emission wavelength plots of the various stained components.

2.7.2 Bodipy staining

Stationary phase cells were prepared for viewing as described (2.7.1), stained with Bodipy 505/515 (Sigma Chemicals Co.) at final concentration of 1.24 mg/ml (from a stock of 6.2 mg/5ml of DMSO) (Cooper *et al.*, 2010). According to Cooper *et al.* (2010), the emission wavelengths of phospholipids are unknown. They reported the use of the 488 nm laser to excite

the bodipy dye which exhibited moderate red autofluorescence from endogenous chlorophyll and carotenoid molecules. Chlorophyll fluorescence was detected using a 514 nm argon excitation laser and a 588 to 753 nm band pass filter. Similarly, bodipy signal for lipidic fluorescence was captured using a 488 argon nm excitation laser and the emission was captured between 500 to 580 nm. This allowed for the visualization of the spectrally distinct green fluorescence of lipidic bodies. Spatial overlap of the lipidic bodies and chloroplasts results in a yellow fluorescence as acquired in the merged micrographs using the Zen 2008 software.

2.8 Extraction and analyses of protein from microalgal oil

2.8.1 Extraction of protein from oil

Sunflower (Flora) and Norwegian salmon oil (Vital capsule) were included in the protein extraction procedure to compare protein associated with algal oil. Algal, salmon (Vital oil capsule) and sunflower (Flora) oils of 400 µl each were mixed with an equal volume of *n* - hexane. Two hundred microlitres of each oil - hexane mixture were subject to protein extraction separately (Wang *et al.*, 2009), using an equal volume of the following extractants:

- i. 10 % w/v sodium dodecylsulphate (SDS) (Merck)
- ii. 6 M urea (Merck)
- iii. 10 % w/v SDS plus 6 M urea (Merck).

The mixtures were contained in Eppendorf tubes and penetrated into a flat polystyrene platform. The platform was affixed onto the vibrating stub of a Genie vortex (Genie) and shaken at moderate speed for 72 hours at “room temperature”. The tubes were centrifuged for 5 minutes at 5000 rpm (G force: Appendix B), followed by removal of the upper aqueous phase.

2.8.2 Protein quantification

Protein concentrations of the algal oil samples were approximated using the Bio - Rad RC - DC protein assay (Bio - Rad) and estimated using a linear regression fit to the BSA standard curve. A standard curve was generated using the microfuge tube assay protocol by preparing, in triplicate, six dilutions of a bovine serum albumin (BSA) standard of 1.4 mg/ml (Bio - Rad) ranging from 1 µg/ml to 10 µg/ml. Distilled water minus BSA was used as the control. The colorimetric assay entailed adding 125 µl RC reagent I to 25 µl of each standard into a clean, dry microfuge tube which was then vortexed and incubated at room temperature for 1 minute. Subsequently, 125 µl RC reagent II was added to the sample, vortexed and then microfuged at 10000 rpm (G force: Appendix B) for 5 minutes. Inversion of the tube allowed for the supernatant being discarded and 127 µl reagent A' was added to each tube. Tubes were then incubated for 5 minutes at room temperature and vortexed before proceeding with the addition of 1 ml of DC reagent. Samples were incubated for 15 minutes at room temperature, followed by mixing using a vortex and reading of the absorbance against the control at 750 nm.

2.8.3 Protein profiling

Aqueous aliquots of 5 µl from the extracted algal oil samples, including 7.5 µl of sunflower and salmon oil standards were separately solubilised in 1:1 volume sample buffer which constituted the following; 1.2 ml of 0.5 M Tris - HCl, pH 6.8; 1.0 ml glycerol; 2.0 ml of 10 % (w/v) SDS; 0.5 ml of 0.1 % (w/v) bromophenol blue and 4.8 ml deionised water (Appendix A). Prior to use, 50 µl β - mercaptoethanol was added to 950 µl of buffer in an Eppendorf tube which constituted the SDS reducing sample buffer. Broad range unstained SDS - PAGE standards (Bio - Rad) and samples were diluted 1:20 in the reducing buffer, which was then inserted into a flat polystyrene platform and immersed in a 95 °C water bath for 4 minutes. Samples were run on a mini - PROTEAN Tetra Cell SDS polyacrylamide gel electrophoresis system using mini - PROTEAN TGX 10 % w/v precast gels (Bio - Rad, USA) (Berkelman *et al.*, 2009). The 10 X

electrode (running) buffer, pH 8.3, (Appendix A) constituted 7.5 g Tris base; 36 g glycine, 2.5 g SDS which was added to 250 ml deionised water. For the electrophoresis run, 50 ml of the 10 X running buffer was diluted with 450 ml deionised water. On each gel, 10 µl of the samples were loaded per well and run at 80 V for 150 minutes or until the dye front reached near the bottom of the gel. Standards of equal volume to the samples were also run on each gel and polypeptides were visualized using coomassie blue R - 250 staining solution (0.1 w/v %) and silver staining (Appendix A). Standard curves were generated by plotting the logarithm of the molecular weight of each standard versus relative migration distance (UKZN Biochemistry, 1992 undergraduate practical manual). The relative migration distance was determined as follows:

$$\text{Relative migration distance} = \frac{\text{distance of protein migration (mm)}}{\text{length of gel after destaining (mm)}} \times \frac{\text{length of gel before staining (mm)}}{\text{distance of dye migration (mm)}}$$

The molecular weight of the purified protein was estimated by extrapolation of a standard curve which presented a negative slope. Linear regression was used to adjust the curve and the antilog function revealed the molecular weight values.

2.9 Derivatization and analyses of fatty acid methyl esters (FAMES)

2.9.1 Derivatization of FAMES

Fatty acid methyl esters were derived from the hexane extracted hydrocarbon oil fractions (2.5.1). Based on the separation of components by thin layer chromatography, it was presumed that the major source of fatty acids is the acylglycerol fraction. Based on an average theoretical molecular weight for fatty acid groups acylated to glycerol, namely 870 (Montes D' Oca *et al.*, 2011), the derivatization reactions were set up as follows in terms of molar ratio; 30 : 1 : 0.2

CH₃OH - lipid - H₂SO₄, respectively. The mixture was treated at 60 °C for 4 hours in an orbital shaker - incubator (Polychem Supplies) set at 200 rpm. Following incubation, the reaction mixture was cooled in ice to enable quenching. The reaction mixtures were dried in an oven (Elektro Helios) and the residue weighed and diluted with 1 ml of hexane. The fatty acid methyl esters of *C. vulgaris* and *D. primolecta* were determined using gas chromatography (2.9.2).

2.9.2 Analyses of fatty acid methyl esters (FAMES) by gas chromatography

The fatty acid profiles were determined using a Shimadzu GC - 2014 (Shimadzu) with autosampler AOC - 20s. Using the linear velocity mode and column SP 2380 - FAME (30 m length x 0.25 mm id. x 0.25 µm film thickness), the parameters were as follows: flow rate: 1.32 ml/min., injector: SPL - 2014, 250 °C, split injection 1:100, injection volume: 1 µl, with a total analysis time of 25 minutes and detector temperature of 260 °C. The carrier gas used was nitrogen (N₂) and an oven temperature programme of initial temperature of 60 °C was held for 2 minutes, followed by a rate increase of 10 °C per minute to reach 160 °C and thereafter a rate increase of 7 °C per minute to reach 240 °C. The tentative identification of fatty acids was achieved using the retention times of standards listed by the NIST library and an internal standard, methylated heptadecanoic acid (C17:0) (10 mg/ml hexane) (Sigma Chemicals Co.). Approximately 1 µl of internal standard was mixed with the algal oil samples to achieve a total injection volume of 2 µl.

CHAPTER THREE

RESULTS AND DISCUSSION

3.1 Growth dynamics of algal cultures

3.1.1 Cell density

Typically the axenic growth of algal cultures can be represented in five phases; the lag phase, exponential or logarithmic phase, growth decline phase, stationary phase and death phase. As shown by growth curve representations (Figures 3.1 and 3.2), from day 0 to 4, propagation began with relatively slow growth as seen by the smaller increments in cell number. Initially when introduced to an environment, algal cells display the growth phase known as the lag or induction phase which is associated with the physiological adaptation of the cells with regard to their metabolism. Within this adjustment period, enzymes and metabolites required for cell division increase, as is the case involving other cellular processes. The duration of this phase is dependent on several factors including inoculum size and time required for the synthesis of new enzymes essential to metabolize substrates present in the medium.

The logarithmic phase of the cultures was characterized by an exponential increase in the number of cells per unit time. In this phase, cell density can be expressed as a function of time t in accordance with the logarithmic function

(<http://www.fao.org/docrep/003/w3732e/w3732e06.htm>):

$$C_t = C_0 \cdot e^{mt}$$

Where, C_t and C_0 express the cell concentrations at time t and 0 , respectively and m expressing the growth rate which is primarily dependent on the species, temperature and light intensity. Without any hindrance, growth can occur at a constant doubling rate as to increase the cell number and population at each consecutive time period. The ecological adaptation of the test species can be best analyzed within this phase especially when in an experimental environment. Completion of the exponential growth phase (day 14) is brought about by the onset of nutrient depletion and consequent waste accretment.

Within the period of 14 - 32 days and 14 - 28 days of growth for *Chlorella vulgaris* and *Dunaliella primolecta*, respectively, the inhibitory environment impedes a further elevation in cell number, resulting in a phase of decline, followed by a levelling out of the growth response curve. This relatively constant value is due to the increasing rate of algal growth which is counteracted by the mortality rate. During this period, the number of dead cells which had consequently taken up methylene blue greatly increased (Figures 3.1 and 3.2). In addition to nutrient depletion which leads to the stationary phase, the accumulation of toxic by-products may also impede active growth. Progression of the stationary phase results in the death phase in which the conditions become detrimental to the survival of cells. At the onset of the death phase, algal cells were immediately harvested (2.4) to alleviate further decline in the cell number. It is also known that the stored lipids are most abundant when in the advanced stationary phase (Lv *et al.*, 2010). However, in the case of *D. primolecta*, clumping of cells occurred at approximately 28 days of growth in BG11 test media, hence all experimental procedures (2.3) were terminated as cell counting proved to be cumbersome and difficult to achieve reliable counts. In spite of this, the stationary phase was still assessed using optical density reading at 680 nm and sufficient oil was extracted from *D. primolecta* cells to enable further analyses. The precise causes of clumping in this flagellated microalga require further investigation. In yeast, similar clumping or "flocculation" may be influenced by cell outgrowths called fimbriae which provide functional groups implicated in Ca^{2+} - bridges between cell aggregates (pers.comm. Gupthar, A. S. 2012).

No visible growth pattern was observed with the control algal cultures. The exclusion of nitrates from the media correlated with adverse growth involving both *C. vulgaris* and *D. primolecta* (Figures 3.1 and 3.2). As nitrogen is the primary source of the metabolic activities of the cell, it is therefore evident that algae are “stressed” when exposed to nitrogen - limiting conditions (Bigogno *et al.*, 2002; Qin, 2005; Guschina and Harwood, 2006; Khozin - Goldberg and Cohen, 2010; Lv *et al.*, 2010). *Dunaliella tertiolecta* showed loss of cell protein and chlorophyll when grown in nitrogen - deficient conditions which subsequently affected both the photosynthetic rate and cell division (Geider *et al.*, 1993).

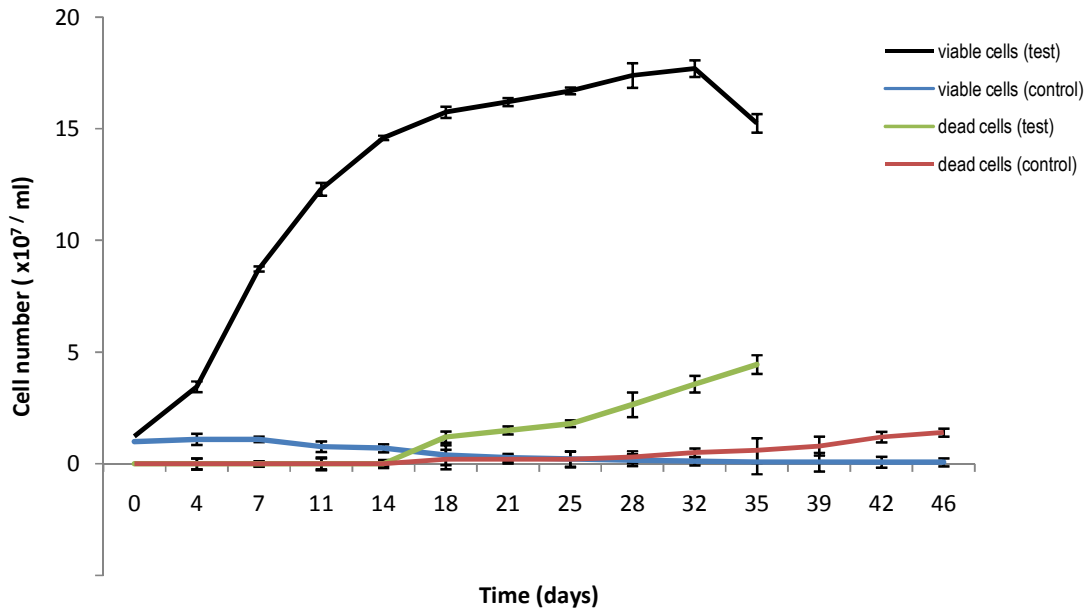


Figure 3.1. Cell density (cells/ml) of *Chlorella vulgaris* growth in BG11 test and BG11 nitrate deficient control media over time (days).

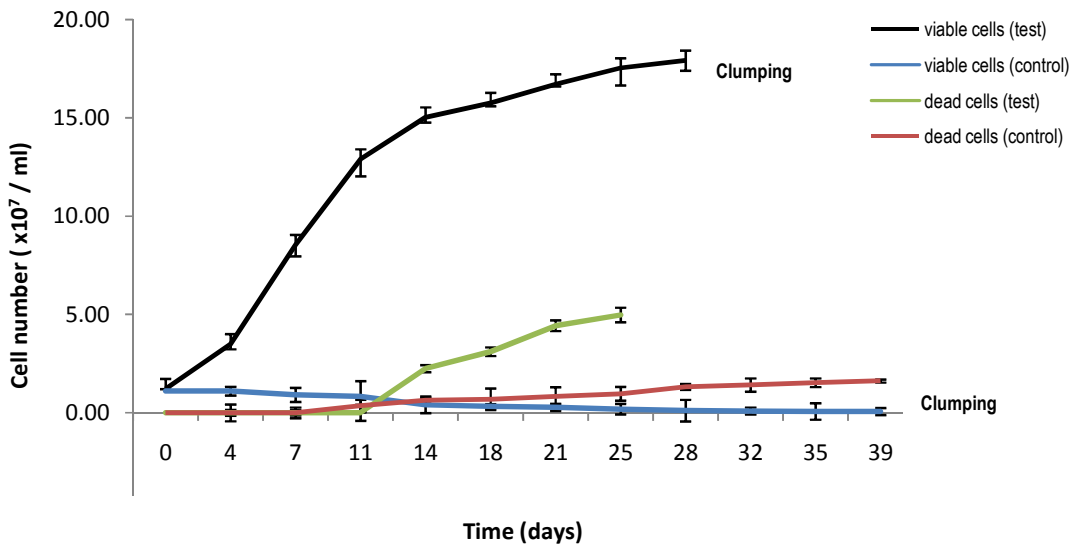


Figure 3.2. Cell density (cells/ml) of *Dunaliella primolecta* growth in BG11 test and BG11 nitrate deficient control media over time (days).

3.1.2 Optical density

In keeping with the trend of the algal growth phases (3.1.1) the turbidity measured at OD_{680 nm} was directly proportional to the cell number. Figures 3.3 and 3.6 reveal that the test cultures displayed the most turbidity during the logarithmic phase owing to the exponential growth of cells. On the basis of the data generated by the control cultures, no significant pattern of growth could be detected or linked to increases in turbidity. The deficiency of nitrates correlated with “stress” among algal cultures and inability to grow actively. Regression equations (R^2) were established for plots OD_{680 nm} versus cell density. Theoretically, the aforementioned equation is utilized in order to determine the relationship, if any, between the X and Y axes. A non - linear relationship is evident by a regression value closer to 0.0 and a horizontal best - fit line that passes through the mean of all the Y values. Conversely, a value closer to 1.0 and a best - fit line, which passes through all the points to form a straight line graph with no evidence of scatter, represents a directly proportional relationship between the X and Y axes. The regression values of the plots of OD_{680 nm} versus cell density (Figures 3.4 - 3.8) were close to 1.0 indicating a virtual proportional relationship.

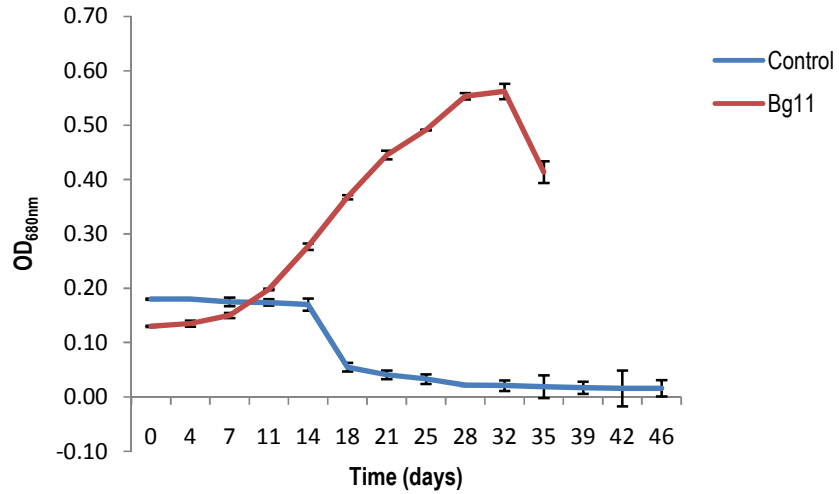


Figure 3.3. Optical density of *Chlorella vulgaris* growth in BG11 test and BG11 control media.

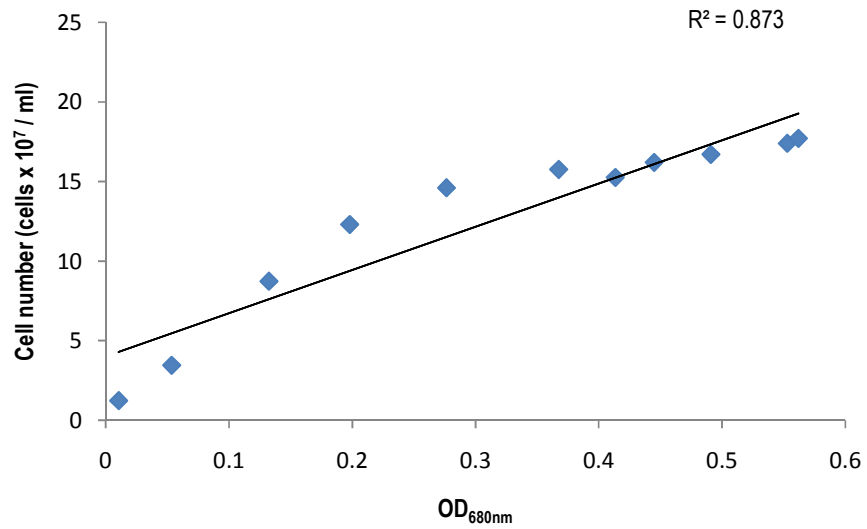


Figure 3.4. Relationship between OD_{680nm} and algal cell count (cells/ml) of *Chlorella vulgaris* grown in BG11 test medium.

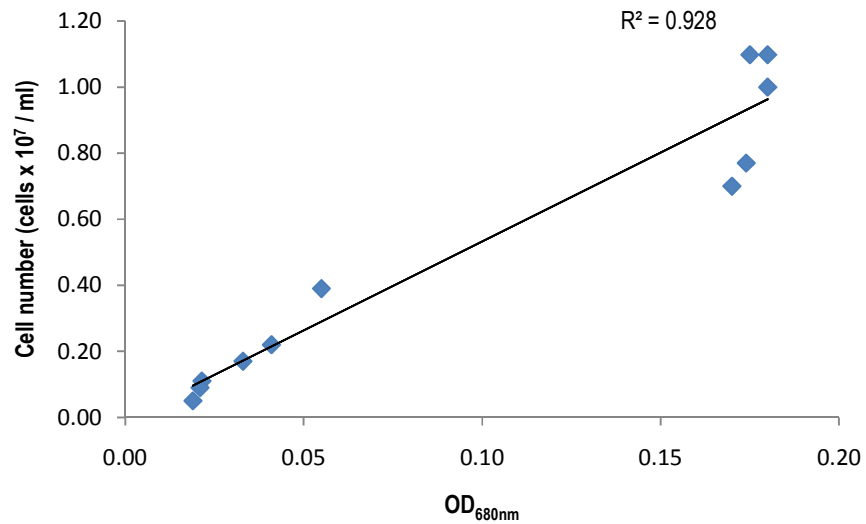


Figure 3.5. Relationship between OD_{680nm} and algal cell density (cells/ml) of *Chlorella vulgaris* grown in BG11 control medium.

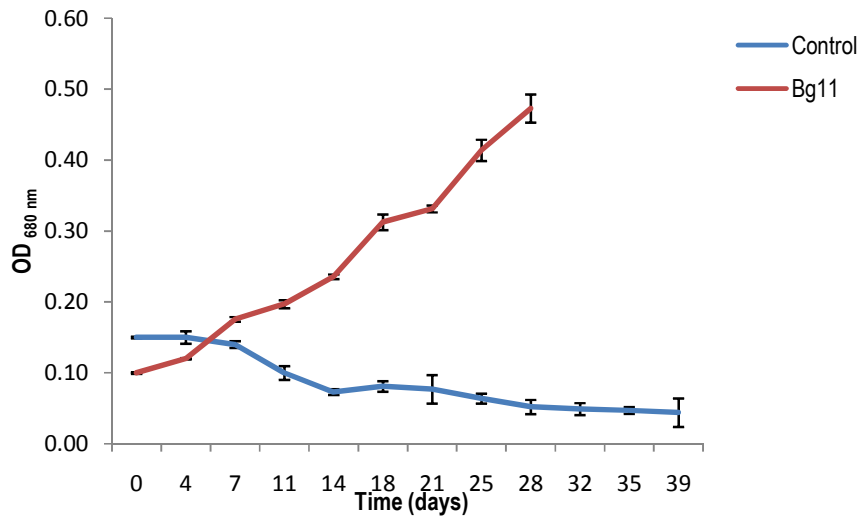


Figure 3.6. Optical density of *Dunaliella primolecta* grown in BG11 test and BG11 control media.

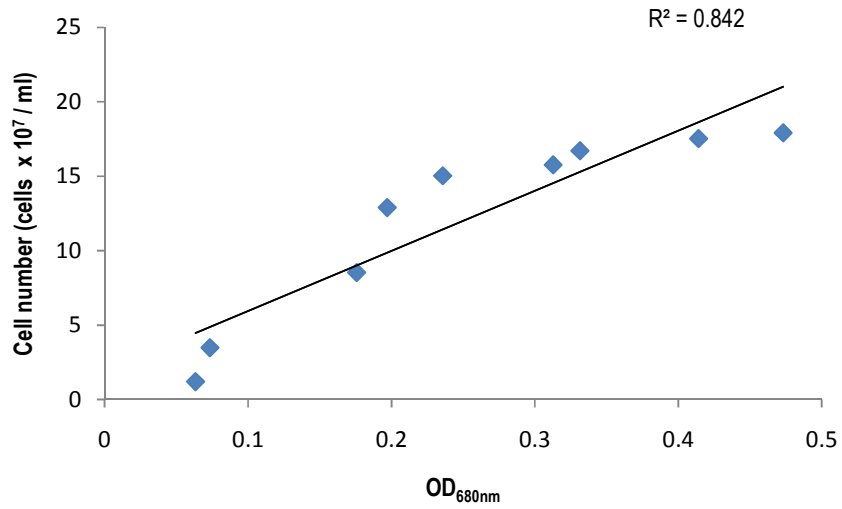


Figure 3.7. Relationship between OD_{680nm} and algal cell count (cells/ml) of *Dunaliella primolecta* grown in BG11 test medium.

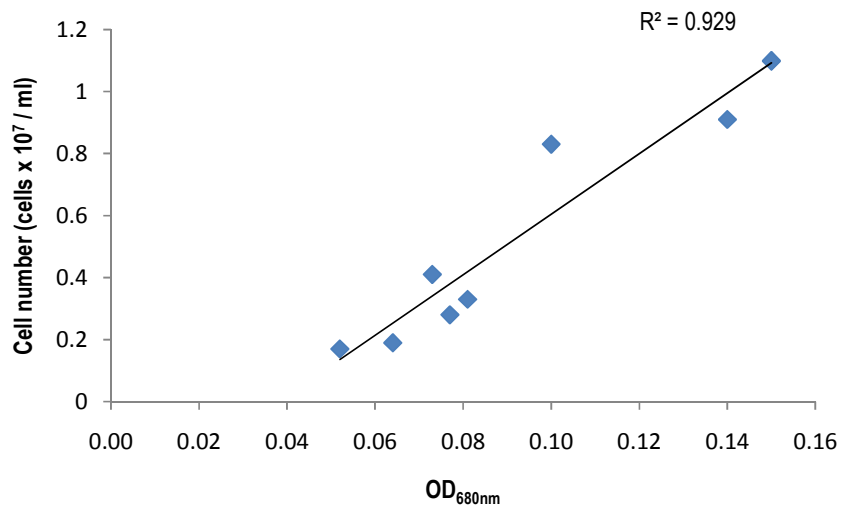


Figure 3.8. Relationship between OD_{680nm} and algal cell count (cells/ml) of *Dunaliella primolecta* grown in BG11 control medium.

3.1.3 Biomass determination

Biomass of *C. vulgaris* and *D. primolecta* freeze - dried cultures were determined in triplicate. Photoautotrophic propagation of the algae produced average biomass yields of 0.15 g and 0.18 g for *C. vulgaris* and *D. primolecta* test cultures (Tables 3.1 and 3.2), respectively. Growth is dependent on the utilization of energy for the conversion of CO₂ into biomass. In this instance natural sunlight served as the sole source of energy without added glucose to promote rapid growth. In addition, it is known that algae utilize approximately 10 % of sunlight (Golueke and Oswald, 1968). These yields were sufficiently high to enable oil extraction (2.8) from the algae, given that the laboratory conditions of growth were different from that of the natural habitat.

A relatively high doubling time generally corresponds to a low specific growth rate. The average doubling time for green algae is 24 hours, corresponding to an average growth rate (μ) of 0.69 day⁻¹. For Cyanobacteria, the average doubling time is 17 hours and the corresponding average growth rate (μ) is 0.96 .day⁻¹ and for other taxa approximately 18 hours and a corresponding growth rate of 0.92 .day⁻¹. The average doubling time calculated for Chlorophyta and other taxa with regard to growth rate all lie in the range 7 to 8 hours ($\mu = 2.08 - 2.38$ day⁻¹). In the case of species being grouped according to culture environment rather than taxa, no dominant trend in growth rates or lipid contents is seen. The average doubling time for marine or saltwater species is 19 hours ($\mu = 0.88$ day⁻¹), whilst freshwater species is 20 hours ($\mu = 0.83$ day⁻¹) (Griffiths and Harrison, 2009). In this study, growth rates were not followed as the emphasis was biomass collection in the stationary phase of growth. However, it was evident from cell counts that the stressed nitrate - limiting conditions did slow the rate of growth (Figures 3.5 and 3.6). However, there is no correlation that increased cell density of the cultures yields a higher biomass (Figures 3.1 and 3.2; Tables 3.1 and 3.2). The determination of cell density proved to be difficult as cell clumping was especially prevalent in *D. primolecta* cultures. In this study, the determination of “biomass” reveals the measure of the constant mass of freeze dried cells (2.4.1). The total mass of different metabolites produced in these cells by the algae, as a result of the different growth conditions, may account for the lack of correlation between increased “cell density” and “biomass yield”.

According to Cheng and Ogden (2011), nitrogen - limiting conditions impose stimulation in the production of lipids. For green algae, nitrogen deprivation has been reported to increase lipid content, with the exception of *Chlorella sorokiniana* which show similar trends (Griffiths and Harrison, 2009). *Dunaliella salina* was shown to produce lipids reaching a maximum as high as 450 mg lipid/litre culture, as a result of high biomass growth. This halophilic marine microalga shows great potential to provide large quantities of hydrocarbons which contribute to biodiesel production (Weldy and Huesemann, 2007). In this study, the yields obtained for the controls of *C. vulgaris* and *D. primolecta* cultures (Tables 3.1 and 3.2) indicate that a higher biomass generates a greater oil yield (Tables 3.3 and 3.4).

Table 3.1. Biomass yield recorded from test and control cultures of *C. vulgaris*

Sample number	Test	Control
	Biomass (g)	Biomass (g)
1	0.12	0.18
2	0.19	0.14
3	0.15	0.19
Average ± SD	0.15 ± 0.035	0.17 ± 0.027

SD: standard deviation

Table 3.2. Biomass yield recorded from test and control cultures of *D. primolecta*

Sample number	Test	Control
	Biomass (g)	Biomass (g)
1	0.16	0.26
2	0.19	0.39
3	0.18	0.43
Average ± SD	0.18 ± 0.015	0.36 ± 0.089

SD: standard deviation

Although the oil yields of the control cultures were higher than that of the test cultures, this increment appeared more apparent with *D. primolecta* cultures than *C. vulgaris* (Tables 3.3 and 3.4). This could probably suggest that the growth conditions, especially the salt composition of BG 11 media, were more conducive for the propagation of *D. primolecta* as it is a saltwater

species, compared with the freshwater alga *C. vulgaris*. Complete characterization of the photosynthetic apparatus of *Dunaliella tertiolecta*, in response to nitrogen - deficient conditions, has been demonstrated by LaRoche *et al.* (1993). This limitation in the growth environment of the alga leads to alterations in its photosynthetic efficiency, which decreases as is shown by a lower biomass yield, and pigment composition. It has also been reported that cell size increases under nitrogen - depletion conditions (Rabbani *et al.*, 1998).

3.1.4 pH

In the initial period (0 - 7 days) of the growth cycle when *C. vulgaris* and *D. primolecta* were first introduced to BG 11 test and BG 11 control media, the pH of the cultures remained unchanged at 7.4 (Figures 3.9 and 3.10). Thereafter an increment in the pH of the test algae was observed suggesting that the cultures produced waste products of an alkaline nature. The control cultures displayed a trend opposite to that of the test algae in that the pH decreased. Currently, there is no published literature to explain the decline in pH of the control cultures. However, it can be speculated that the nitrate deficiency prompted the accumulation of more acidic metabolites. The deficiency of nitrates in the control media imposed greater stringency for survival. Cell death appeared to be more prominent as a direct result of the depletion of available nitrogen resources (Figures 3.1 and 3.2).

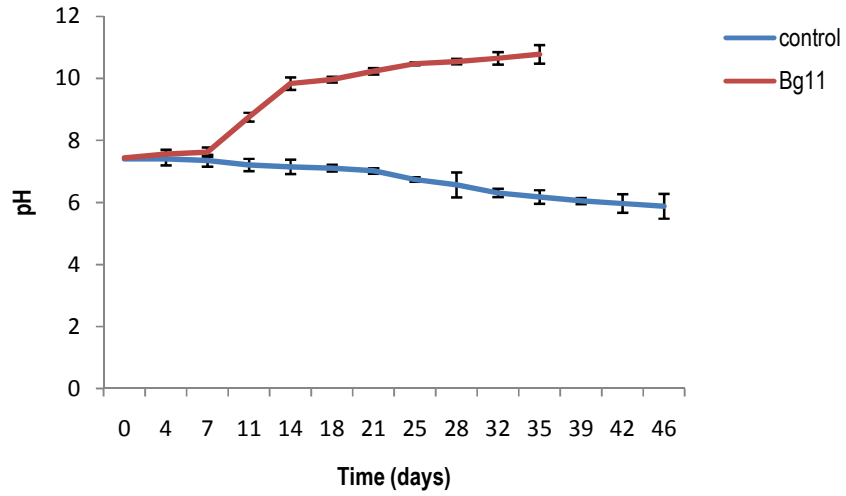


Figure 3.9. Changes in pH of *Chlorella vulgaris* cultivation in BG11 test and BG11 control media.

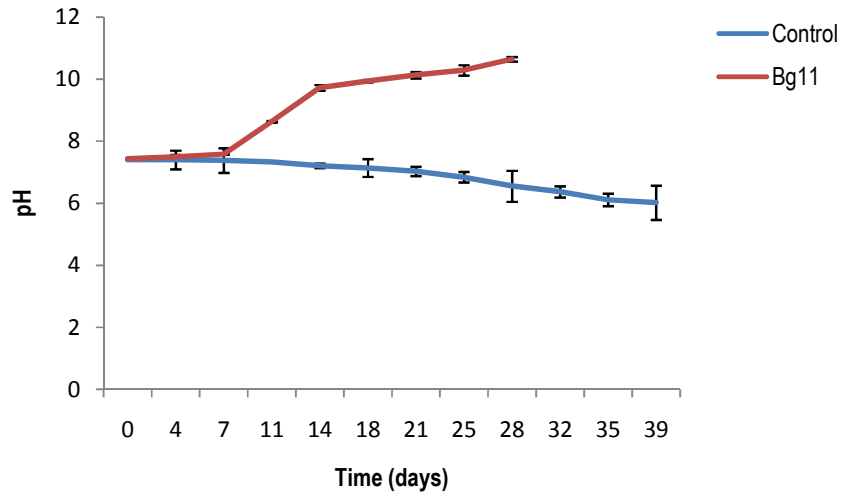


Figure 3.10. Changes in pH of *Dunaliella primolecta* cultivation in BG11 test and BG11 control media.

3.2 Analyses of the oil - hydrocarbon fraction

3.2.1 Determination of oil - hydrocarbon mass

Microalgal enzymes and pathways that trigger and control the accumulation of storage triacylglycerol (TAG) have not been well established at the molecular level. The first genetic engineering effort to manipulate algal lipid production was conducted in the diatom *Cyclotella cryptica* and this was accomplished by over - expressing the endogenous gene encoding acetyl - CoA carboxylase (ACCase) (Khozin - Goldberg and Cohen, 2010). Initially it was demonstrated that an increase in ACCase activity played an important role in the induction of TAG accumulation in cells of the aforementioned nutrient - deprived alga. However, an over - expression of ACCase did not have a significant effect on lipid synthesis in either *C. cryptica* or another diatom, *Navicula saprophila*. Nitrogen depletion induces ultra - structural changes in the cells of *Chlamydomonas reinhardtii* such as the reduction of stacked thylakoid membranes. This is accompanied by the accumulation of starch granules (Wang *et al.*, 2009) and the appearance of lipid droplets or oil bodies in such cells (Khozin - Goldberg and Cohen, 2010).

In cultures where nutrients are abundant, linolenic acid (C18:3) constitutes 33.2 % of the weight of the cells of *C. vulgaris*, whilst in nitrogen - starved cells it makes up 39.6 % (Chen *et al.*, 2010). In keeping with literature reports that nitrogen - deficient conditions promote an increase in oil production, the hydrocarbon - oil yields obtained from the control cultures were higher than that of the cultures grown in BG11 medium (Tables 3.3 and 3.4). *C. vulgaris* and *D. primolecta* control cultures yielded hydrocarbon - oil masses of 0.0040 g and 0.0051 g, respectively, with the latter alga producing double the amount of oil - hydrocarbon in a nitrate deficient environment rather than when grown in nitrate enriched BG 11 medium (Tables 3.3 and 3.4). *C. vulgaris*, being a freshwater chlorophyte, displayed a lower biomass yield and hence, only a slight increment in the oil - hydrocarbon production when exposed to nitrogen - depleted conditions (3.1.3). The overall yields of both algae were relatively low; however, cultivation was conducted in a photoautotrophic environment without an added carbon source to enhance growth (3.1.3). Lv *et al.* (2010) reported that cells are known to adapt themselves at

the time of inoculation to an unfamiliar environment and may not assimilate nutrients. This suppresses cell division but promotes lipid accumulation.

3.2.2 Oil - hydrocarbon yield

Don - Hee *et al.* (1998) reported that oil - hydrocarbon production in *Dunaliella salina* displays a close relation to the growth stages of cultivation. Crude oil - hydrocarbon levels remain constant irrespective of a decline in the cell density. When exposed to a 12:12 light/dark cycle, cell growth and oil - hydrocarbon production were shown to increase during the light phase, followed by a subsequent decrease in the dark period.

In this study, the amount of oil - hydrocarbon extracted was greater under nitrogen - depleted BG 11 medium; as yields were 0.02 % and 0.01 % higher than that recorded from BG 11 growth media for *C. vulgaris* and *D. primolecta*, respectively (Tables 3.3 and 3.4). According to Volova *et al.* (2003), the greatest content of intracellular oil - hydrocarbons, making up 12 - 13 % of cell weight, in a *Botryococcus sp.* corresponded to a physiologically active state of culture at the end of the exponential growth phase and the onset of the phase of decline.

Table 3.3. Oil - hydrocarbon yield of *C. vulgaris* test and control cultures

Sample number	Test culture			Control culture		
	Oil - hydrocarbon mass (g)	Biomass (g)	Oil - hydrocarbon (%)	Oil - hydrocarbon mass (g)	Biomass (g)	Oil - hydrocarbon (%)
1	0.0038	0.12	3.17	0.0028	0.18	1.55
2	0.0055	0.19	2.895	0.0052	0.14	3.71
3	0.0018	0.15	1.20	0.0039	0.19	2.05
Average ± SD	0.0037 ± 0.002		2.42 ± 1.067	0.0040 ± 0.001		2.44 ± 1.131

SD: standard deviation

Table 3.4. Oil - hydrocarbon yield of *D. primolecta* test and control cultures

Sample number	Test culture			Control culture		
	Oil - hydrocarbon mass (g)	Biomass (g)	Oil - hydrocarbon (%)	Oil - hydrocarbon mass (g)	Biomass (g)	Oil - hydrocarbon (%)
1	0.0014	0.16	0.875	0.0036	0.26	1.38
2	0.0028	0.19	1.47	0.0035	0.39	0.90
3	0.0033	0.18	1.83	0.0082	0.43	1.91
Average \pm SD	0.0025 \pm 0.001		1.40 \pm 0.483	0.0051 \pm 0.003		1.41 \pm 0.505

SD: standard deviation

3.3 Thin layer chromatography (TLC) and spectrophotometry

Constituents of algal oil - hydrocarbon samples were separated by TLC, and identified tentatively using standards, where available, and a lipid manual (Gurr and James, 1980). The solvent *n* - hexane - diethyl ether - acetic acid (35:15:0.5 v/v/v) which is capable of resolving ordinary and α - hydroxyl fatty acids (Heftmann, 2004), was used successfully in this study to achieve separation of various oil components (Figure 3.11). For the visualization of the separated lipids, the use of iodine vapour and sulphuric acid, followed by charring (2.6.1) enabled detection of low quantities of various components. Iodine vapour is suggested to have a high affinity for unsaturated and aromatic compounds (Schneiter and Daum, 2006), including the large amounts of polyunsaturated fatty acids found in algal oils (Carvalho and Xavier Malcata, 2004). Positive standards for the microalgal carotenoid and chlorophyll species were not available to enable a comparison involving the cell extracts of both components.

The lipid composition of algae is associated with both the structural integrity and physiological nature of the organism. This includes the functionality of the membrane - embedded assembly associated with the photosynthetic electron transport system in thylakoids or mitochondrial respiration. (Vieler *et al.*, 2007). The dominant lipid class of diatoms under light limitation is known to be monogalactosyldiacylglycerol (MGDG), which is present exclusively in chloroplasts, particularly in thylakoid membranes. Digalactosyldiacylglycerol (DGDG) and sulfoquinovosyldiacylglycerol (SQDG) are also restricted to chloroplasts, whereas

phospholipids also occur in non - chloroplast membranes (Mock and Kroon, 2002). In the green alga, *Chlamydomonas reinhardtii*, the lipids phosphatidylcholine (PC) and phosphatidylserine (PS) are not present in their membranes. The predominant membrane is a betaine lipid, diacylglyceryltrimethylhomoserine (DGTS). Guschina and Harwood (2006) reported a very high content of eicosapentaenoic acid (EPA) in the marine green alga, *Chlorella minutissima*. As a result of this high content, EPA is found at the *sn* - 1 and *sn* - 2 positions of DGTS, in contrast to the asymmetric distribution in other algae. In this chlorophyte, PC was the dominant phospholipid and the level of DGTS showed a marked rhythmic fluctuation with time which was inversely correlated with the level of MGDG, the other major lipid in this alga. Analysis of the thin layer chromatograms, in this study, showed different compounds and migration patterns between the test and control algal extracts. Some of these compounds could be identified tentatively using the standards listed, and guidelines presented by Gurr and James (1980) although published literature on oil - hydrocarbon extracts from microalgae grown in nitrate - deficient media is limited.

The spectra presented (Figures 3.12 - 3.15) reveal λ_{\max} for chlorophyll fractions of both algae which were detected close to 665 nm. The intensity of the peak generated was not as elevated as expected, probably due to the content of the present chlorophyll and low concentration extracted. Chlorophyll content is adversely affected by depletion in nitrogen as the pigment is structurally arranged to contain four nitrogen atoms which becomes cumbersome for the cells to synthesize in the presence of low nitrogen concentrations (Pisal and Lele, 2005). However, the spectra generated for chlorophyll fractions of test media were similar for both algae (Figures 3.12 and 3.13) and comparable with the spectra produced under stress conditions (Figures 3.14 and 3.15). Likewise, the carotenoid spectra generated (Figures 3.12 - 3.15) reveal peaks close to 665 nm. However, as per literature the aforementioned peaks have been shown to occur at 663 nm (Garcia *et al.*, 2007). Under nitrogen deficient conditions, *Dunaliella sp.* cultures have shown to yield higher peaks as a result of the excessive formation of free radicals under stress (Ben - Amotz *et al.*, 1989; Pisal and Lele, 2005). β - carotene contains antioxidant properties known to quench free radicals, restoring physiological balance. Additional β - carotene is synthesized for the protection of the cells and the continuation of cell growth. Hence, the concentration of the aforementioned pigment is markedly increased in the case of nitrogen deficiency (Pisal and Lele, 2005). This was not quantified in the current study.

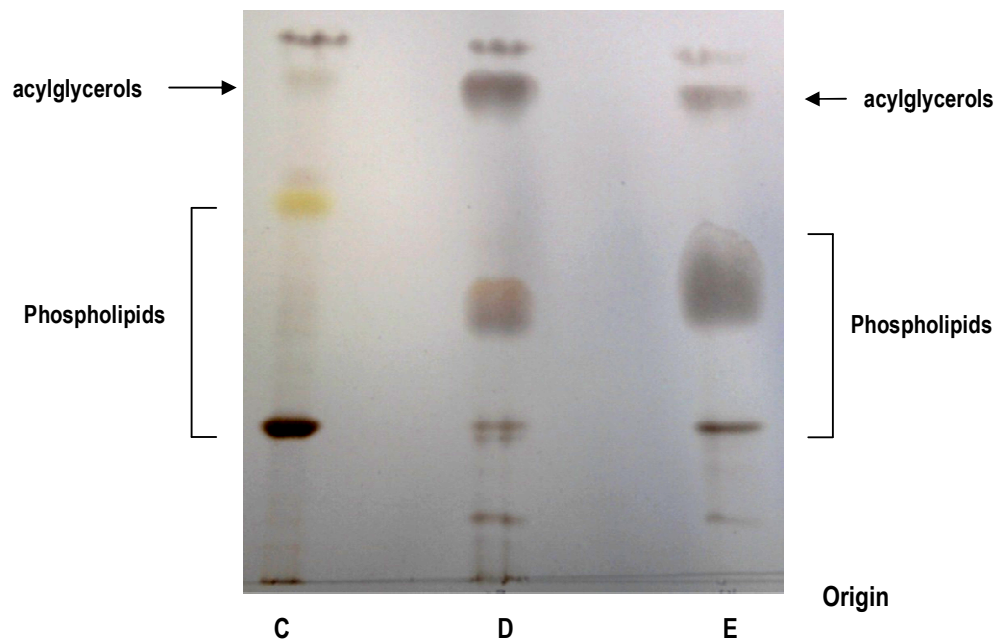
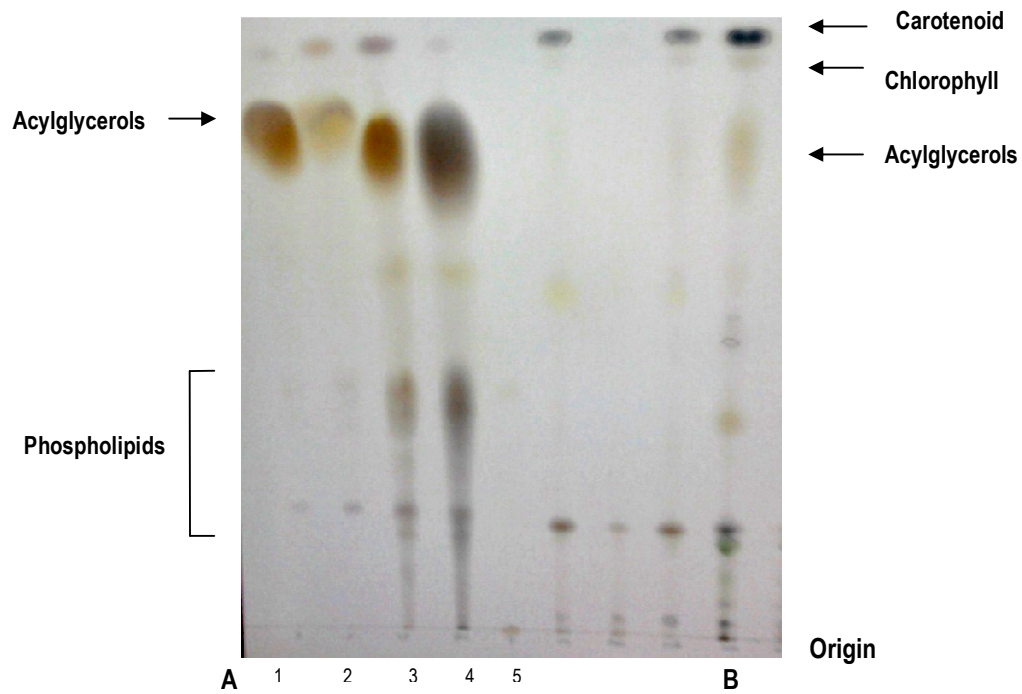


Figure 3.11. TLC image showing separation of lipids. **A:** Standards 1 - 5 (sunflower oil, olive oil, evening primrose oil, salmon oil, DOPE [R - L]); **B:** *Dunaliella primolecta* algal oil in hexane (test); **C:** *Chlorella vulgaris* algal oil in hexane (test); **D:** *Dunaliella primolecta* algal oil in hexane (control); **E:** *Chlorella vulgaris* algal oil in hexane (control).

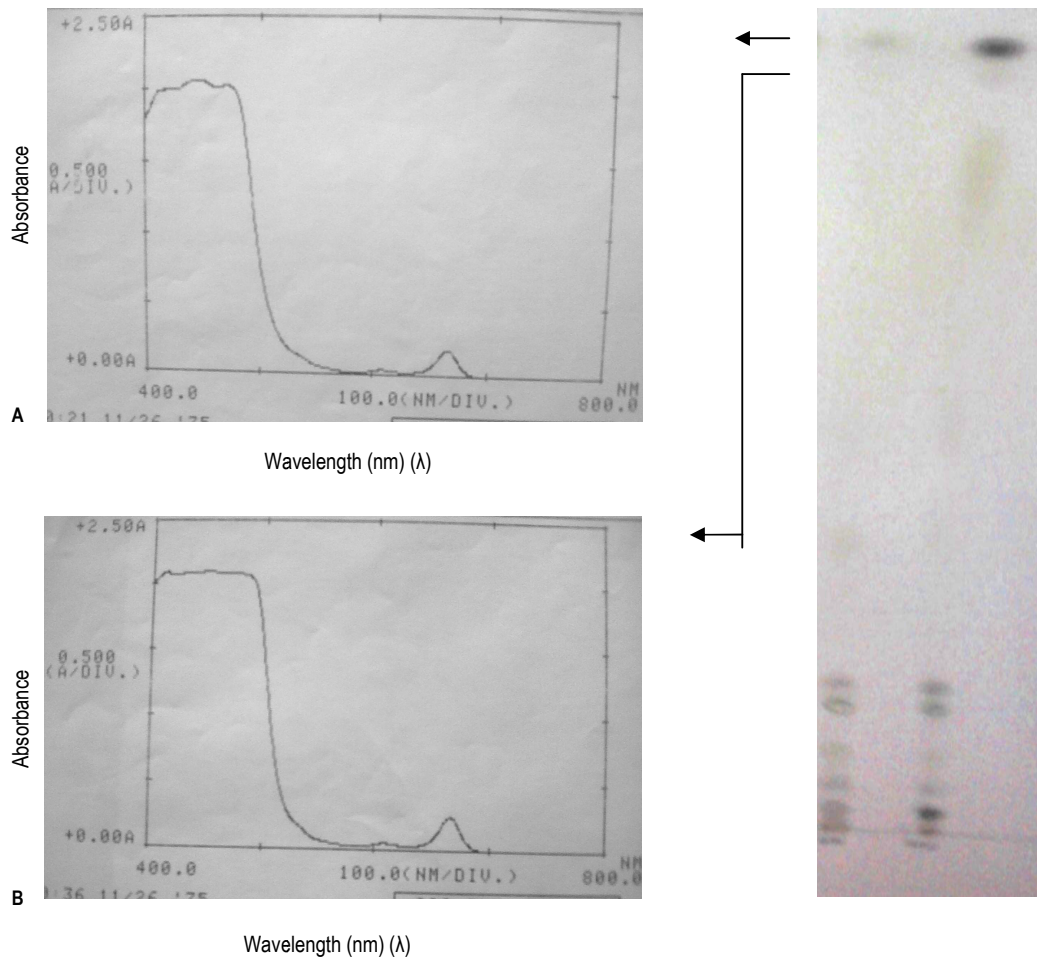


Figure 3.12. TLC image showing, *Dunaliella primolecta* algal oil (test) extracted in acetone (left) and methanol (right) with corresponding spectra of carotenoid (A) and chlorophyll (B) fractions, respectively.

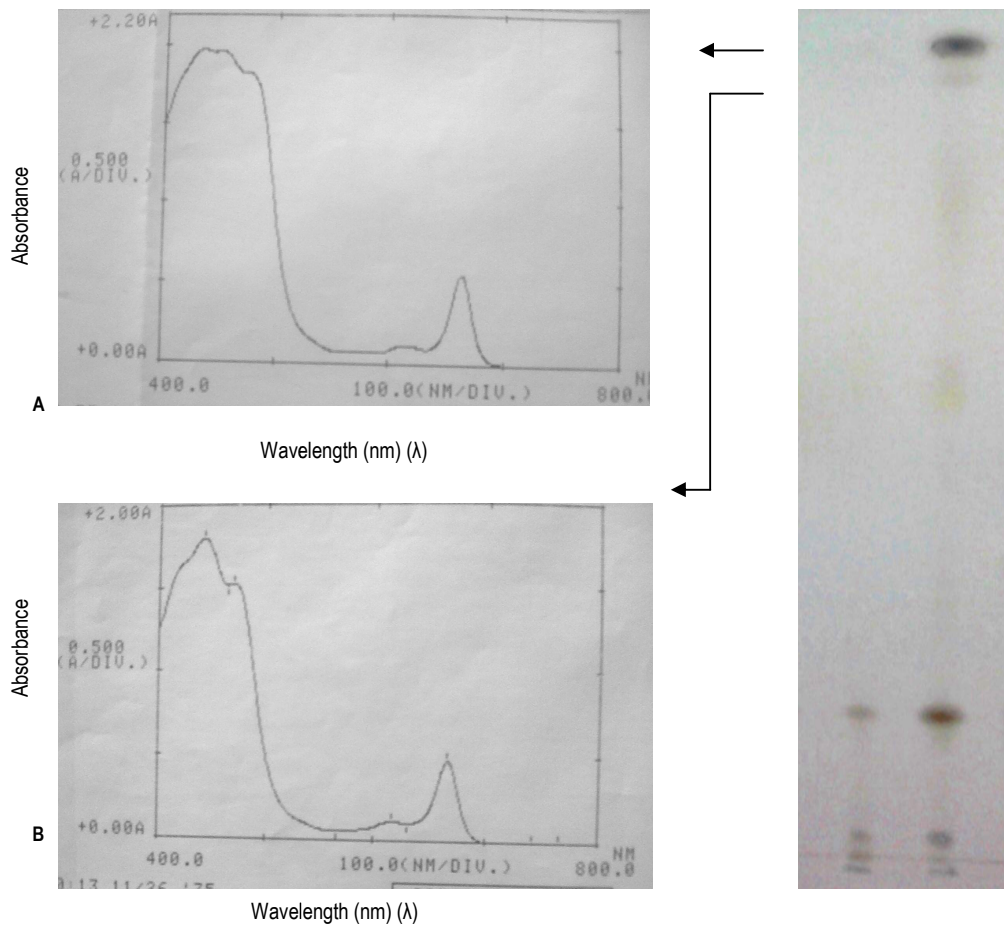


Figure 3.13. TLC image showing *Chlorella vulgaris* algal oil (test) extracted in acetone (left) and methanol (right) with corresponding spectra of carotenoid (A) and chlorophyll (B) fractions, respectively.

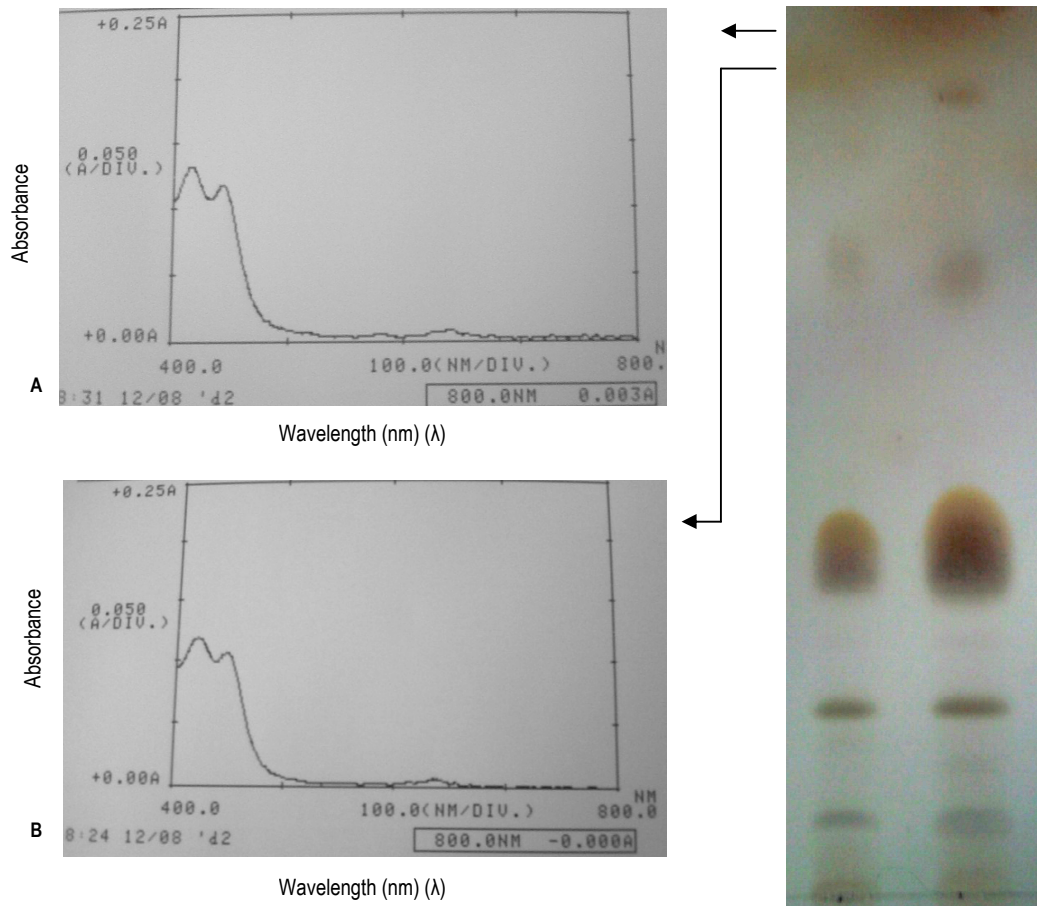


Figure 3.14. TLC image showing *Chlorella vulgaris* algal oil (control) extracted in acetone (left) and methanol (right) with corresponding spectra of carotenoid (A) and chlorophyll (B) fractions, respectively.

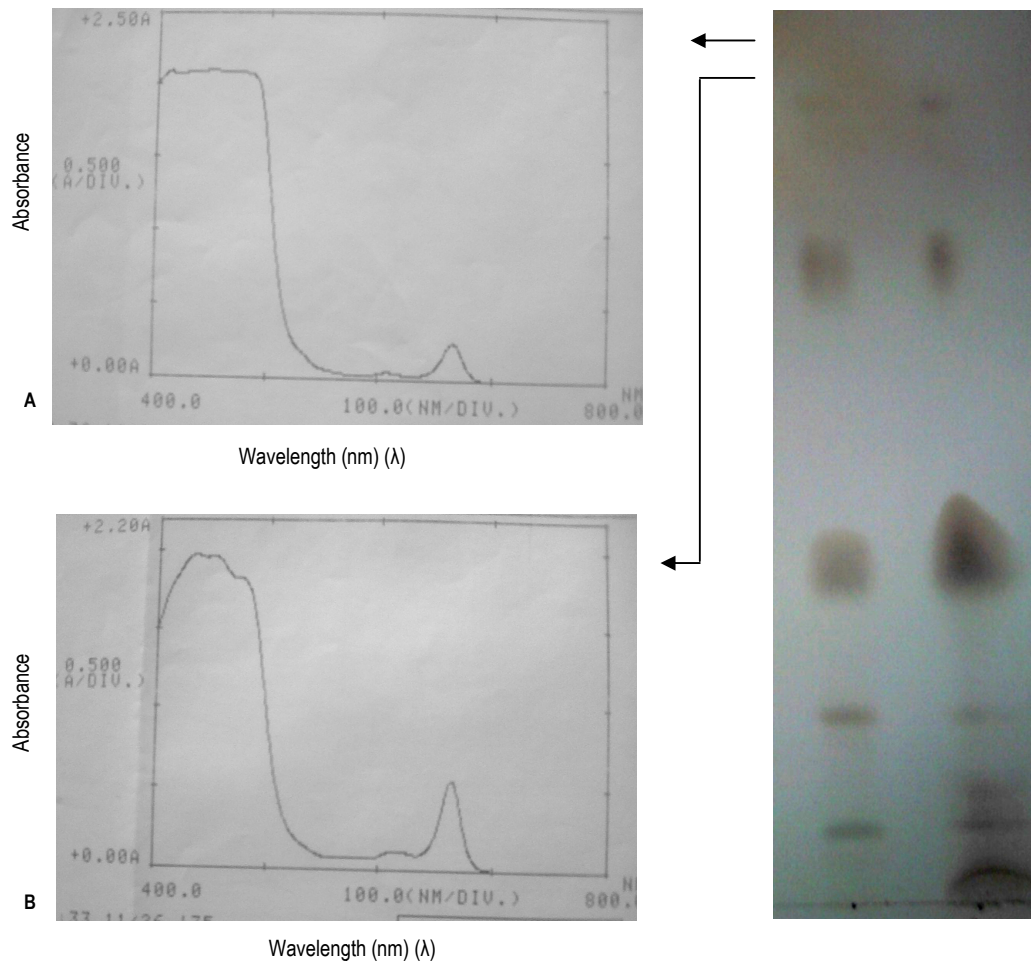


Figure 3.15. TLC image showing *Dunaliella primolecta* algal oil (control) extracted in acetone (left) and methanol (right) with corresponding spectra of carotenoid (A) and chlorophyll (B) fractions, respectively.

3.4 Protein profiling

3.4.1 Protein quantification

The approximate quantity of protein present in the algal oil - hydrocarbon extract was estimated using the Bio - Rad RC - DC kit and bovine serum albumin (BSA) to construct standard curves (Figures 3.16 - 3.19). Curves were also generated, accommodating SDS and/or urea as these substances could possibly act as interfering agents (2.8.1). As per the RC - DC protein kit, the protein concentrations (Tables 3.5 and 3.6) were as extrapolated from the respective standard curves (Figures 3.16 - 3.19) which showed differences due to supplements of either SDS or urea or both.

Table 3.5. Protein concentration of extracted algal oil samples

	Protein concentration ($\mu\text{g}/\mu\text{l}$)			
	BSA standard curve	BSA, SDS standard curve	BSA, Urea standard curve	BSA, SDS, Urea standard curve
<i>C. vulgaris</i> (test)	1.93 ± 0.101	1.95 ± 0.005	1.92 ± 0.008	1.87 ± 0.009
<i>C. vulgaris</i> (control)	1.88 ± 0.112	1.85 ± 0.111	1.74 ± 0.012	1.90 ± 0.010
<i>D. primolecta</i> (test)	1.96 ± 0.140	2.23 ± 0.007	1.91 ± 0.017	1.93 ± 0.151
<i>D. primolecta</i> (control)	1.95 ± 0.009	1.88 ± 0.009	1.94 ± 0.007	1.98 ± 0.143

SD: standard deviation

Values above indicate mean and standard deviation involving triplicate samples

Table 3.6. Protein concentration of extracted oil standards

	Protein concentration ($\mu\text{g}/\mu\text{l}$)			
	BSA standard curve	BSA, SDS standard curve	BSA, Urea standard curve	BSA, SDS, Urea standard curve
Sunflower oil	3.65 ± 0.123	3.71 ± 0.111	3.91 ± 0.143	3.68 ± 0.135
Salmon oil	3.70 ± 0.121	3.73 ± 0.009	3.72 ± 0.136	3.82 ± 0.121

SD: standard deviation

Values above indicate mean and standard deviation involving triplicate samples

For the algal oils, 10 µl of various extracted samples (2.8.1) were loaded per gel in order to attain approximately 20 µg of protein for detection. Likewise, 5 µl of extracted sunflower and salmon oil (2.8.1) were utilized to achieve a similar outcome.

Among microalgae generally, manipulations such as the influence of dissolved nitrogen on the proximate composition of *Dunaliella primolecta* cells can lead to protein content reaching 20 to 50 % of total dry weight (Uriarte *et al.*, 1993). It has been reported that under these conditions, the protein content of *D. primolecta* from outdoor cultures that had not been acclimated to their nutrient regimes decreased from 50 % to 12 %. Following acclimation for three weeks, the minimum content dropped to 8 % and only reached a maximum of 40 % (Uriarte *et al.*, 1993).

3.4.2 Protein composition of the lipidic body

Typically *Chlamydomonas reinhardtii* has been used in several studies relating to the isolation of genes and the identification of proteins involved in the assembly of the lipidic body. Khozin - Goldberg and Cohen (2010) purified a lipid droplet - enriched fraction from the *C. reinhardtii* and identified 16 proteins involved in lipid biosynthesis using mass spectrometry. These included acyl - CoA synthetases and acyltransferases, which play a significant role in the production of lipids and the transfer of acyl groups between the rough endoplasmic reticulum membrane and neutral lipids. A major protein, designated major lipid droplet protein (MLDP) was also isolated and its mRNA abundance appeared to correlate with the accumulation of TAG during the time course of nitrogen deprivation. This hydrophobic protein was recorded as being specific to the green algal lineage of photosynthetic organisms and displayed no similarity to oleosins. The functional significance of MLDPs was further examined by RNAi silencing in which an expression cassette containing the nitrate reductase (*NIT 1*) promoter, inducible by nitrogen starvation, was used in order to drive the expression of an *MLDP* genomic sense cDNA antisense RNAi hairpin. An increment in the average lipid droplet size was observed in the *MLDP* - RNAi lines, but the levels of TAG or rate of TAG mobilization upon nitrogen replenishment rendered no further change; thus indicating a structural role for MLDP in oil - body formation (Khozin - Goldberg and Cohen, 2010). In similar studies conducted by

Moellering and Benning (2010), in which the lipid droplet size was analysed by the RNA interference silencing of an MLDP in the model alga, *C. reinhardtii*; a 27 KDa MLDP was identified as being predominant as it was based on a 10 - fold overabundance of spectral counts for its peptides. The inactivation of MLDP resulted in an increase in lipid droplet size. Despite an extensive screening in transgenic lines, expression of the MLDP gene could be reduced by only approximately 60 % in the best RNAi lines leading to a moderate yet significant increment in the size of the oil droplet of these lines. Repression of MLDP gene expression using this approach led to the changes in lipid droplet size yet no change in TAG content or metabolism was observed.

Prior to subjecting the algal oil samples to SDS - polyacrylamide gel electrophoresis (PAGE) in this study, protein was extracted from sunflower and salmon oils which served as reference samples. The samples were suspended in 10 % SDS, 6 M urea and 10 % SDS - 6 M urea mixture (Wang *et al.*, 2009). Of these, proteins were only detected in extracts treated separately using 10 % SDS and 6 M urea (Figure 3.16). Sunflower oil extracts derived from SDS extraction produced bands of 198, 96, 70 and 58 KDa while urea treatment yielded a band of 200 KDa (Figure 3.16 , lanes D and E). Salmon oil treated with SDS and urea yielded bands of 195, 27 KDa, and 198 KDa respectively, as well as common bands of 68 and 64 KDa (Figure 3.16, lanes B and C). These proteins may be intact or might be a dissociation of subunit structure. However, the combination of extractants SDS and urea, could have possibly been too harsh and may have denatured any protein in the sample, hence accounting for a lack of visible banding patterns (data not shown). Moellering and Benning (2010) used mass spectrometry to identify 259 proteins associated with the lipid droplet of the green alga *Chlamydomonas reinhardtii* but reported on the enrichment of a 27 KDa MLDP which was detected using polyacrylamide gels. In an earlier study, Vechtel and co - workers (1992) isolated among other proteins, 4 discrete polypeptides of 28, 26, 25 and 23 KDa associated with the lipid droplet of *Eremosphaera viridis* which was grown under conditions of nitrogen deficiency. It is evident from the literature that lipid - associated protein varies in different algal oils and may be implicated in the assembly of lipidic bodies.

According to Wang *et al.* (2009), when protein - extracted lipidic bodies of *C. reinhardtii* were run on SDS PAGE gels, two protein bands of 20 and 16 KDa were detected using coomassie blue

staining. However, no discrete bands of *C. vulgaris* or *D. primolecta* were detectable with coomassie blue or silver staining. The electrophoresis conducted in the current study generated smears which suggest that the proteins found in the algal oils lie in the range of 98 - 200 KDa and 200 - 58 KDa for *C. vulgaris* and *D. primolecta* test cultures, respectively (Figure 3.17). For the algae grown in nitrogen - restricted media, these ranges were shown to be 200 - 115 KDa. for the algal oils extracted in SDS and 200 - 95 KDa for the algal oils extracted in urea (Figure 3.18). A possible explanation could be that the proteins were denatured as a result of the harsh treatment of the oils, hence resulting in a smeared banding pattern for the test culture extracts in urea and for the control culture extracts in SDS and urea; and thus the attempt in identifying protein of discrete size present in the algal oils (Figures 3.17 and 3.18) proved difficult. The use of combination extractants SDS and urea gave no results (data not shown).

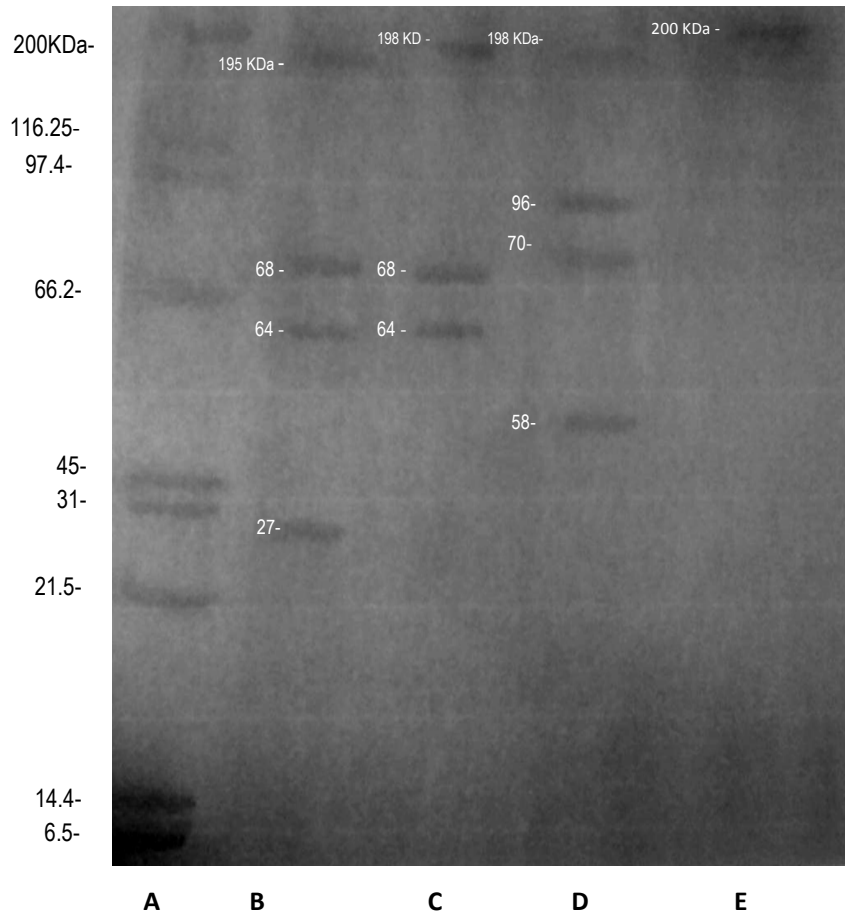


Figure 3.16. SDS PAGE gel: **A:** Bio - Rad protein standards (lane A); **B:** salmon oil extracted with SDS (lane B); **C:** salmon oil extracted with urea (lane C); **D:** sunflower oil extracted with SDS (lane D); **E:** sunflower oil extracted with urea (lane E).

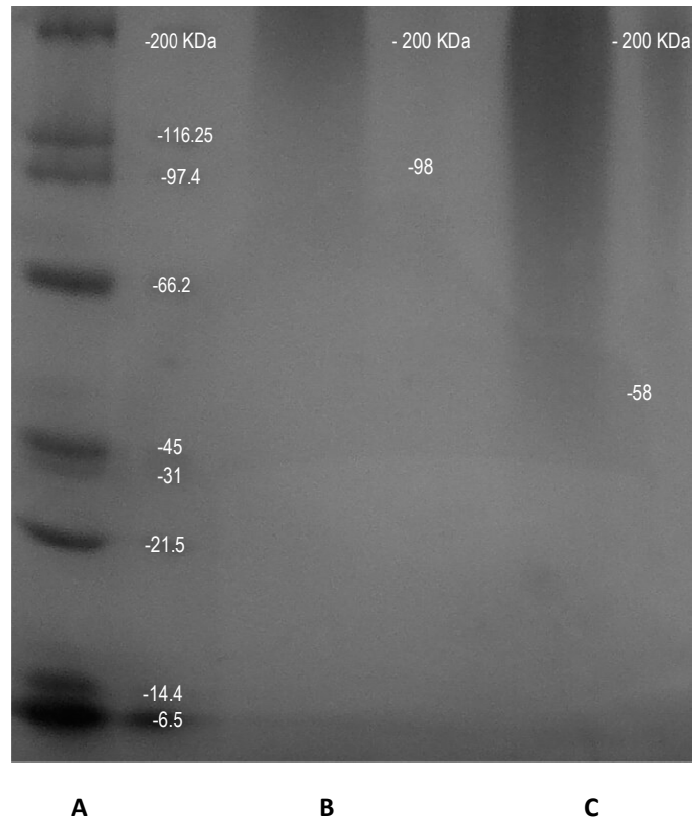


Figure 3.17. SDS PAGE gel: **A:** Bio - Rad protein standards (lane A); **B:** *C. vulgaris* algal oil (test) extracted with urea (lane B); **C:** *D. primolecta* algal oil (test) extracted with urea (lane C).

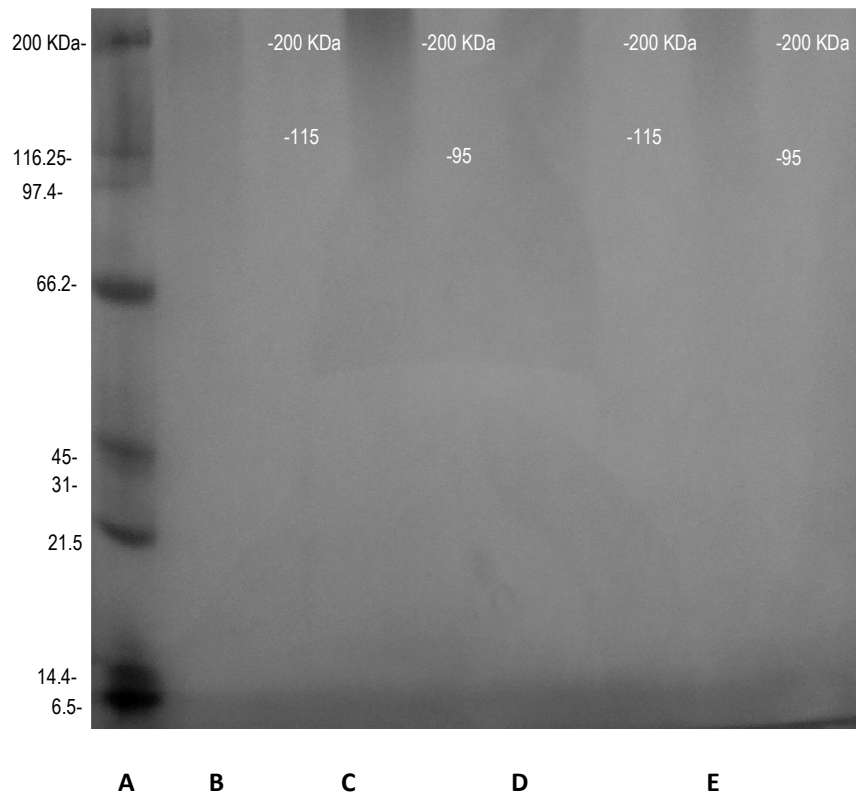


Figure 3.18. SDS PAGE gel: **A:** Bio - Rad protein standards (lane A); **B:** *D. primolecta* algal oil (control) extracted with SDS (lane B); **C:** *D. primolecta* algal oil (control) extracted with urea (lane C); **D:** *C. vulgaris* algal oil (control) extracted with SDS (lane D); **E:** *C. vulgaris* algal oil (control) extracted with urea (lane E).

3.5 Analyses of fatty acid methyl esters (FAMEs) using gas chromatography (GC)

The genus *Chlorella* includes several species that vary in the amount and type of cellular lipids produced. The lipid content in cells of *Chlorella vulgaris*, *Chlorella ellipsoidea* and *Chlorella pyrenoidosa* constitute 14 - 22 , 4.49 and 2 - 11.9 (w/w) %, respectively (Montes D'Oca *et al.*, 2011). Johnson and Wen (2009) reported the heterotrophic microalga, *Schizochytrium limacinum* is capable of producing high levels of biomass and total fatty acid and has the potential of producing the omega - 3 polyunsaturated fatty acid, docosahexaenoic acid (DHA) (C22:6 n - 3). This alga presents a relatively simple fatty acid profile comprising of myristic acid (C14:0), palmitic acid (C16:0), docosapentaenoic acid (C22:5) and docosahexaenoic acid (C22:6) as the major fatty acids.

Marine microalgae are the major producers of omega - 3 PUFAs (polyunsaturated fatty acids), namely EPA (eicosapentaenoic acid) and DHA. The freshwater microalgae predominantly produce saturated or monosaturated fatty acids (Patil *et al.*, 2007), which is known to be the ideal precursor of biodiesel (Khozin - Goldberg and Cohen, 2010). *Dunaliella* spp. produce of 27 - 29 % saturated fatty acids and 71 - 73 % unsaturated fatty acids under conditions of nitrogen deficiency, with linolenic acid being the predominant unsaturated fatty acid (C18:3) (Chen *et al.*, 2010). Analysis of the FAMEs extracted from the algal oils (Table 3.9) in this study revealed that saturated fatty acids were present solely (Table 3.8) in the freshwater alga, *C. vulgaris* when grown in nitrate - deficient medium (Figure 3.20). For the same alga grown in conventional BG 11 medium, 12.5 % of the fatty acids extracted were unsaturated (Table 3.8; Figure 3.19) whilst approximately 87.5 % represented saturated methyl esters. However, the marine alga, *D. primolecta*, displayed unsaturated fatty acid methyl esters of approximately 13.9 % and 7.5 % of those extracted when grown in the test and control media, respectively (Table 3.8). For all the algal cultures, except the *D. primolecta* control culture, the internal standard (C17:0) showed the greatest peak (Figure 3.22) and therefore presented as the predominant fatty acid methyl ester in the mixture of algal oil (Table 3.8). The FAMEs extracted from the algal cultures were shown relative to the internal standard as these were based on

peak area integration. This was expected due to the minute volumes of oil extracted from the algae as a result of the low biomass yields obtained. Analysis of the fatty acid profiles reveal the predominant fatty acid to be palmitic acid (C16:0) (Figure 3.19 - 3.22) in all the algal oil samples subjected to GC analyses (Table 3.9). *D. primolecta* control culture yield approximately 26 % of biodiesel content in the processed oil, a relatively high percentage when compared with the other algal cultures; which exhibited < 7 % biodiesel content. However, these yields are low as Johnson and Wen (2009) reported FAME content as high as 66.37 (m/m) % when producing biodiesel from the microalga *Schizochytrium limacinum* (Johnson and Wen, 2009). A reason for low yields in the production of FAMES in this study correlates with the low algal oil harvests (3.2.2). Listed in Table 3.7 are the names of the FAMES extracted, *n* represents the location of the first double bond from the methyl end of the fatty acid chain along with the carbon number following this notation. The symbols “c” and “t” denote “cis” and “trans”, respectively in unsaturated fatty acids.

Arachidonic acid (AA, 20:4 ω 6) is almost excluded from the lipids of freshwater microalgal species and in most marine species, it does not account for more than a few percent of total fatty acids. The only alga known to produce AA in significant quantities is *Porphyridium cruentum* (Bigogno *et al.*, 2002). Under logarithmic growth, the major PUFA of this alga is EPA, but when exposed to unfavourable conditions, AA accumulates and accounts for 40 % of the total fatty acids. When present, long chain - PUFAs are predominantly located in the polar membranal lipids, whereas TAG (triacylglycerol) generally contains very little PUFAs as side chains (Bigogno *et al.*, 2002).

Using the following equation (Shimadzu application book, volume 4), the fatty acid methyl ester content C in % (m/m) present in the oils can be calculated as follows:

$$C = \frac{(\sum A) - A_{ISTD}}{A_{ISTD}} \times \frac{C_{ISTD} \times V_{ISTD}}{m} \times 100 \%$$

Where,

$\sum A$ total signal area of all methyl esters from C14:0 up to C24:1 (15734000 μ V*s)

A_{ISTD} signal area of the internal standard heptadecanoic acid methyl ester C17:0 (2644200 μ V*s)

C_{ISTD} concentration of the heptadecanoic acid methyl ester in the internal standard solution used (10 mg/mL)

V_{ISTD} volume of the internal standard solution added (5 mL)

m mass of the weighed biodiesel sample (250 mg)

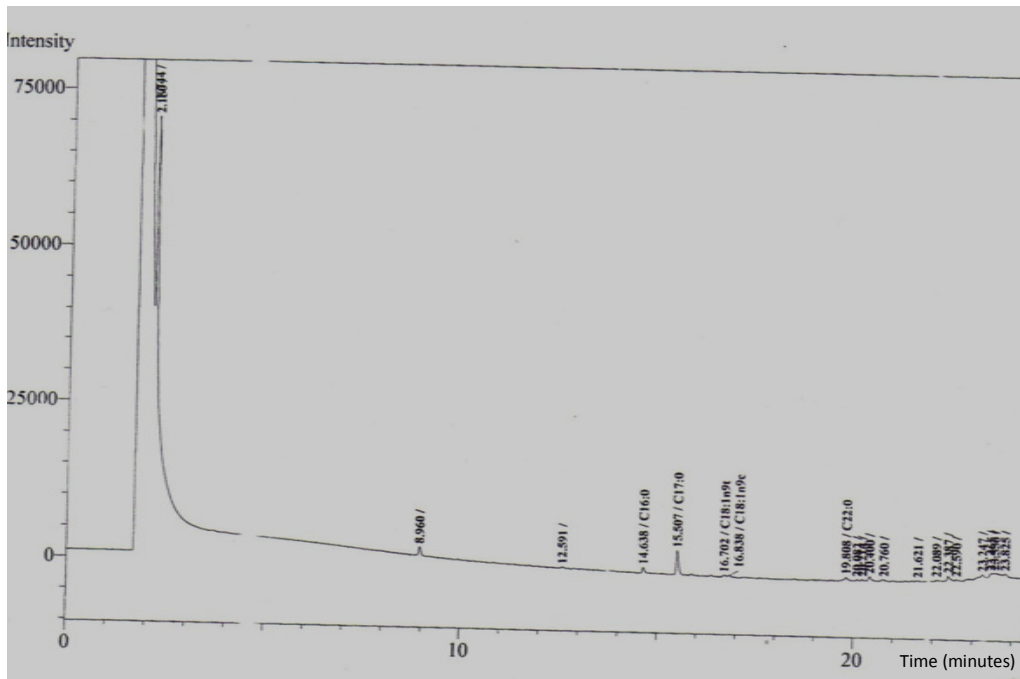


Figure 3.19. Gas chromatogram of FAMES derived from oil of unstressed *C. vulgaris* cultures.

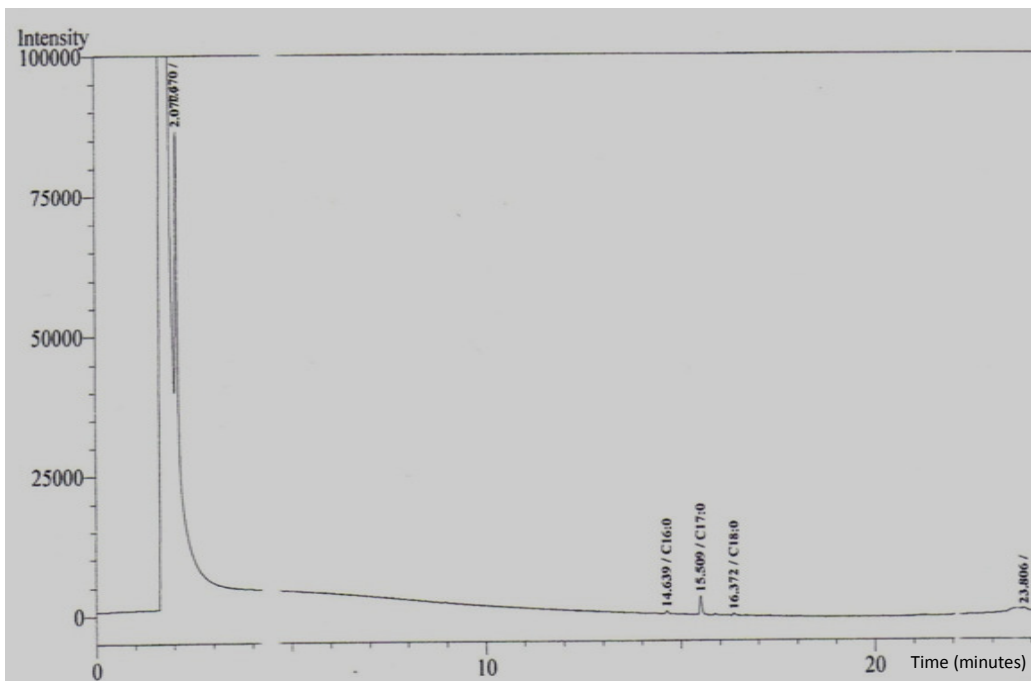


Figure 3.20. Gas chromatogram of FAMES derived from oil stressed *C. vulgaris* cultures.

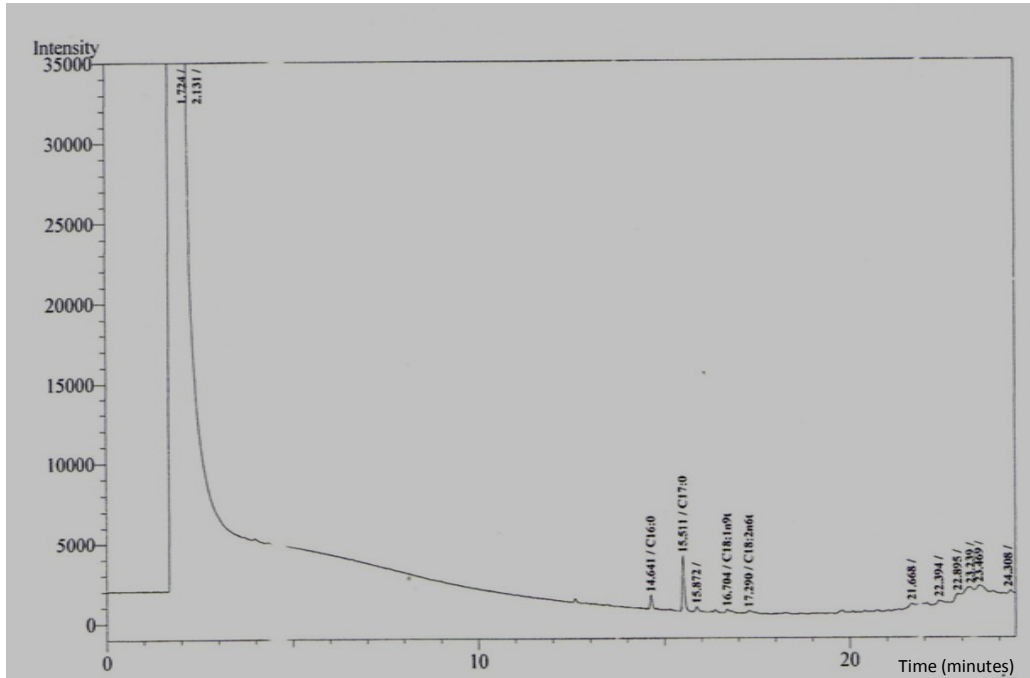


Figure 3.21. Gas chromatogram of FAMES derived from oil of unstressed *D. primolecta* cultures.

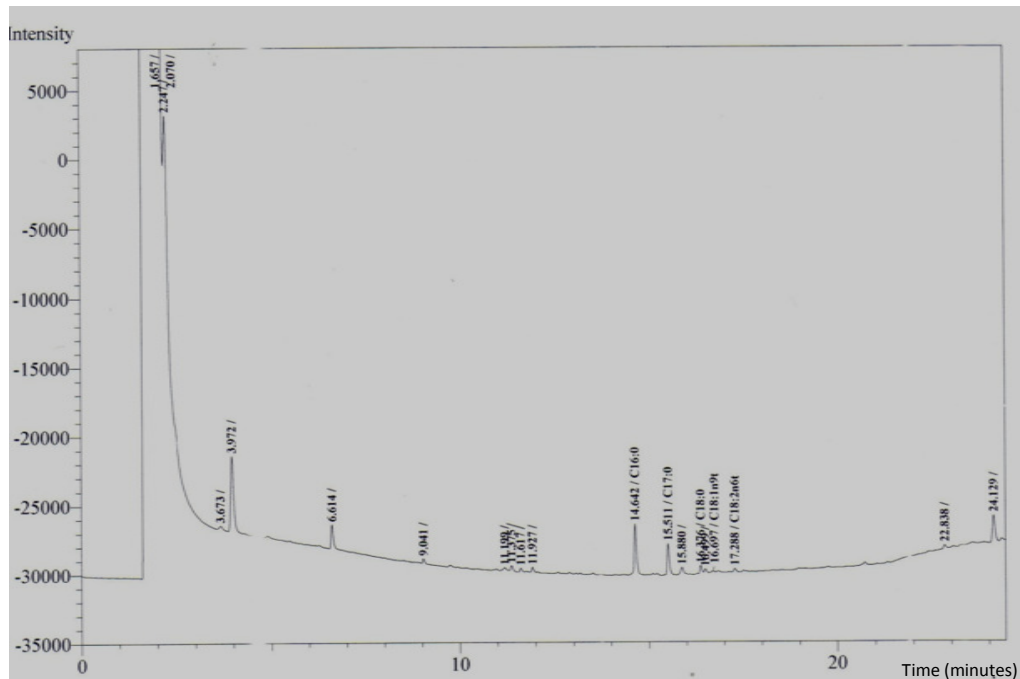


Figure 3.22. Gas chromatogram of FAMES derived from oil of stressed *D. primolecta* cultures.

Table 3.7. Nomenclature of FAMES extracted from algal oils

Shorthand notation of algal oil	Names of FAMES
C16:0	Palmitic acid methyl ester
C17:0	Heptadecaenoic acid methyl ester
C18:0	Stearic acid methyl ester
C18:1nt	<i>trans</i> -9-elaidic methyl ester
C18:1nc	Methyl <i>cis</i> -9-oleic methyl ester
C18:2n6t	Linolelaidic acid methyl ester or <i>trans</i> , <i>trans</i> -octadeca-9,12-dienoic acid methyl ester
C22:0	Docosanoic acid methyl ester

Table 3.8. Percentage composition of individual fatty acids relative to an internal standard

Algal culture	Internal standard mixed in ^a	% FAMES extracted					
		C16:0	C18:0	C18:1n9t	C18:1n9c	C18:2n6t	C22:0
<i>Chlorella vulgaris</i> (test)	61.260	13.227	-	6.722	5.775	-	13.016
<i>Chlorella vulgaris</i> (control)	78.256	11.845	9.899	-	-	-	-
<i>Dunaliella primolecta</i> (test)	69.698	16.370	-	6.458	-	7.474	-
<i>Dunaliella primolecta</i> (control)	31.125	53.332	8.001	3.414	-	4.128	-

a) Internal standard of C17:0 of 1 µl was mixed in a total injection volume of 2 µl. The algal oil extract was 1 µl.

Table 3.9. FAME content in % of algal oil

<i>C. vulgaris</i> (test)	6.57
<i>C. vulgaris</i> (control)	2.42
<i>D. primolecta</i> (test)	5.87
<i>D. primolecta</i> (control)	26.11

3.6 Detection of lipids and other fluorescent components using confocal microscopy

3.6.1 Nile red staining of microalgal cells

Nile red, 9 - diethylamino - 5H - benzo [α] phenoxazine - 5 - one, is a dye that fluoresces in organic solvents and hydrophobic lipids. It is known to be fully quenched in water and is therefore considered to act as a fluorescent hydrophobic probe. Nile red is an uncharged heterocyclic molecule (Figure 3.23), which accounts for its solubility in organic solvents such as dimethylsulphoxide (DMSO) and methanol. Traditional analysis of lipid content has been accomplished by gravimetric determination, solvent extraction and the use of GC or HPLC. Chen *et al.* (2009) discovered that high neutral lipid content was obtained from the aforementioned methods but was not detectable by Nile red staining *in vivo*. It was then speculated that the reason for this was due to the composition and structure of the rigid cell wall found in the algae which prevented the penetration of the dye. This was overcome by pre - exposure of the cells to chemicals that affected the integrity of the cell wall thus facilitating the penetration of Nile red. Chen *et al.* (2011) also reported the use of microwave pretreatment of cells to enhance Nile red penetration in green microalgae. Disadvantages of the conventional techniques are that the steps required to both extract and derivatize the fatty acids for GC analysis are numerous and time - consuming. Also, a substantial amount of biomass must be cultured for the extraction and derivatization. If the accurate measurement of lipid content of the microalgal cells was possible *in situ*, the preparation time and amount of sample required would be reduced. Quantitation of lipids using dye fluorescence is however complicated by autofluorescence in most algal cells (Brennan *et al.*, 2012). The use of Nile red as a lipid - soluble dye exhibits several advantages; these include the photostability of the dye, intense fluorescence in various organic solvents and staining ability in hydrophobic environments. The fluorescence maxima of Nile red varied depending on the relative hydrophobicity of the surrounding environment (Fowler and Greenspan, 1985). This allows the differentiation between neutral and polar lipids using the appropriate choice of the excitation and emission wavelengths which differ for the different dye solvents (http://en.wikipedia.org/wiki/Nile_red).

The excitation and emission wavelengths for fluorescence of cellular neutral lipids using Nile red are 530 nm and 575 nm, respectively (Chen *et al.*, 2009). These results were recorded using DMSO as the solvent to stain microalgal cells.

Chen *et al.* (2009) also revealed that Nile red fluorescence was strongly influenced by temperature and duration of staining with high temperatures or lengthy staining periods leading to the quenching of the fluorescence. Under the experimental conditions of Chen *et al.*, algal cells stained with Nile red at 40 °C for 10 min were found to yield optimal neutral lipid - derived fluorescence. In this study, Nile red - stained microscope slides were freshly prepared and immediately viewed under the microscope to prevent subsequent fading of the dye.

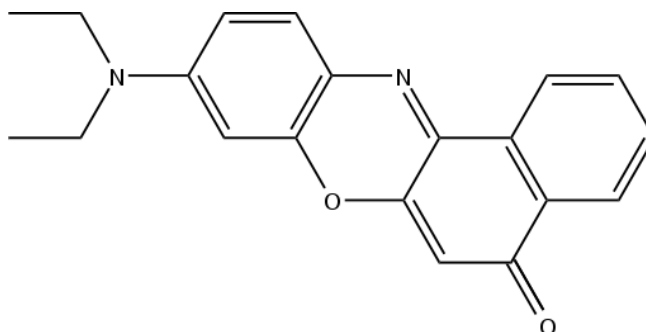


Figure 3.23. Chemical structure of Nile red (www.wikipedia/nile_red).

3.6.1 Bodipy 505/515 staining of microalgal cells

Bodipy (4,4 - difluoro - 1,3,5,7 - tetramethyl - 4 - boro - 3a,4a - diaza - s - indacene) is a fluorescent lipophilic dye which can be used to monitor oil storage within algal cells (Cooper *et al.*, 2010; Govender *et al.*, 2012). It is composed of dipyrromethene complexed with a disubstituted boron atom (Figure 3.24). These dyes are typically recognized for their small Stokes shift, high environmentally - independent fluorescence quantum yields which can reach 100 % in water and sharp excitation and emission peaks that contribute to the overall

brightness and resolution. These attributes enables bodipy to be an essential tool in several imaging applications. In solvents of different polarity, the position of the absorption and emission bands are unaltered as a result of the dipole moment and the transition dipole being orthogonal to each other (<http://en.wikipedia.org/wiki/BODIPY>).

Lack of photodamage to processed cells suggests that bodipy 505/515 might be used in conjunction with FACS (fluorescence - activated cell sorters) (Brennan *et al.*, 2012) to establish new lineages of algal cells with high lipid content. FACS measurements could possibly also be made in bodipy 505/515 - labelled algal cultures as the algal cells store different lipids in response to changes in environmental conditions such as temperature, nutrient load and light regime (Khozin - Goldberg and Cohen, 2006; Weldy and Heusemann, 2007; Chisti, 2007; 2008; Lv *et al.*, 2010). This type of information may be significant in optimizing oil harvests at commercial algal farms (Cooper *et al.*, 2010).

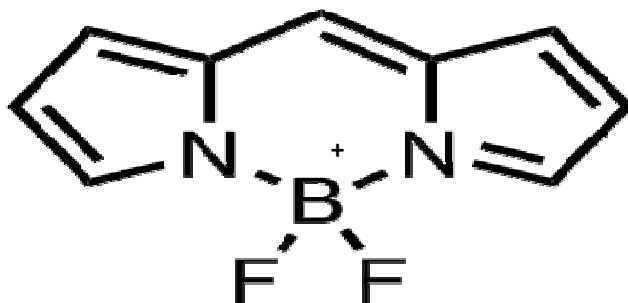


Figure 3.24. Chemical structure of bodipy (http://wikipedia_BODIPY).

3.6.3 Use of DMSO as a dye solvent

Algal cells characteristically comprise thick cell walls which, as a consequence impede the penetration of dyes and hence renders the staining process cumbersome (Cooper *et al.*, 2010). Therefore, DMSO is used as a vehicle to enhance and accelerate the permeation of dyes into

these relatively difficult target cells. In this study, 0.800 ml and 0.625 ml of DMSO was used in conjunction with bodipy and Nile Red, respectively (2.7.1; 2.7.2). In spite of the capability of bodipy to stain lipidic bodies of varied morphological or topological diversity, DMSO is used to promote dye permeation in algae with thick cell walls, especially those embellished with delicate scales or thecal plates, (Cooper *et al.*, 2010). This solvent enables good quality imaging and lipid detection in *Dunaliella primolecta* and *Chlorella vulgaris*. The penetration of Nile Red differs amongst algal species (Wang *et al.*, 2009). Cooper *et al.* (2010) reported that high levels of DMSO (20 - 30 % v/v) at elevated temperatures (40°C) were used to permeate the algal cells with Nile Red. However, whether or not, the algae were capable of surviving at these temperatures was not reported. In this study, considerably lower levels of DMSO were used at “room temperature” of approximately 25 °C.

3.6.4 Autofluorescence

Algae are capable of exuding natural fluorescence from endogenous carotenoid molecules and chlorophyll (Cooper *et al.*, 2010). This autofluorescence constrains the differentiation between natural and lipidic - dye emissions of light. Hence, manipulation of the confocal microscope is required in order to visualize and distinguish between the different forms of fluorescence as shown in the current study.

3.6.4.1 Autofluorescence detection in algal chloroplasts

Natural fluorescence is seen as a red hue (Figures 3.25 and 3.26) emitted by the endogenous chloroplasts. As stated by Cooper *et al.* (2010), the algal chloroplast is detected as “red” pigmentation. This pigmentation is the fluorescence exuded by the alga when unaided by the use of a dye. The detection of lipidic bodies necessitates staining with a dye as these organelles do not exhibit autofluorescence. This allows for the visualisation of characteristic

fluorescent emissions which differs in phospholipid and neutral lipid - dye complexes and hence, the extent of accumulation of such lipidic bodies can be assessed. However, the differentiation of the lipids in the study was resolved further using TLC and GC analyses (2.6.1; 2.9).

Autofluorescence was captured in both stressed and unstressed cells of *C. vulgaris* and *D. primolecta*, as the nitrogen - deficient growth condition promotes the accumulation of lipidic bodies (2.2) (Lv *et al.*, 2010).

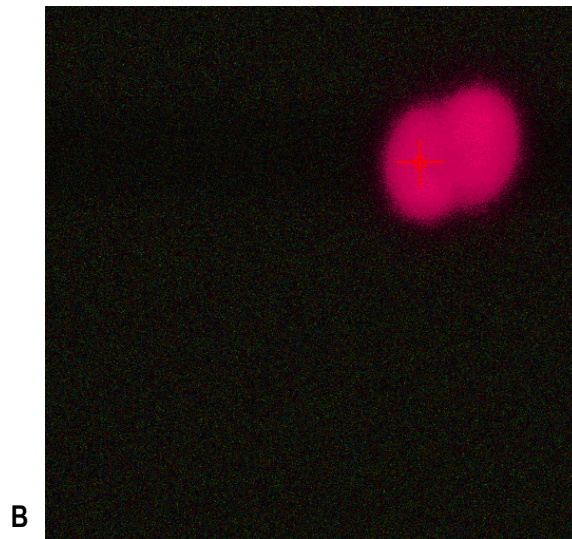
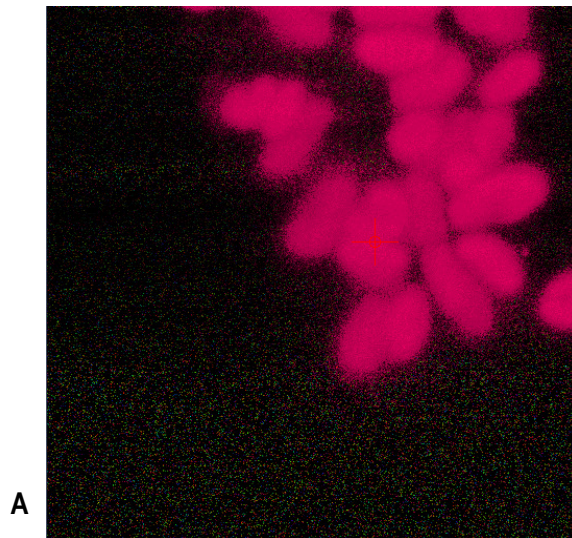


Figure 3.25. Confocal Micrographs showing (A) Autofluorescence of unstressed cells of *C. vulgaris*. (B) Autofluorescence of stressed cells of *C. vulgaris*.

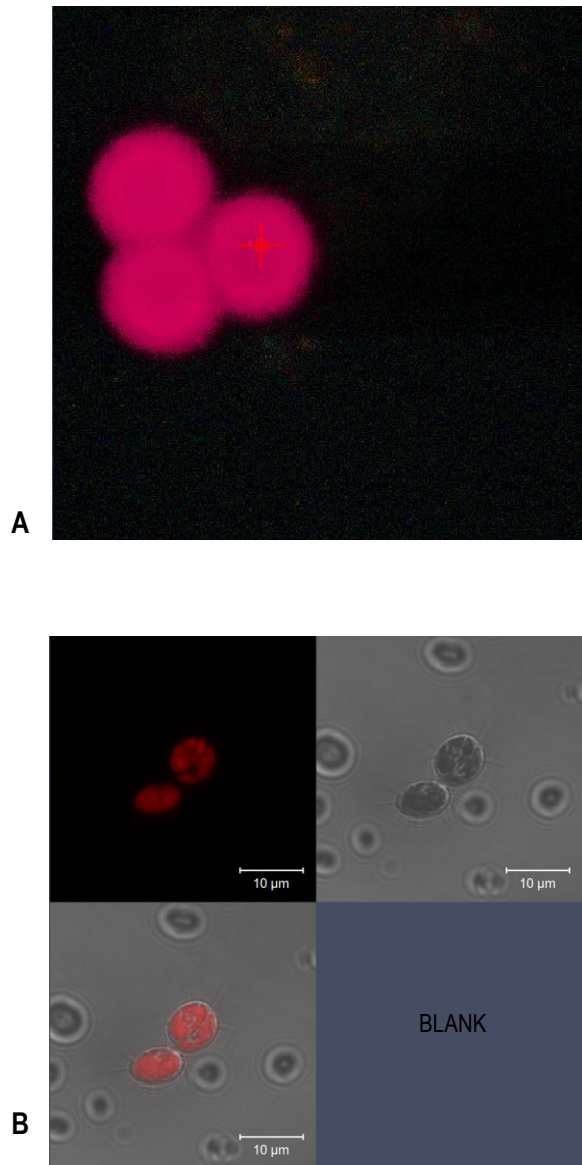


Figure 3.26. Confocal micrographs showing **(A)** Autofluorescence of unstressed *D. primolecta* cells. **(B)** Split image of autofluorescence of stressed *D. primolecta* cells (top left and bottom left) and * DIC image of the chlorophyll (top right).

* DIC: differential interference contrast (imaging)

As previously mentioned, the stressing of the algae was induced in order to create an environment of nitrogen deprivation. Under this condition, the algae are known to incorporate much of their endogenous nitrogen into its pigments (Figueroa *et al.*, 2010). In a habitat of sufficient nitrogen and other nutrients, algae are known to increase their rate of production of light - harvesting complexes, phycobilisomes and associated pigments. Hence, an increase in photosynthetic capacity is brought about as a result of an increase in photosynthetic pigments. The converse is apparent in that nitrogen depletion correlates with decreases in the rates of photosynthesis (Pinchetti *et al.*, 1998; Voronova *et al.*, 2009). Lv *et al.* (2010) confirmed that lipids do in fact accumulate in algal cells when grown in N - limiting conditions rather than in N - enriched media. They reported that the N - depletion condition imposed a reduction in the cellular abundance of ACCase with a concomitant loss of the activity of the enzyme. Cell division almost ceased as cells accumulated lipids. These studies conducted by Lv *et al.* continued to reveal that moderate CO₂ levels (1.0 %) induced the production of *Chl a* and accordingly enhanced the activity of ACCase, therefore promoting lipid accumulation.

If the stressed conditions lower the rate of production of the photosynthetic apparatus; then it would be expected that the amount of chlorophyll decreases and consequently the fluorescence emitted will be less intense. This hypothesis is supported by the graphical representations generated in this study (Figures 3.27 - 3.30) in which the intensity of fluorescence is lower in the stressed cells of *D. primolecta* alga rather than the unstressed. A split image (Figure 3.26) was acquired in which 1 track and 2 channels were opened to allow for the identification of the chlorophyll (red) (channel 1) and the *DIC image to be visualised. The use of 1 track means that the settings of the microscope will remain the same when detecting fluorescence in 2 channels. For this detection, a 488 - excitation filter and 415 - 726 nm band pass filter were used to capture the natural fluorescence exuded. Cognizance should be taken that the red and green peak emissions do not indicate the presence of 2 different algal body components but rather chlorophyll detection at different locations in the algal cell (Figure 3.30). Analysis of the graphical plots of *C. vulgaris* cells from the stressed and unstressed media revealed a similar intensity of autofluorescence yet sharper peaks were obtained in the former (Figure 3.27 and 3.28). The Argon 488 nm - excitation laser was used for both *D.*

primolecta and *C. vulgaris* cells and the emissions were captured in the same wavelength range (Figures 3.31 - 3.34).

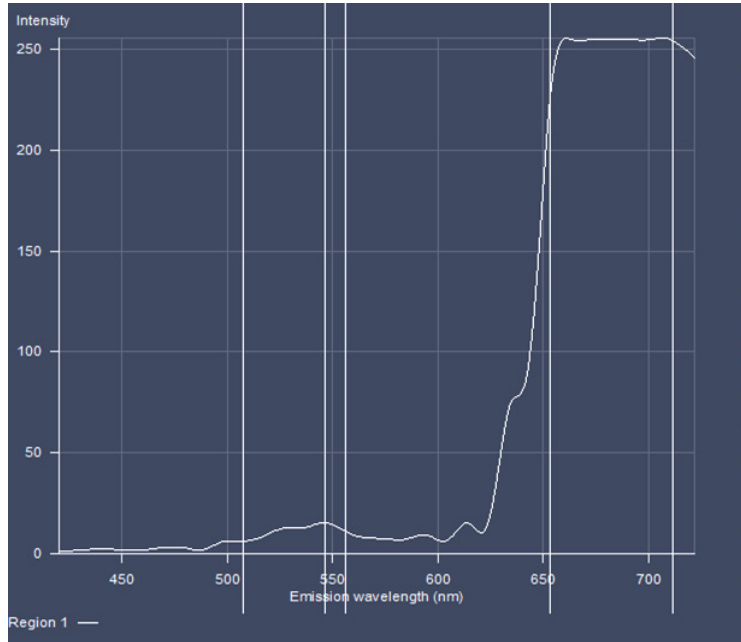


Figure 3.27. Graphical representation of the intensity of autofluorescence (red hue) emitted by unstressed *C. vulgaris* cells at a range of 420 - 722nm.

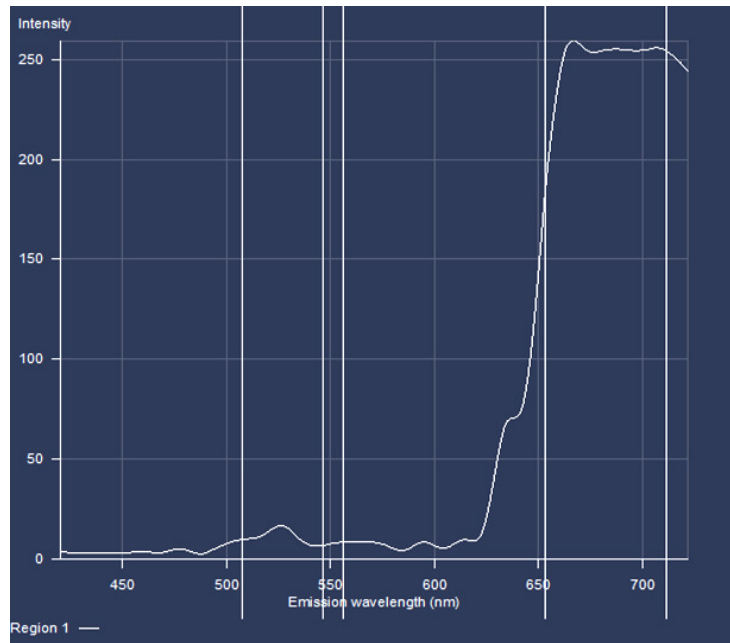


Figure 3.28. Graphical representation of the intensity of autofluorescence (red hue) emitted by stressed *C. vulgaris* cells at a range of 420 - 722nm.

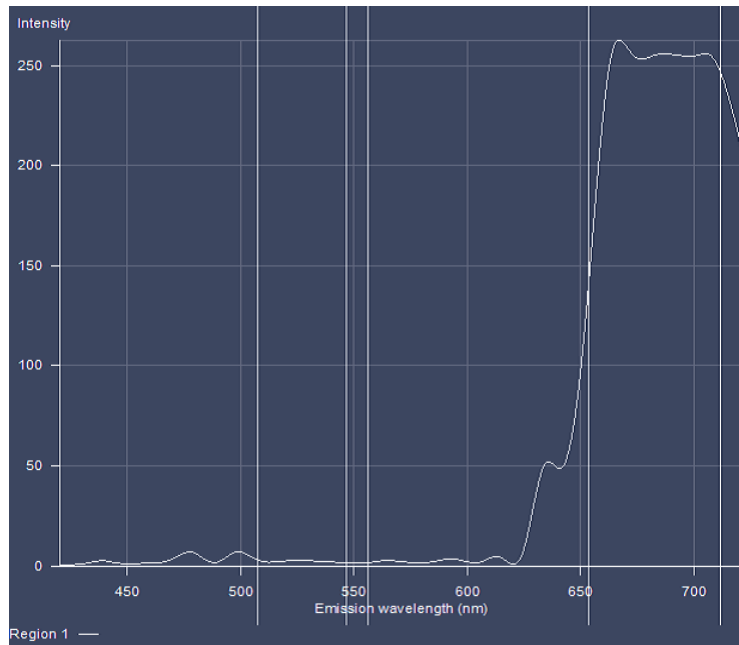


Figure 3.29. Graphical representation of the intensity of autofluorescence (red hue) emitted by unstressed *D. primolecta* cells at a range of 420 - 722nm.

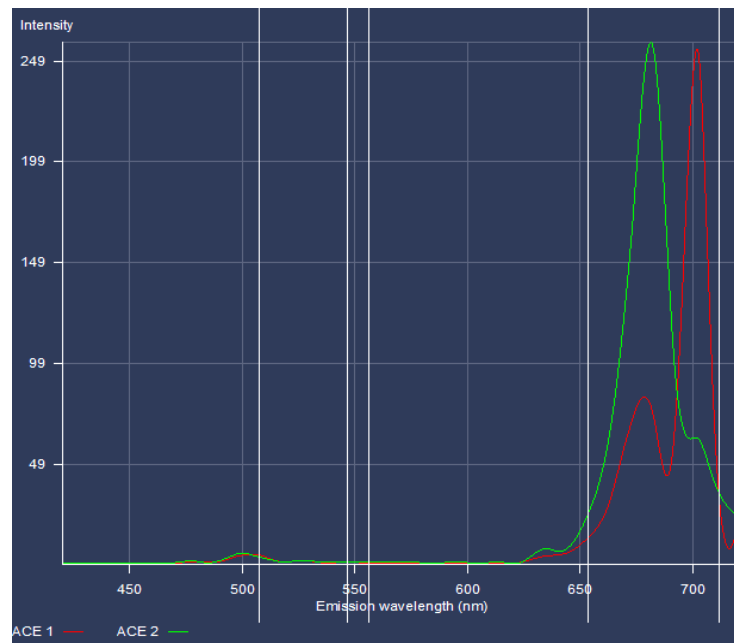


Figure 3.30. Graphical representation of the intensity of autofluorescence (red hue) emitted by stressed *D. primolecta* at a range of 420 - 722nm.

It is known that the fluorophores found in the chloroplast of algae emit fluorescence in the wavelength range of 415 - 726 nm (Chen *et al.*, 2009). More specifically, *chl a* and *chl b* emit fluorescence in the ranges 500 - 550 nm and 550 - 640 nm, respectively (Chen *et al.*, 2009). In a recent study conducted by Wang *et al.* (2009) various fluorescent components of *Chlamydomonas reinhardtii* were reported to give fluorescence in similar wavelength ranges. Peaks at approximately 655 nm and 670 nm were detected in the acquisition of natural fluorescence for *C. vulgaris* test and control cultures, respectively (Figures 3.27 and 3.28). Literature has also stated that chlorophyll fluorescence has been detected at a wavelength range of 650 - 694 nm (Wang *et al.*, 2009; Moellering and Benning, 2010). Cooper *et al.* (2010) confirmed this finding when they reported chlorophyll fluorescence captured at 694 nm. It is widely known that each algal cell differs from the next and hence, likewise the fluorescence patterns obtained. According to the plots obtained (Figures 3.27 and 3.30), autofluorescence was detected as peaks at approximately 663 - 673 nm and 702 - 712 nm for cells of the unstressed *D. primolecta* alga (Figure 3.29). Similarly, peaks for the stressed alga were obtained at approximately 683nm (green fluorescence emission), 663 nm - 673 nm (red fluorescence emission) and 702nm (red fluorescence emission), respectively. The green and red peak emissions do not indicate different components but rather different regions chosen in the algal cell. The Zeiss LSM 710 Axio observer Z1 microscope with "smart setup" programme, accommodated chlorophyll fluorescence standards which enabled a comparison of similar fluorescence obtained in this study.

A useful feature found in CSLM is the acquisition of a composite image showing fluorescence over the desired wavelength range. Wavelength scanning or lambda stack is a three - dimensional dataset which comprises a collection of images that uses the same specimen subject to scanning at different wavelength bands, each which spans a limited region of the emission spectra (www.microscopyu.com/tutorials/flash/spectralimaging.html). The lambda stacks for *D. primolecta* and *C. vulgaris* revealed patterns in which strong autofluorescence is emitted at wavelengths corresponding to the peaks obtained in the associate graphical plots (Figures 3.31 - 3.34).

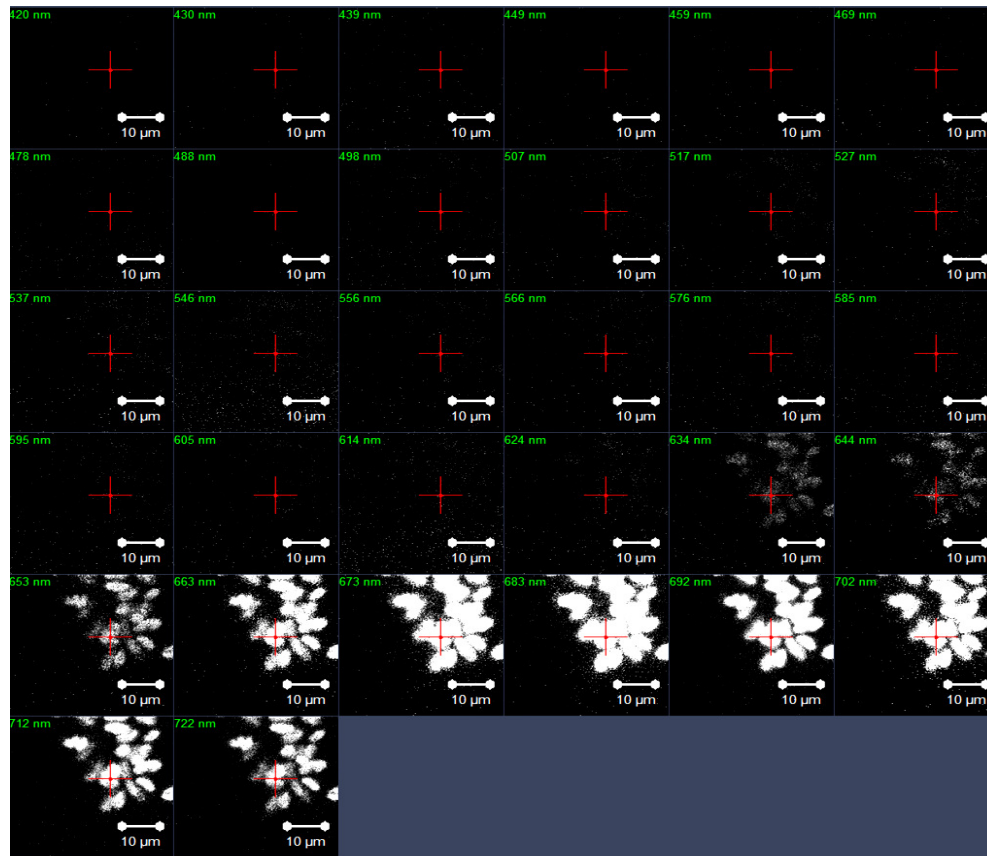


Figure 3.31. Wavelength scanning of the autofluorescence pattern observed in unstressed cells of *C. vulgaris*.

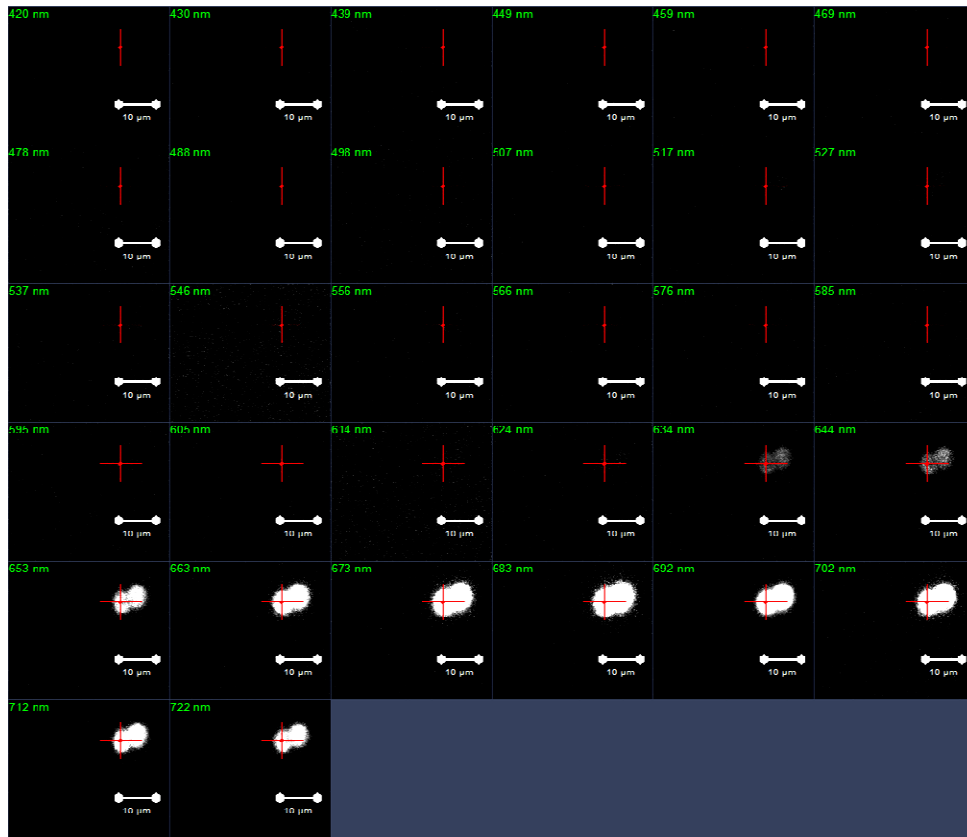


Figure 3.32. Wavelength scanning of the autofluorescence pattern observed in stressed cells of *C. vulgaris*.

Table 3.10. Confocal parameters used for autofluorescence detection in *C. vulgaris*

Unstressed <i>C. vulgaris</i>			
Confocal microscope setting	Digital parameters		
	Microscope image	Lambda stack and graphical representation	
Master gain	550	900	
Digital gain	1	1	
Digital offset	0	1	
Bit depth	8	8	
Pinhole	170.2 (1 AU) airy unit	176.3 (1 AU) airy unit	
Average number	2	2	
Frame size	512 x 512	512 x 512	
Stressed <i>C. vulgaris</i>			
Confocal microscope setting	Digital parameters		
	Confocal image	*DIC	Lambda stack and graphical representation
Master gain	561	550	900
Digital gain	1.2	1	1
Digital offset	1	1	1
Bit depth	8	8	8
Pinhole	52.6 (1 AU)	67.2 (1 AU)	176.3 (1 AU)
Average number	2	4	2
Frame size	512 x 512	512 x 512	512 x 512

* DIC: differential interference contrast (imaging)

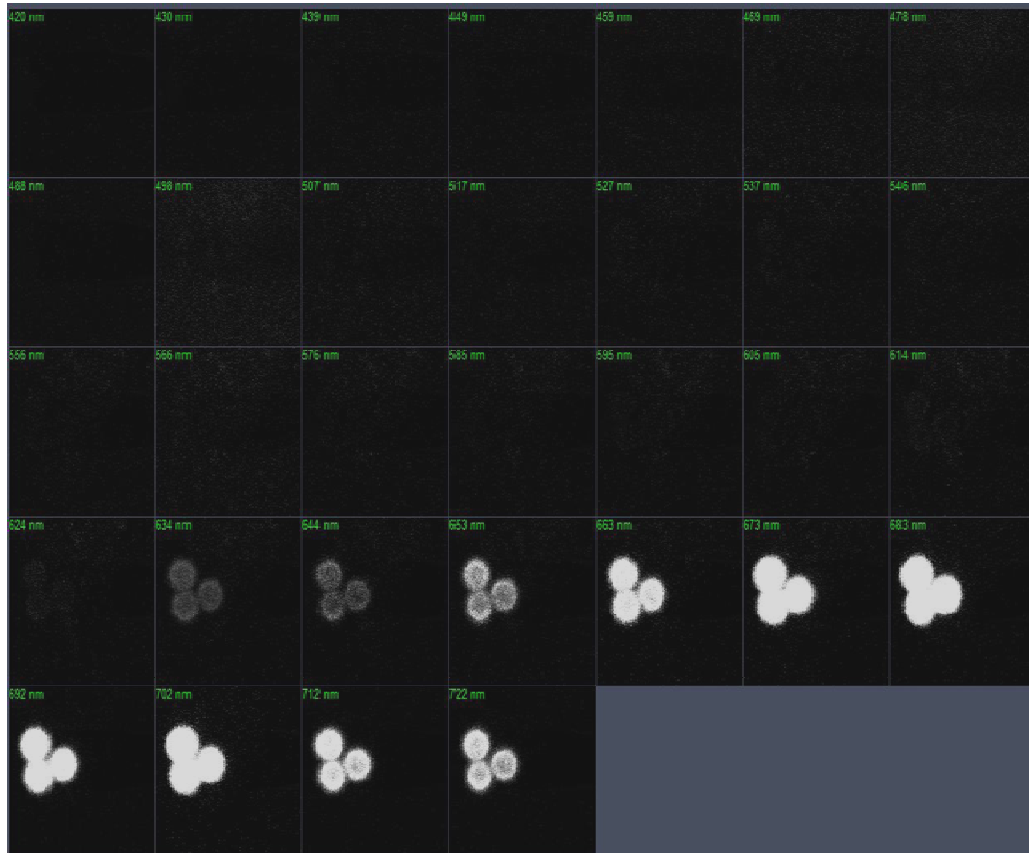


Figure 3.33. Wavelength scanning of the autofluorescence pattern observed in unstressed cells of *D. primolecta*.

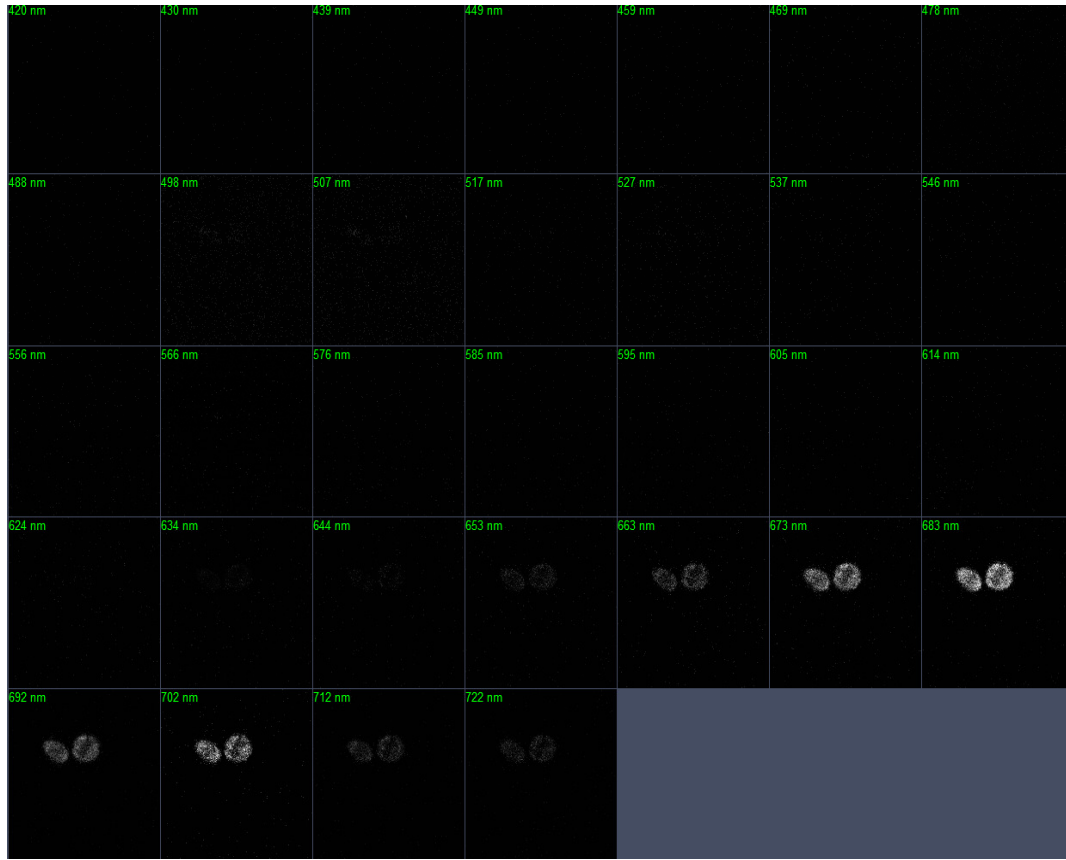


Figure 3.34. Wavelength scanning of the autofluorescence pattern observed in stressed cells of *D. primolecta*.

Table 3.11. Confocal parameters used for autofluorescence detection in *D. primolecta*

Unstressed <i>D. primolecta</i>			
Confocal microscope setting	Digital parameters		
	Microscope image	Lambda stack and graphical representation	
Master gain	947	910	
Digital gain	1	1	
Digital offset	1	1	
Bit depth	8	8	
Pinhole	178.4 (1 AU) airy unit	170.1 (1 AU) airy unit	
Average number	2	2	
Frame size	512 x 512	512 x 512	
Stressed <i>D. primolecta</i>			
Confocal microscope setting	Digital parameters		
	Red channel	*DIC	Lambda stack and graphical representation
Master gain	844	840	900
Digital gain	1	1	1
Digital offset	1	1	1
Bit depth	8	8	8
Pinhole	56.1 (1 AU)	60 (1 AU)	56.1 (1 AU)
Average number	2	4	2
Frame size	512 x 512	512 x 512	512 x 512

* DIC: differential interference contrast (imaging)

3.6.5 Lipidic fluorescence detection

Neutral lipids and phospholipids, unlike chloroplasts, do not exude a natural fluorescence but rather require the aid of a dye stain. The fluorescence hue emitted by the oil bodies is dependent on the dye used and type of lipid making up the oil body structure.

3.6.5.1 Fluorescence of algal lipidic bodies using Nile red dye stain

The maximum wavelength of emission with neutral lipids is shorter than that shown by polar lipids and the fluorescent intensity is also higher than the latter when complexed with Nile red. The fluorescence intensity of lipids composed of unsaturated fatty acids is stronger than that composed of saturated fatty acids (Kimura *et al.*, 2004). Nile red undergoes a solvatochromic shift in fluorescence, emitting a yellow fluorescence after entering algal lipid bodies and thereby, becoming solvated by the neutral lipids in these organelles (excitation 450 - 500 nm, emission > 528 nm). When the dye is dissolved in more polar solvents, red fluorescence by phospholipids is given off at approximately 590 nm, following excitation at 515 - 560 nm. Depending upon the hydrophobicity of the solvent, the excitation and emission maxima of Nile red fluorescence can vary over a range of 60 nm (Greenspan *et al.*, 1985).

Greenspan *et al.* (1985) reported that the emission wavelengths for the detection of neutral lipids and phospholipids were > 528 nm and > 590 nm, respectively. For the visualization of the aforementioned biomolecules, several channels (Tables 3.12 and 3.13) were opened and assigned specific band - pass filters. This allowed for the acquisition of a split image which permits the visualization of each component independently for identification and analytical purposes, as well as a composite image which demonstrates the assorted fluorescent components which can be superimposed on each other. For the detection of neutral lipids, a 516 - 547 nm band pass filter was employed with a 488 nm excitation filter, as the excitation wavelength for triacylglycerol - rich lipids is 450 - 500 nm. Similarly, a 528 - 615 nm band pass filter was applied for the capture of fluorescence emitted by phospholipid fluorophores after

being excited by a 512 nm excitation filter. For the identification of chlorophyll fluorescence (green fluorescence), a 633 nm laser was utilized for the excitation of the fluorophores and emission was captured employing a 639 nm band pass filter. As previously mentioned, staining with Nile red reveals a yellow fluorescence for neutral lipids and a red fluorescent hue for polar lipids. However, autofluorescence is detected in the range of 415 - 726 nm (3.6.4.1), hence fluorophores overlap when capturing fluorescence emitted by the biomolecules of interest and the chloroplasts. The linear unmixing feature of the ZEN software utilizes a mathematical process whereby the fluorescent light can be re - allocated back to the correct channel. This software also allows for the fluorescent colours to be altered for example, when fluorescence is being captured with the use of several dyes. Pseudo - colouring is seen in the micrographs obtained from the unstressed *C. vulgaris* alga whereby the chlorophyll and neutral lipids are indicated by blue and green fluorescence, respectively (Figure 3.35). Using the image analysis programme, images taken in separate channels can be merged and assigned a specific colour.

Many microalgal cultures divert from the tendency to grow as discrete single cells in suspension to as a flocculated mass of cells (Held and Raymond, 2011). This is evident by the stressed *D. primolecta* micrograph as this microalgal species is known to form clumps in the latter phase of its growth cycle (3.1.1) (Figure 3.38). The typical structure of lipid droplets is conserved in different species with a globular neutral lipid core enclosed by a phospholipid monolayer (Moellering and Benning, 2010). In addition, specific proteins are randomly integrated with the lipidic bodies and play vital roles in the droplet assembly, structure and function (Davidi and Pick, 2012). However, little is currently known at the cellular and molecular levels with regard to the mechanism of oil accumulation and this structure has yet to be confirmed in all green microalgae.

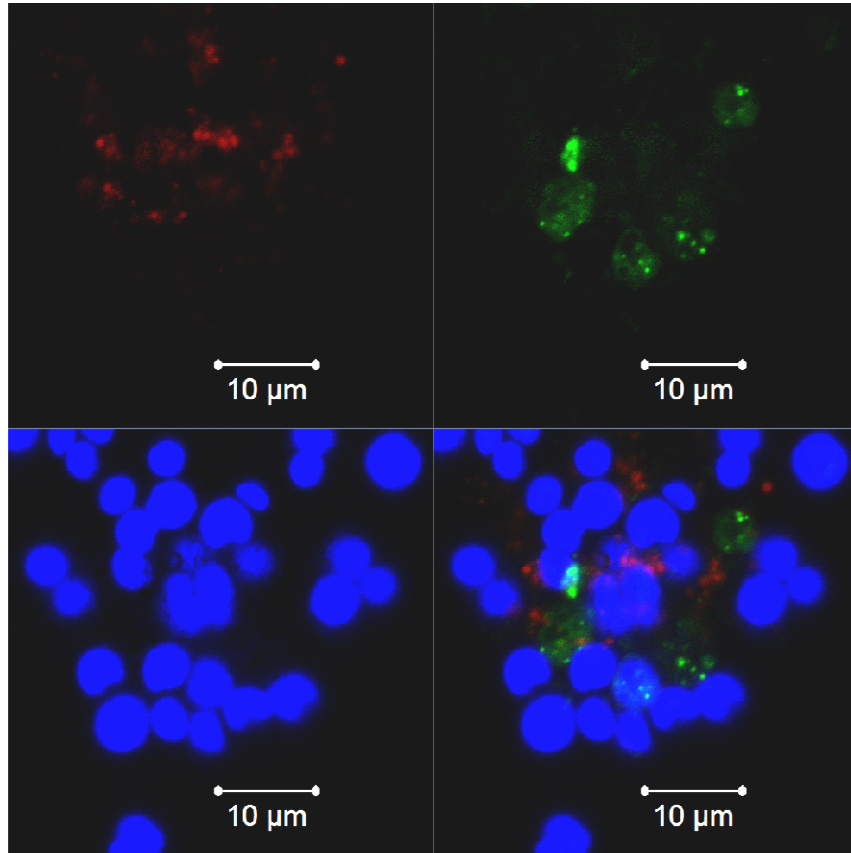


Figure 3.35. Split fluorescence image of unstressed *C. vulgaris* cells using Nile red dye stain visualizing the phospholipids (top left), chlorophyll (bottom left), neutral lipids (top right) and a composite image of all the fluorescence patterns (bottom right).

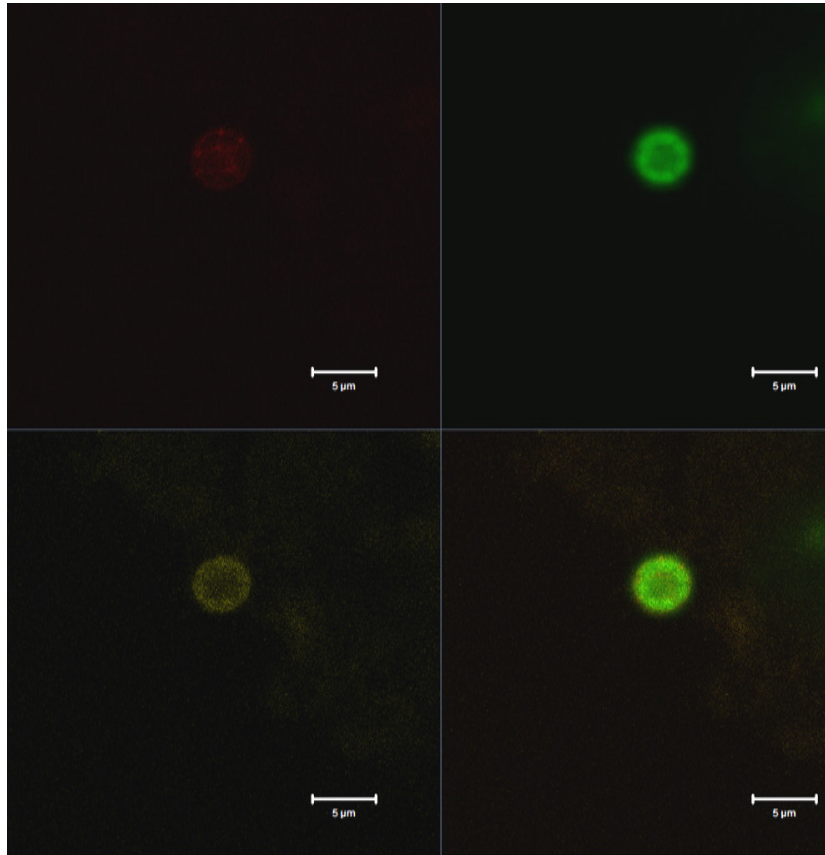


Figure 3.36. Split fluorescence image of stressed *C. vulgaris* cells using Nile red dye stain visualizing the phospholipids (top left), chlorophyll (top right), neutral lipids (bottom left) and a composite image of all the fluorescence patterns (bottom right).

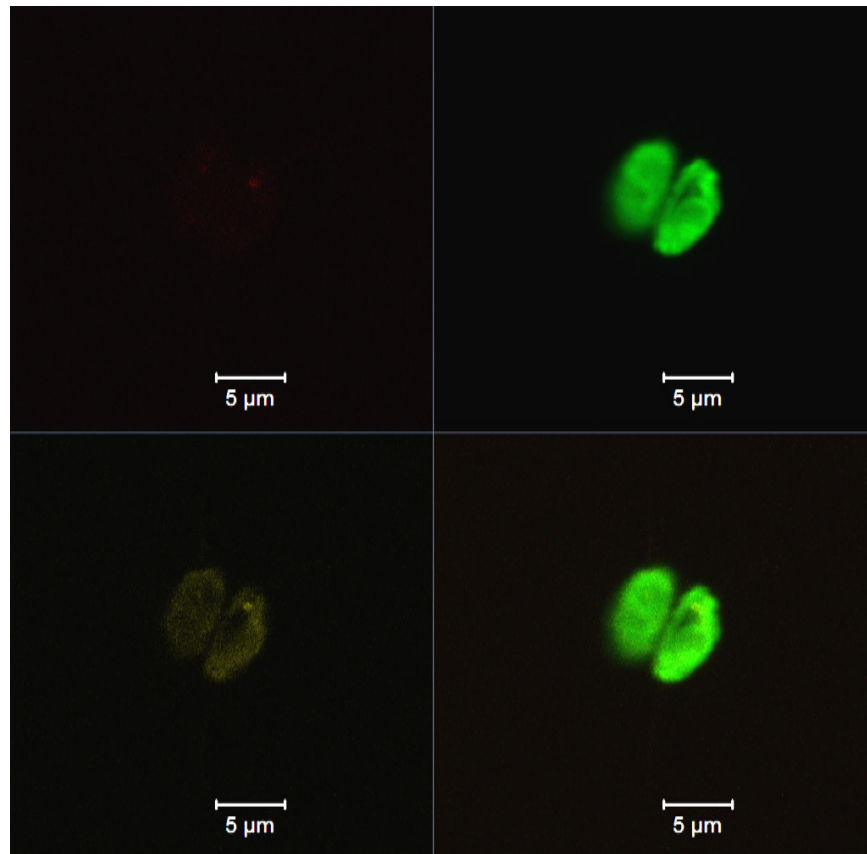


Figure 3.37. Split fluorescence image of unstressed *D. primolecta* cells using Nile red dye stain visualizing the phospholipids (top left), chlorophyll (top right), neutral lipids (bottom left) and a composite image of all the fluorescence patterns (bottom right).

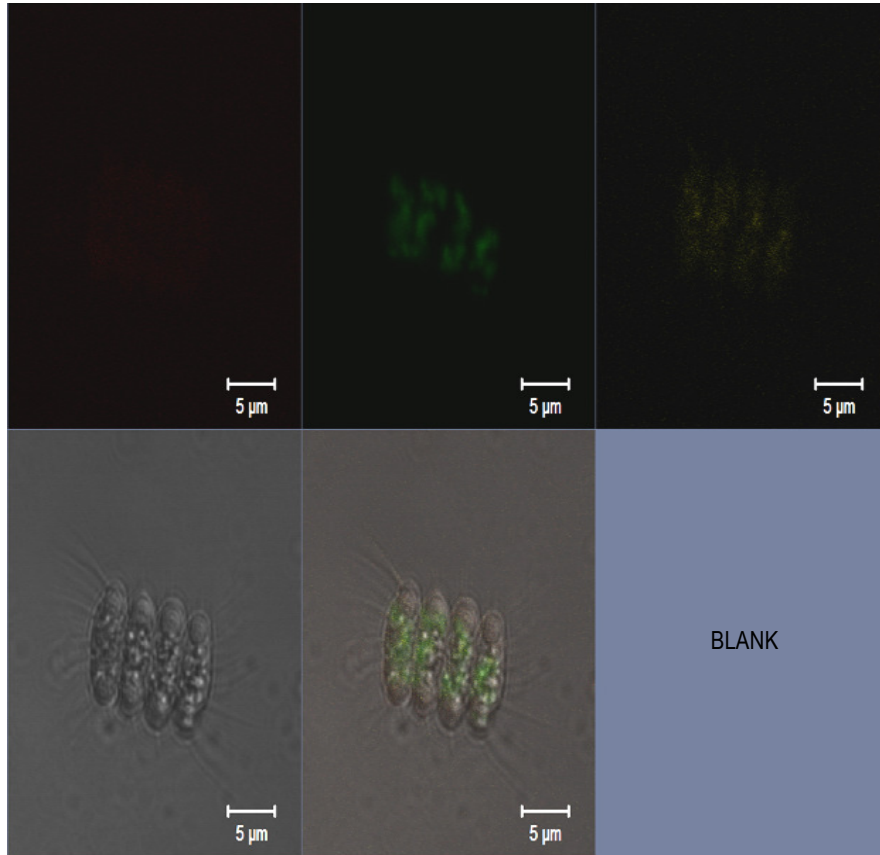


Figure 3.38. Split fluorescence image of stressed *D. primolecta* cells using Nile red dye stain visualizing the phospholipids (extreme top left), chlorophyll (top centre), neutral lipids (extreme top left), DIC image on bottom left and composite image of all the fluorescence patterns (centre right).

*DIC: Differential interference image.

An analysis of the graphical representations reveal the peaks at which fluorescence is optimized, which are in keeping with the respective wavelengths reported by Fowler *et al.* (1987) and is currently used for tentative component identification. The general trend from the aforementioned plots illustrates peaks > 520 nm for neutral lipids, > 560 nm for phospholipids and > 600 nm for chlorophyll. These peaks are evident in the respective lambda stacks (Figures 3.43 - 3.56) which allow for the acquisition of component related fluorescence to be captured over the range of 420 - 722 nm. According to the lambda stack of the stressed *C. vulgaris* alga (Figure 3.44), neutral lipid and phospholipid fluorescence is not seen as the intensity of fluorescence was too low; this is evident by the peaks generated in the corresponding graphical representation (Figure 3.40).

The red, blue and green coloured peak emissions on the graphical representations do not indicate the specific algal components but rather the fluorescence captured at different locations of the algal cells (Figures 3.39 - 3.42). A specific colour indicates a particular region selected on the corresponding micrograph.

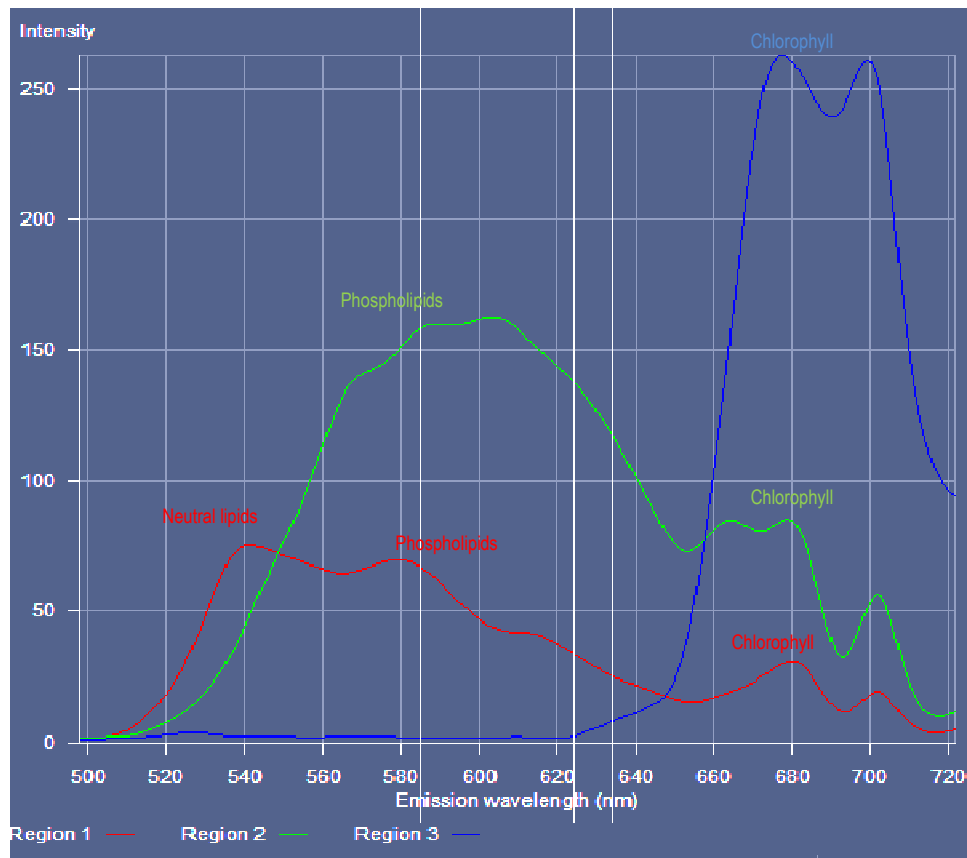


Figure 3.39. Graphical representation of the intensity of fluorescence emitted by unstressed *C. vulgaris* cells using Nile red dye at a range of 420 - 722nm showing neutral lipids, phospholipids and chlorophyll.

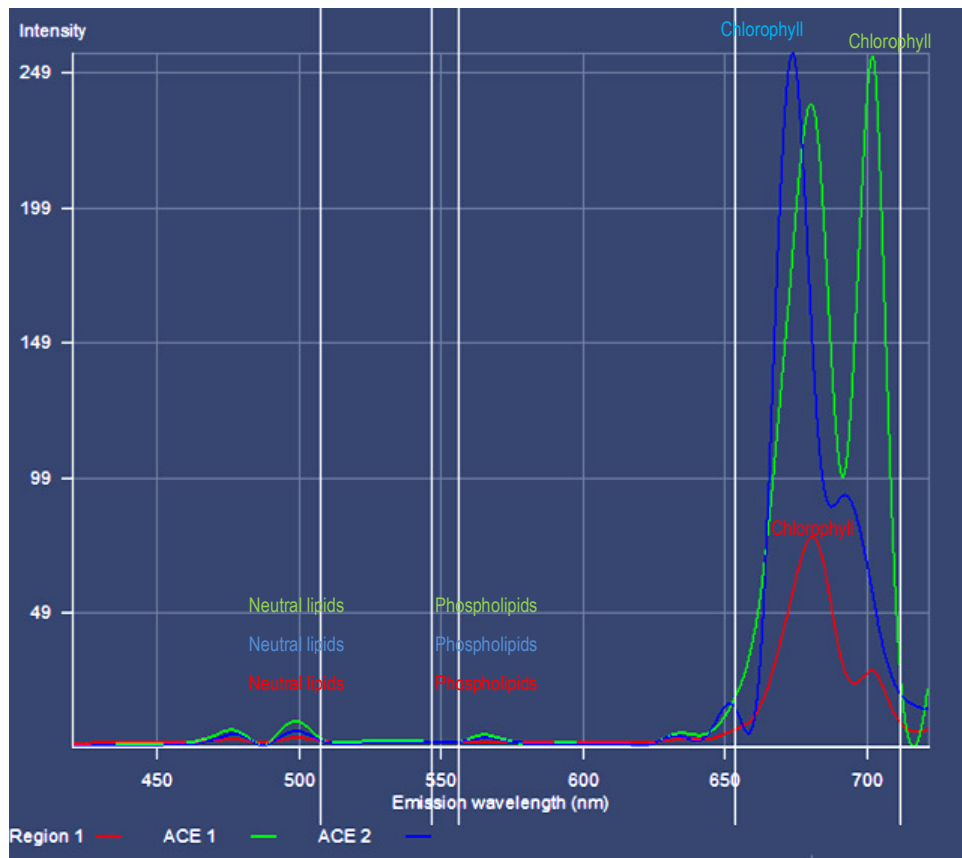


Figure 3.40. Graphical representation of the intensity of fluorescence emitted by stressed *C. vulgaris* cells using Nile red dye at a range of 420 - 722nm showing neutral lipids, phospholipids and chlorophyll.

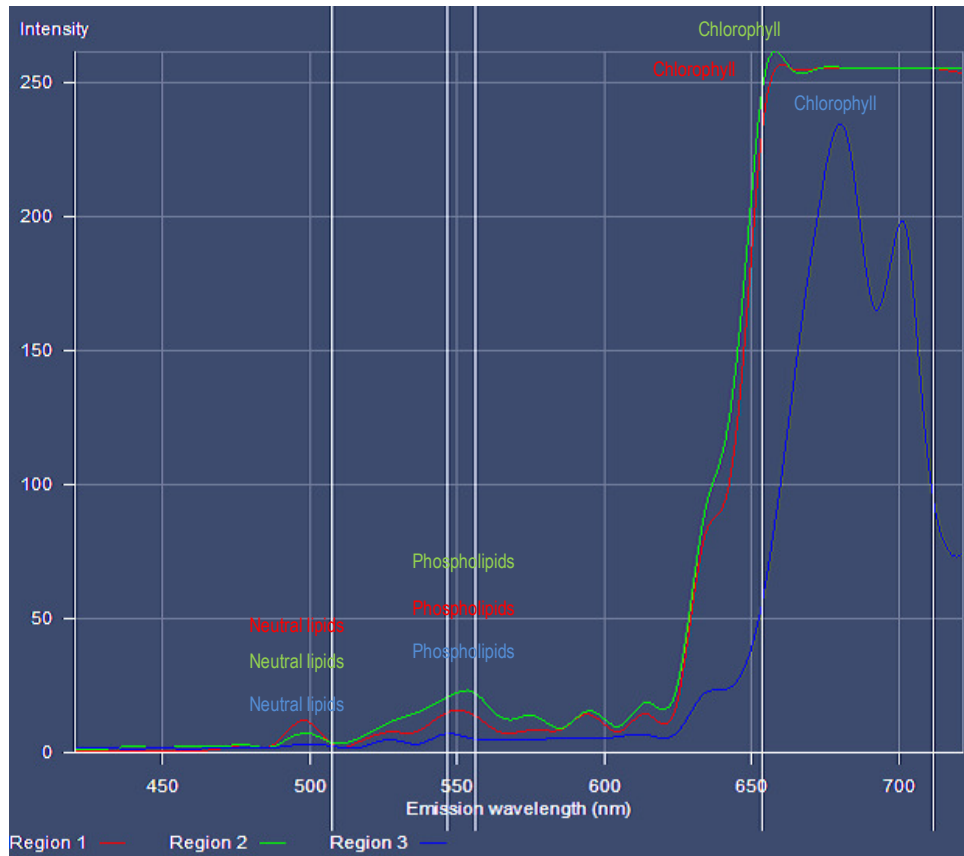


Figure 3.41. Graphical representation of the intensity of fluorescence emitted by unstressed *D. primolecta* cells using Nile red dye at a range of 420 - 722nm showing neutral lipids, phospholipids and chlorophyll.

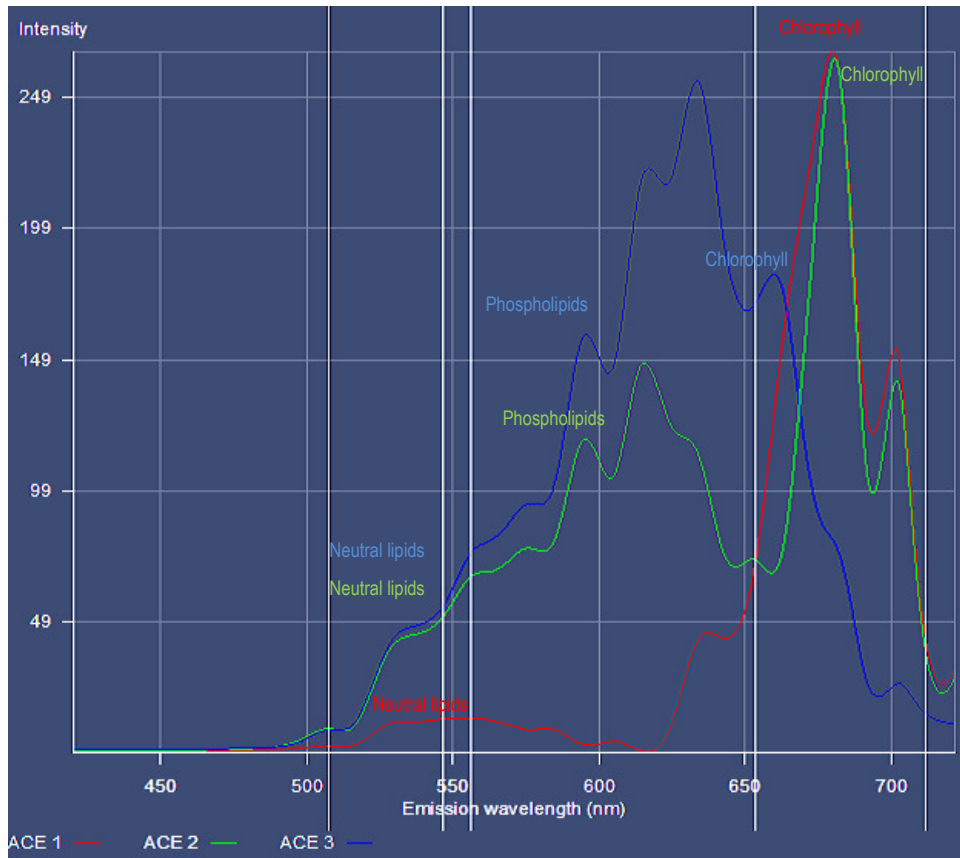


Figure 3.42. Graphical representation of the intensity of fluorescence emitted by stressed *D. primolecta* cells using Nile red dye at a range of 420 - 722nm showing neutral lipids, phospholipids and chlorophyll.

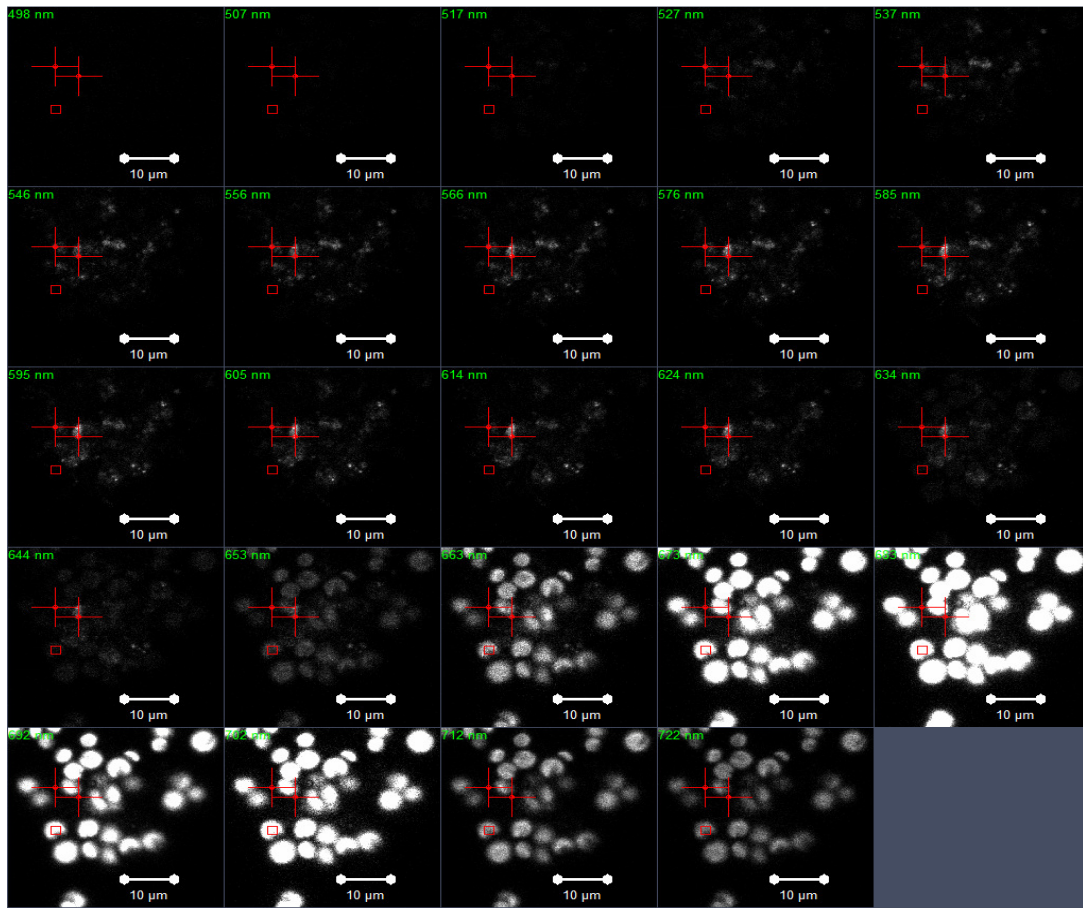


Figure 3.43. Wavelength scanning of fluorescence pattern observed in unstressed *C. vulgaris* cells subject to Nile red staining indicating fluorescent components neutral lipids, phospholipids and chlorophyll at 546, 585 and 673 nm, respectively.

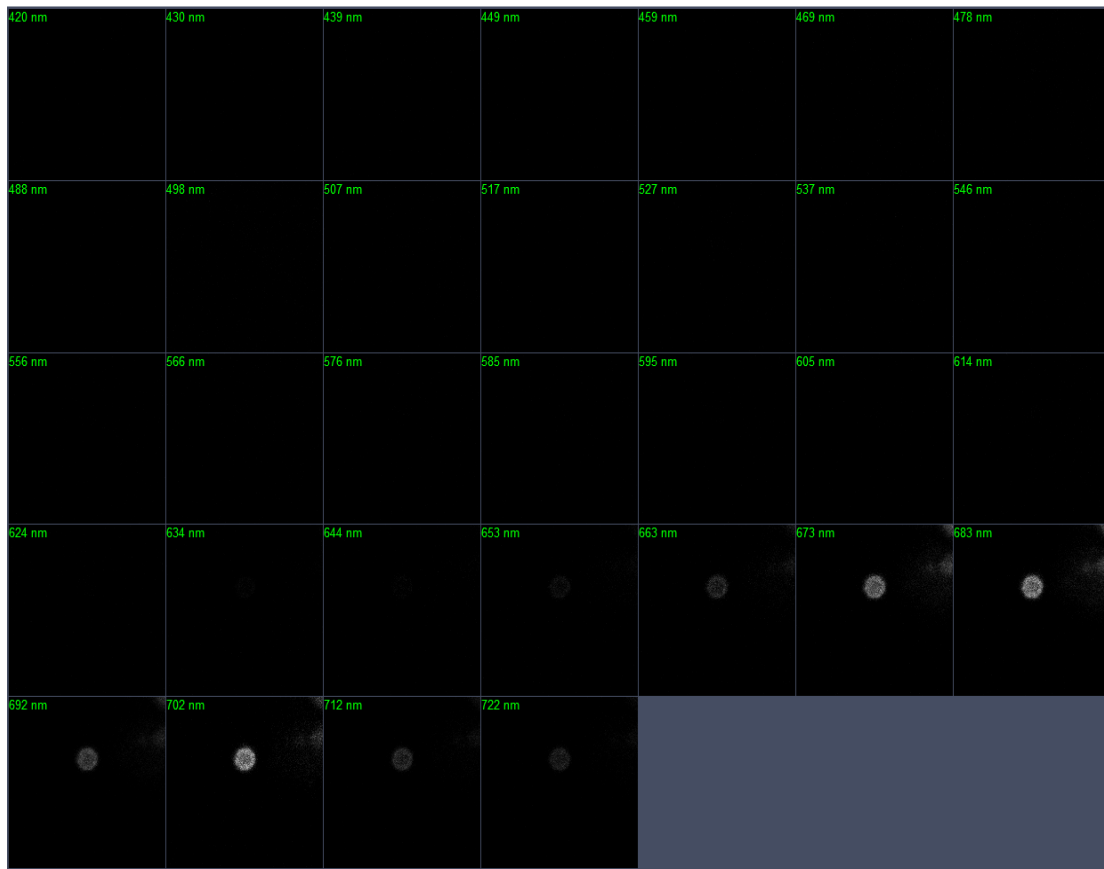


Figure 3.44. Wavelength scanning of fluorescence pattern observed in stressed *C. vulgaris* cells subject to Nile red staining indicating fluorescent component chlorophyll at 683 nm.

Table 3.12. Confocal parameters for lipid detection in Nile red stained *C. vulgaris* cells

Unstressed <i>C. vulgaris</i>				
Confocal microscope setting	Digital parameters			
	Red channel	Green channel	Blue channel	Lambda and graphical representation
Master gain	623	447	910	900
Digital gain	1	1	1	1
Digital offset	0	1	1	1
Bit depth	8	8	8	8
Pinhole	56.3 (1 AU) airy unit	52.2 (1 AU) airy unit	55.3 (1 AU) airy unit	51.4 (1 AU)
Average number	2	2	2	2
Frame size	512 x 512	512 x 512	512 x 512	512 x 512
Stressed <i>C. vulgaris</i>				
Confocal microscope setting	Digital parameters			
	Red channel	Yellow channel	Green channel	Lambda stack and graphical representation
Master gain	540	582	590	900
Digital gain	1.2	1	1	1
Digital offset	1	1	1	1
Bit depth	8	8	8	8
Pinhole	51.1 (1 AU)	63.5(1 AU)	59.6 (1 AU)	178.4 (1 AU)
Average number	2	4	2	2
Frame size	512 x 512	512 x 512	512 x 512	512 x 512

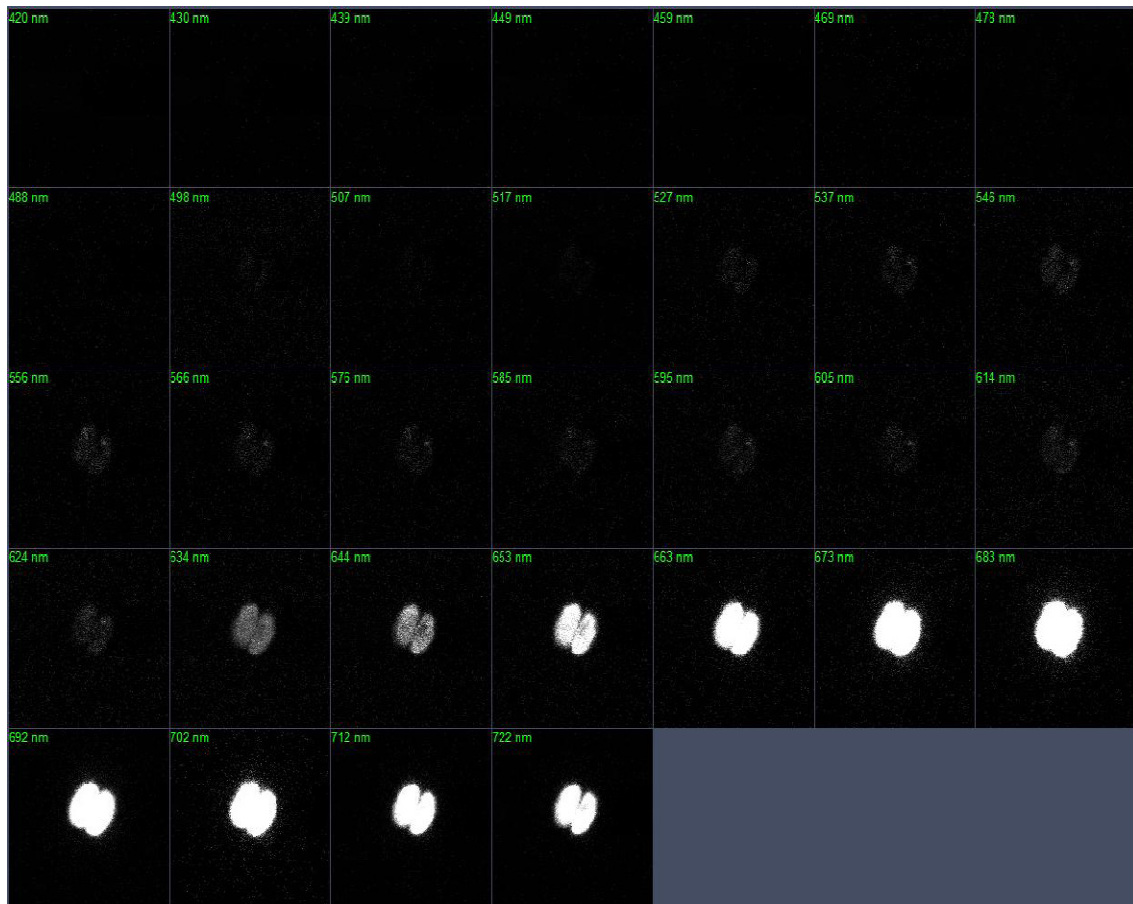


Figure 3.45. Wavelength scanning of fluorescence pattern observed in unstressed *D. primolecta* cells subject to Nile red staining indicating fluorescent components neutral lipids, phospholipids and chlorophyll at 546, 595 and 663 nm, respectively.

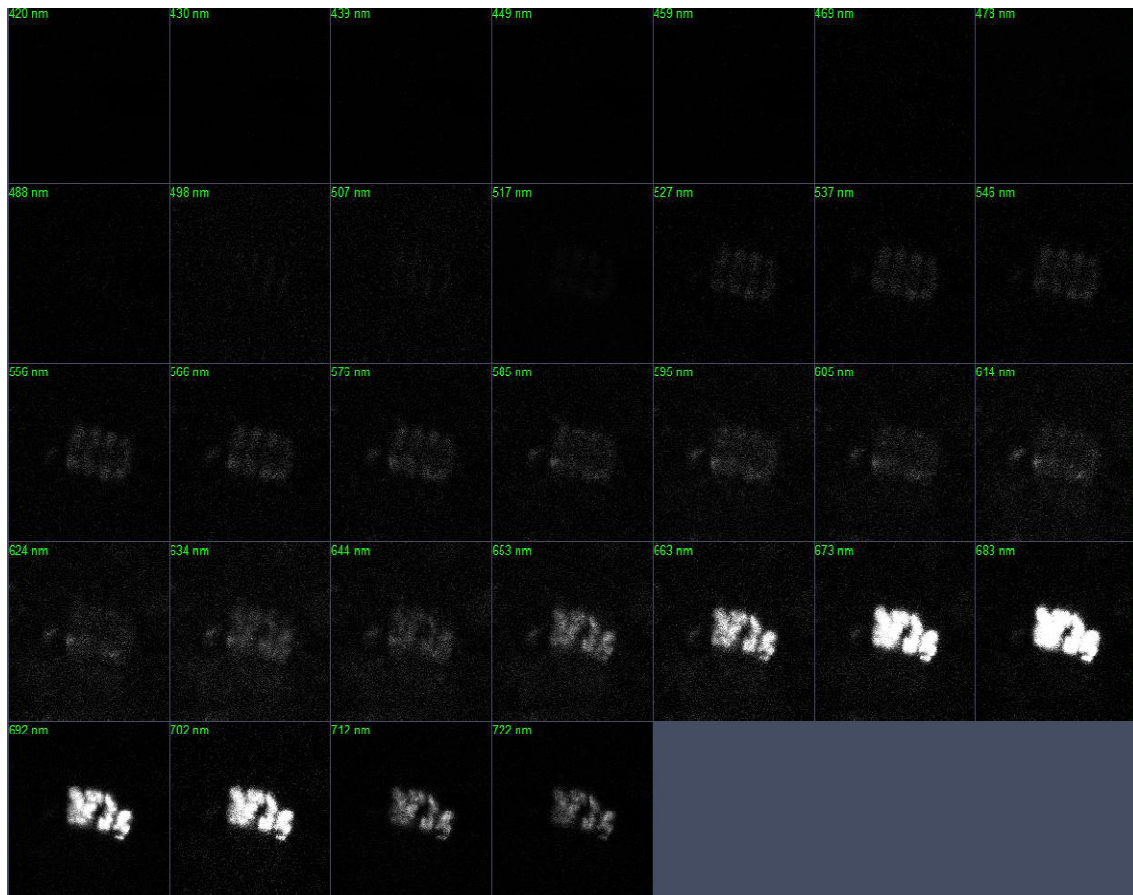


Figure 3.46. Wavelength scanning of fluorescence pattern observed in stressed *D. primolecta* cells subject to Nile red staining indicating fluorescent components neutral lipids, phospholipids and chlorophyll at 527, 595 and 663 nm, respectively.

Table 3.13. Confocal parameters of lipid detection in *D. primolecta* subject to Nile red staining

Unstressed <i>D. primolecta</i>					
Confocal microscope setting	Digital parameters				
	Red channel	Green channel	Yellow channel	Lambda and graphical representation	
Master gain	1030	1030	947	900	
Digital gain	1	1	1	1	
Digital offset	4	4	1	1	
Bit depth	8	8	8	8	
Pinhole	56.1 (1 AU) airy unit	56.1 (1 AU) airy unit	56.1 (1 AU) airy unit	178.4 (1 AU)	
Average number	2	2	2	2	
Frame size	512 x 512	512 x 512	512 x 512	512 x 512	
Stressed <i>D. primolecta</i>					
Confocal microscope setting	Digital parameters				
	Red channel	Yellow channel	Green channel	*DIC	Lambda stack and graphical representation
Master gain	1030	1030	638	951	900
Digital gain	1.2	1	1	1	1
Digital offset	1	1	1	3	1
Bit depth	8	8	8	8	8
Pinhole	51.1 (1 AU)	56.1 (1 AU)	56.1 (1 AU)	56.1 (1 AU)	178.4 (1 AU)
Average number	2	2	2	2	2
Frame size	512 x 512	512 x 512	512 x 512	512 x 512	512 x 512

* DIC: differential interference contrast (imaging)

3.6.5.2 Fluorescence of algal lipidic bodies using bodipy 505/515 dye stain

In contrast to Nile red, this dye has a high quantum yield and accumulates in lipidic intracellular compartments by a diffusion trap mechanism (Cooper *et al.*, 2010). Bodipy 505/515 has a high oil/water partition coefficient thereby granting it easier access to the cell organelles. The selective partitioning of bodipy into lipid bodies allows for the rapid identification and isolation of cells with high oil content relative to other cells within the same sample (Cooper *et al.*, 2010; Govender *et al.*, 2012). This isolation of algal cells with high oil content can be accomplished with the use of a fluorescent-activated cell sorter (FACS) (Brennan *et al.*, 2012). This is an ideal method for isolation as it individually interrogates the cells in contrast to bulk fluorescent measurements which depend upon cell density. Cooper *et al.* (2010) used bodipy 505/515 as a stain for the visualization and monitoring of oil storage within live algal cells. They conducted analysis on various 'green algae' such as *Chrysochromulina* spp. and *Prorocentrum* spp. and reported that the dye serves as an excellent stain for the oil-containing lipid bodies in algae.

Under the same wavelength (488 nm) utilized for the excitation of bodipy 505/515 dye, algal chloroplasts exude moderate red autofluorescence from endogenous chlorophyll molecules (3.6.4.1). Notably, the green emission spectrum of bodipy 505/515 is spectrally separate from algal autofluorescence. Lipidic bodies appear yellow (Figure 3.47) when they overlap spatially with chloroplasts. Unlike with the use of Nile red, which enables the differentiation of algal components, bodipy fluorescence is currently known only to spectrally distinguish between the natural chloroplast autofluorescence and lipidic fluorescence (Figures 3.47 and 3.48).

Cooper *et al.* (2010) stated that the spectral separation, as well as photostability of the bodipy 505/515 fluorophore, permits confocal time-lapse recordings of algal lipidic bodies. This analysis could potentially be performed in transgenic and mutant algal strains to aid the elucidation of genetic pathways involved in intracellular oil accumulation (Cooper *et al.*, 2010). Govender *et al.* (2012) reported that in contrast to Nile red-stained algal cells, bodipy 505/515-stained algal cells showed resistance to photobleaching, maintaining their fluorescence longer than 30 minutes.

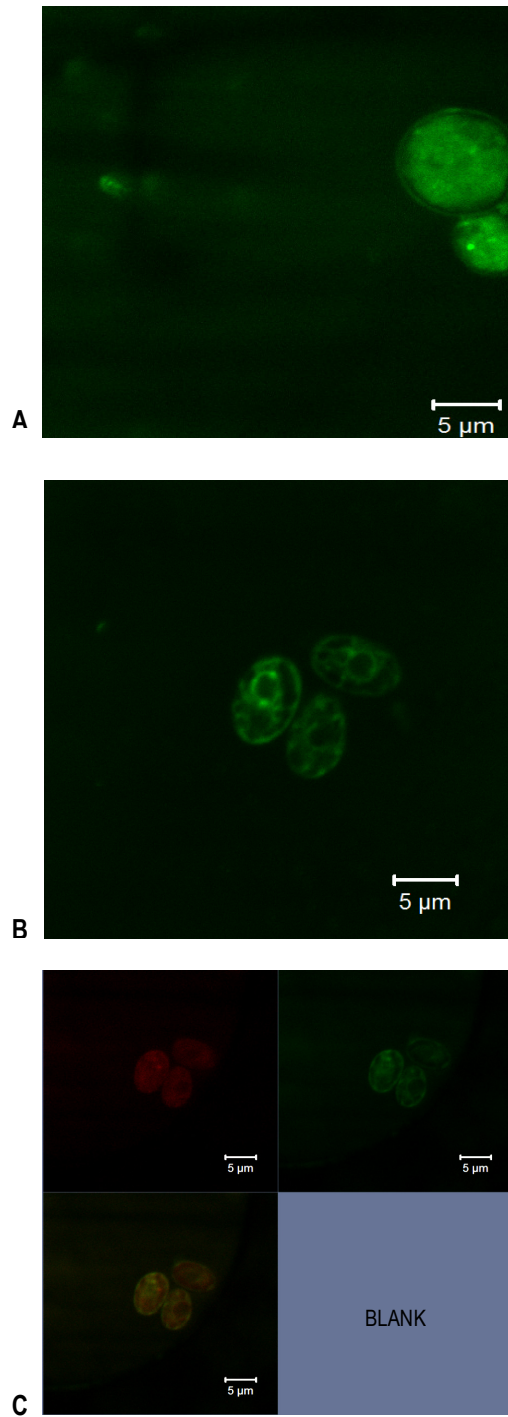


Figure 3.47. Micrograph showing (A) Fluorescence image of unstressed *C. vulgaris* cells using bodipy 505/515 dye stain. (B) Fluorescence image of stressed *C. vulgaris* cells using bodipy 505/515 dye stain. (C) Split fluorescence image of stressed *C. vulgaris* cells using bodipy 505/515 dye stain visualizing the lipid bodies (top left) and chlorophyll (top right) and a composite image of all the fluorescence patterns.

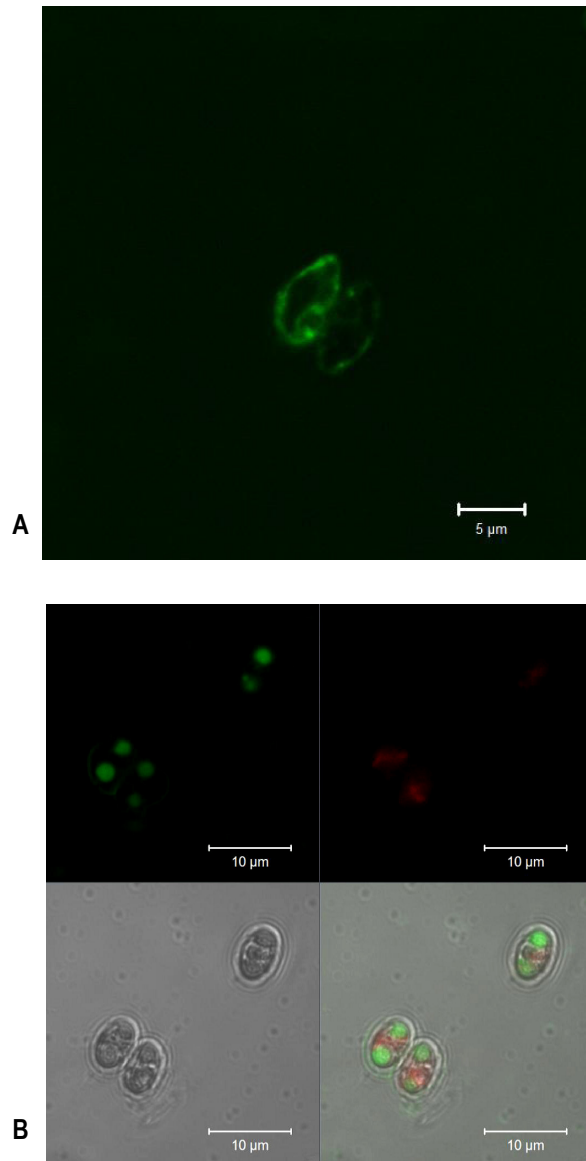


Figure 3.48.

Confocal micrograph showing

(A) Fluorescence image of unstressed *D. primolecta* using bodipy 505/515 dye stain.

(B) Split fluorescence image of stressed *D. primolecta* using bodipy 505/515 dye stain visualizing the lipid bodies (top left) and chlorophyll (top right), DIC image (bottom left) and a composite image of all the fluorescence patterns (bottom right).

* DIC: differential interference contrast (imaging)

Cooper *et al.* (2010) reported that lipidic fluorescence emission was captured using 488 nm excitation wavelength and a 500- to 530- nm band - pass emission filter. Autofluorescence emission was acquired using a 610- nm long - pass filter with the same excitation. In this study, lipidic fluorescence of the unstressed algal cultures was captured in the range of 517 - 537 nm (Figures 3.47A and 3.48A), whilst chloroplast fluorescent emission was attained in the range of 673 - 702 nm (Figures 3.52 and 3.53). For both algal components, the 488 - nm argon laser was used for the excitation of fluorophores. As a result of the minimal literature published on the use of bodipy 505/515 for the visualisation of neutral lipids and phospholipids in algal species, it is difficult to indicate conclusively as to the exact wavelength range that one would detect these specific components. Therefore, one can assume that these components may be detected at a similar wavelength range as produced by the lipidic bodies. In the case of stressed cultures, the 488- nm excitation laser was used for the capture of fluorescence of lipidic bodies in the range of 490 - 540 nm (Figures 3.47B and 3.48B). A 633nm laser was used to read the fluorescence emission from a range of 637 - 721nm (Figures 3.47C and 3.48B). This is the range for chlorophyll detection. Lastly, the 488nm laser was used to read the fluorescence emission from a range of 415 - 726nm for the light microscope image (DIC) of the stressed *C. vulgaris* alga. Analysis of the graphical plots (Figures 3.49 - 3.52) shows sharper peaks in the region of approximately 500 - 540 nm, which is the region known for lipidic fluorescence, in the stressed algal cultures rather than the unstressed. This supports the hypothesis that nitrogen - deficient cultures will develop higher percentage lipid content than N - sufficient cultures (Weldy and Huesemann, 2007).

The fluorescent intensity measurements revealed by the graphical representations (Figures 3.49 - 3.52) correlate with fluorescence emitted by the algal culture when emission is captured in the lambda stack images at the range of 420 - 702 nm (Figures 3.53 - 3.56). According to the lambda stack of the unstressed *C. vulgaris* alga (Figure 3.53), the lipidic fluorescence is not seen as the intensity was too low; this is evident by the peak generated in the corresponding graphical representation (Figure 3.49). The different coloured peak emissions on the graphical representations do not indicate specific algal components but rather different locations in the algal cell.

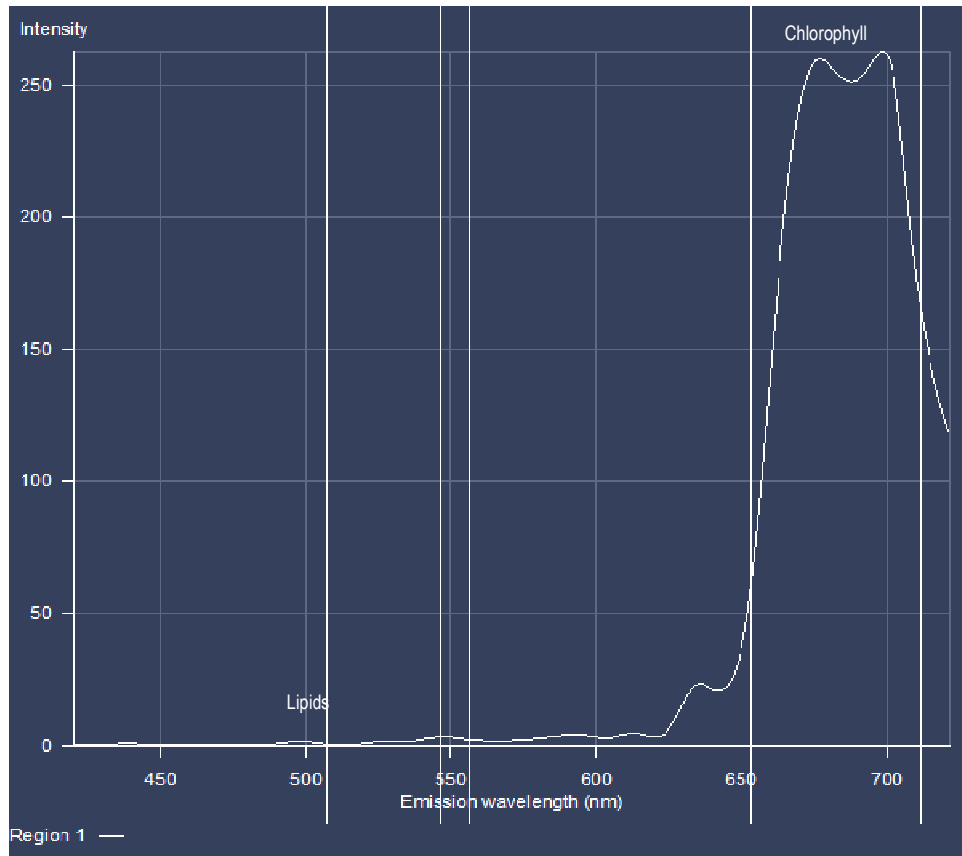


Figure 3.49. Graphical representation of the intensity of fluorescence emitted by unstressed *C. vulgaris* cells in the range of 420 - 722nm.

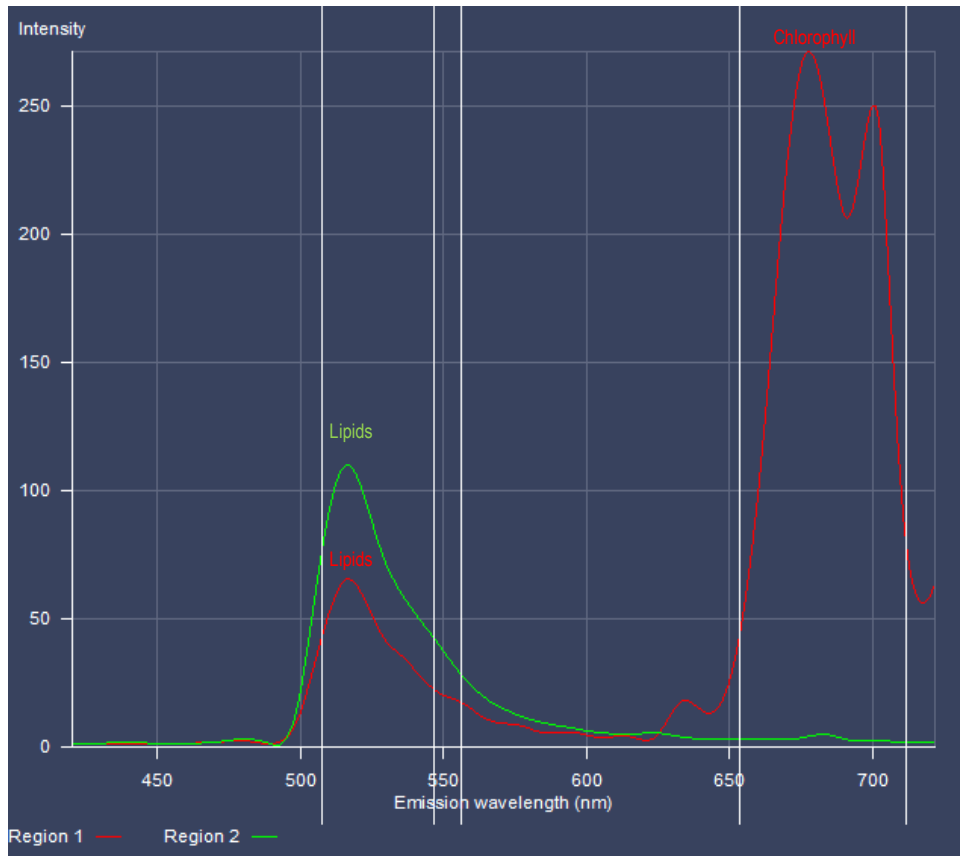


Figure 3.50. Graphical representation of the intensity of fluorescence emitted by stressed *C. vulgaris* cells in the range of 420 - 722nm.

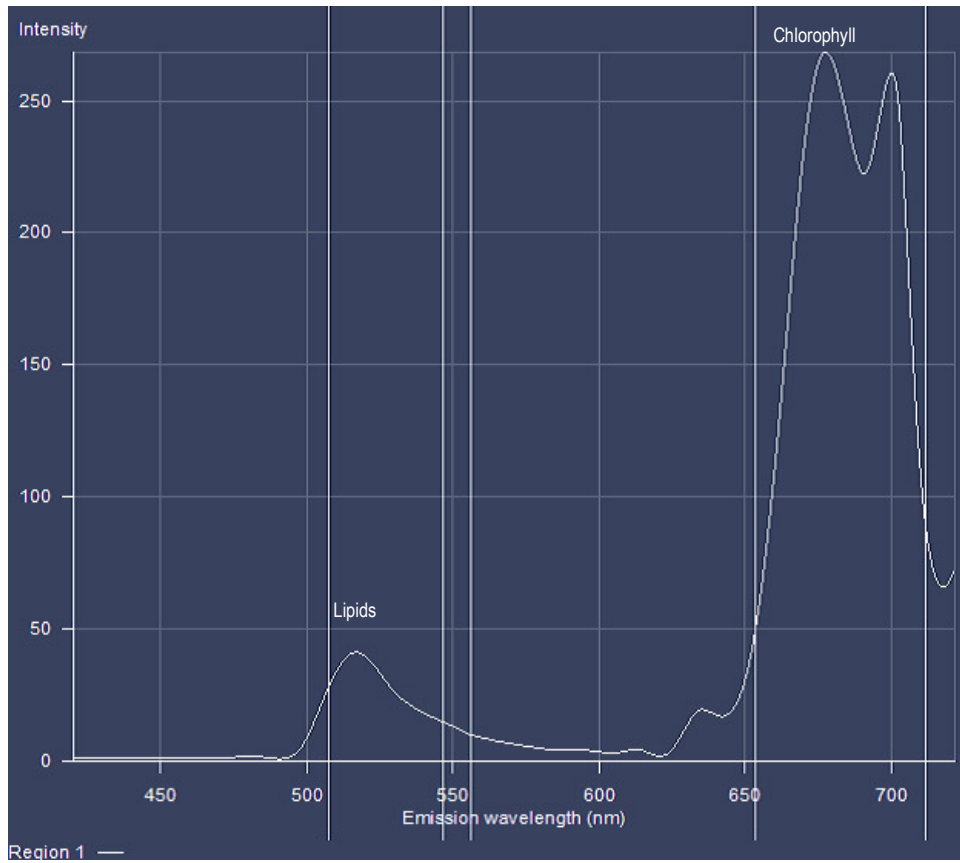


Figure 3.51. Graphical representation of the intensity of fluorescence emitted by unstressed *D. primolecta* cells in the range of 420 - 722nm.

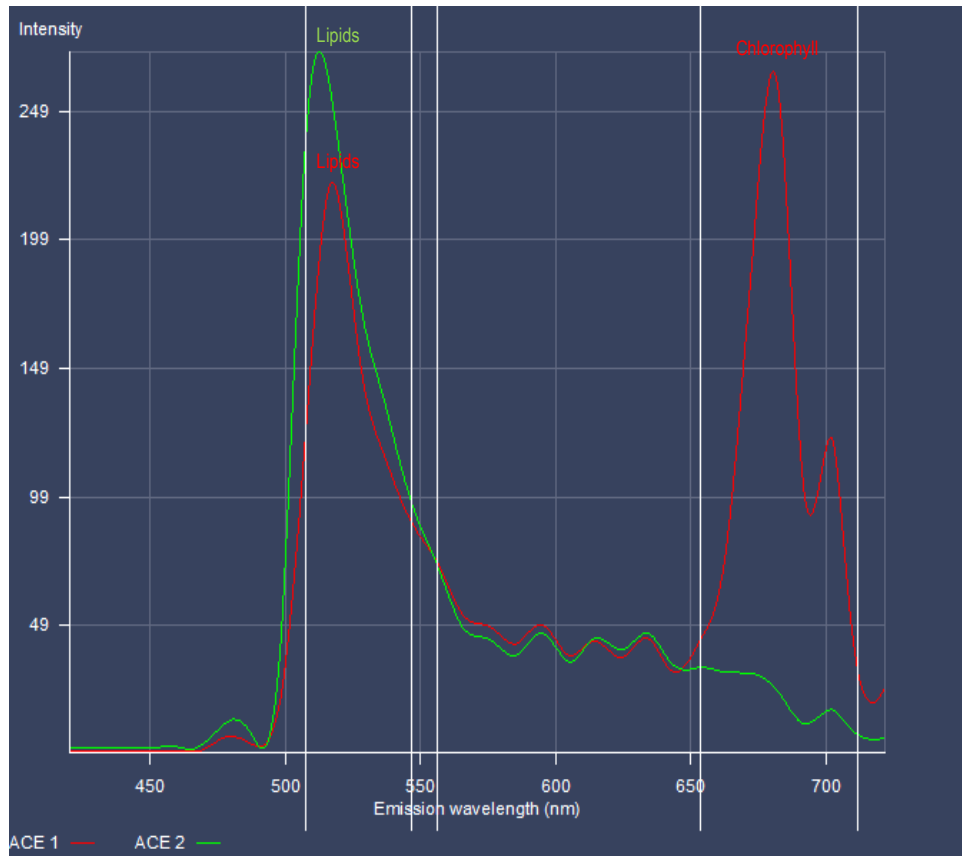


Figure 3.52. Graphical representation of the intensity of fluorescence emitted by stressed *D. primolecta* cells in the range of 420 - 722nm.

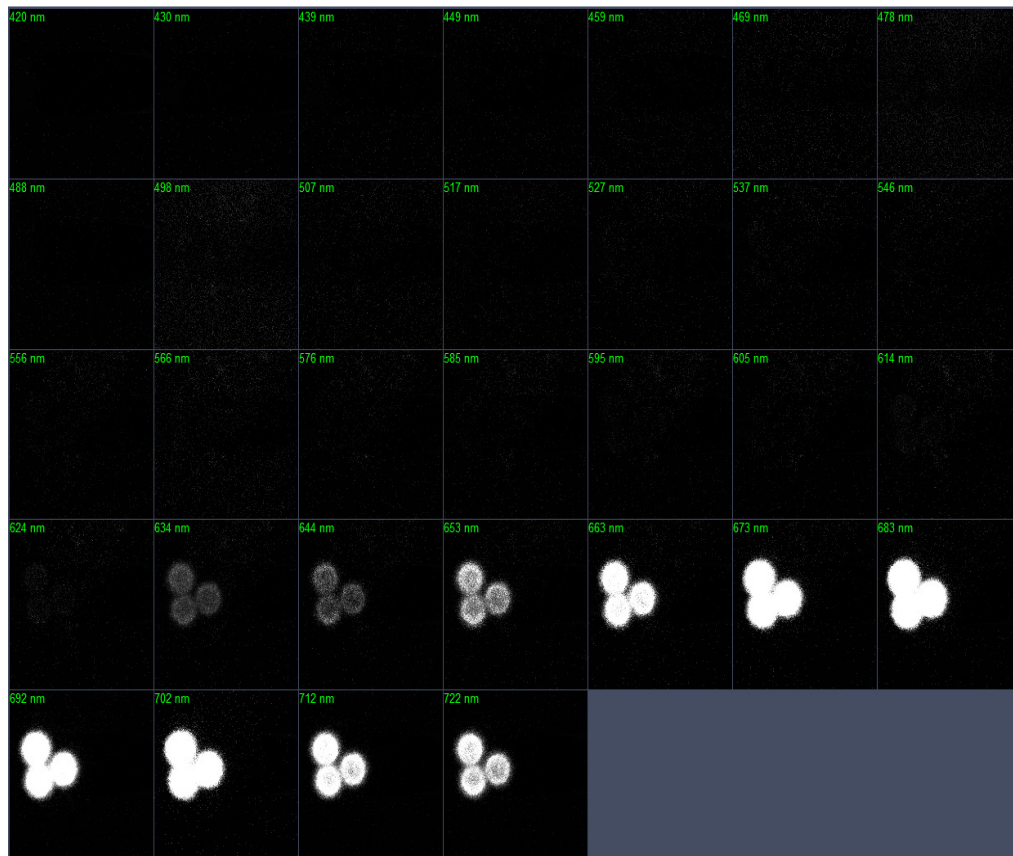


Figure 3.53. Wavelength scanning of fluorescence pattern observed in unstressed *C. vulgaris* cells subject to bodipy staining indicating chlorophyll fluorescence at 673 nm.

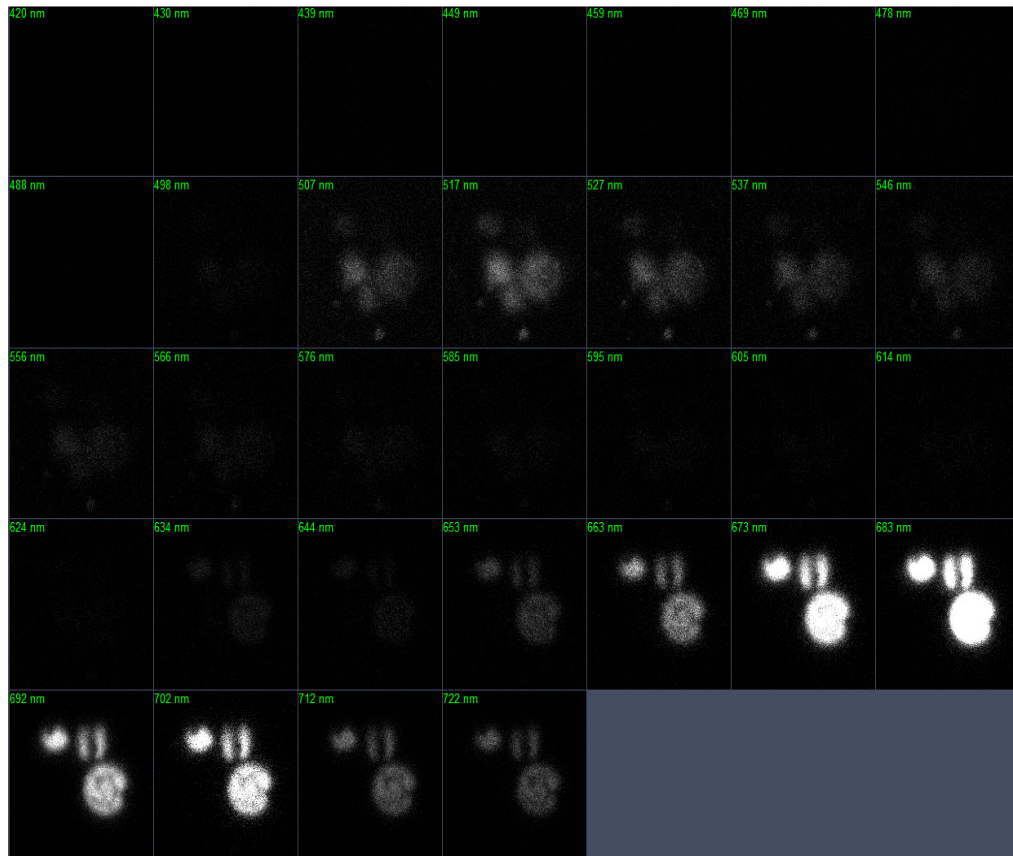


Figure 3.54. Wavelength scanning of fluorescence pattern observed in stressed *C. vulgaris* cells subject to bodipy staining indicating lipidic and chlorophyll fluorescence at 517 and 663 nm, respectively.

Table 3.14. Confocal parameters of lipid detection in *C. vulgaris*

Unstressed <i>C. vulgaris</i>				
Confocal microscope setting	Digital parameters			
	Microscope image	Lambda stack and graphical representation		
Master gain	850	875		
Digital gain	1	1		
Digital offset	1	1		
Bit depth	8	8		
Pinhole	168.4 (1 AU) airy unit	178.4 (1 AU) airy unit		
Average number	2	2		
Frame size	512 x 512	512 x 512		
Stressed <i>C. vulgaris</i>				
Confocal microscope setting	Digital parameters			
	Micrograph (B)	Split image (C) Green channel	Split image (C) Red channel	Lambda stack and graphical representation
Master gain	800	820	700	900
Digital gain	1	1	1	1
Digital offset	1	1	1	1
Bit depth	8	8	8	8
Pinhole	56.1 (1 AU)	60 (1 AU)	60 (1 AU)	56.1 (1 AU)
Average number	2	4	2	2
Frame size	512 x 512	512 x 512	512 x 512	512 x 512

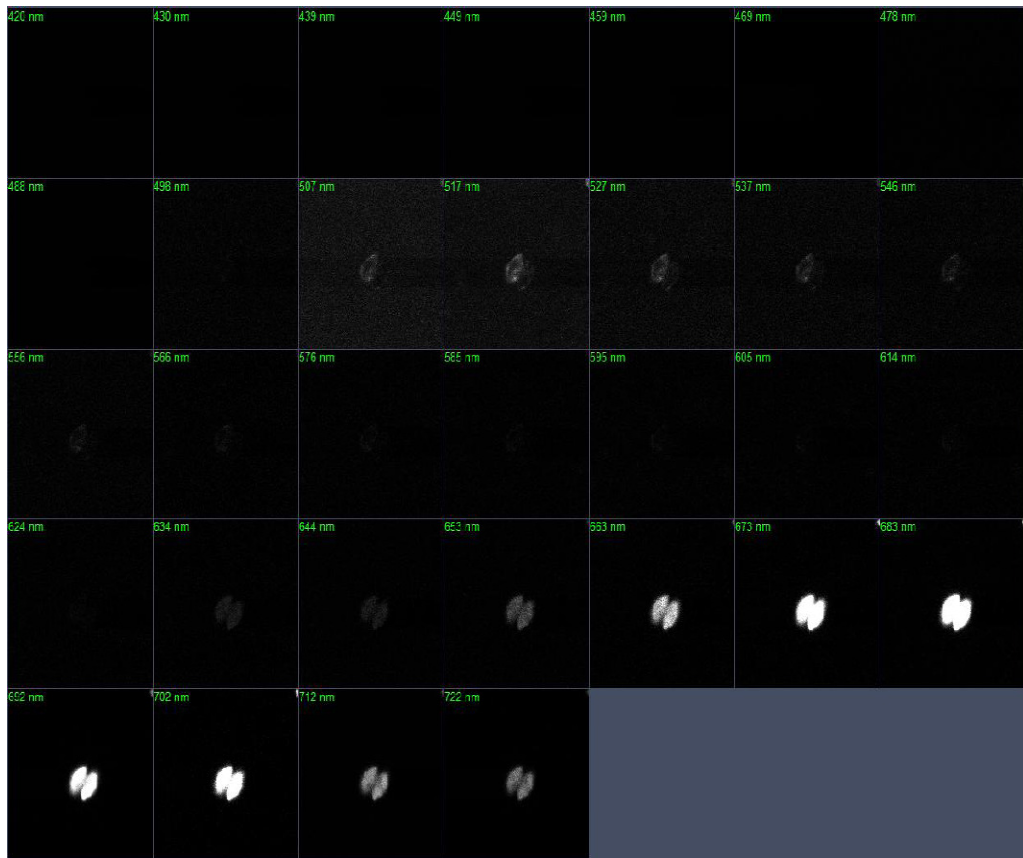


Figure 3.55. Wavelength scanning of fluorescence pattern observed in unstressed *D. primolecta* cells subject to bodipy staining indicating lipidic and chlorophyll fluorescence at 517 and 673 nm, respectively.

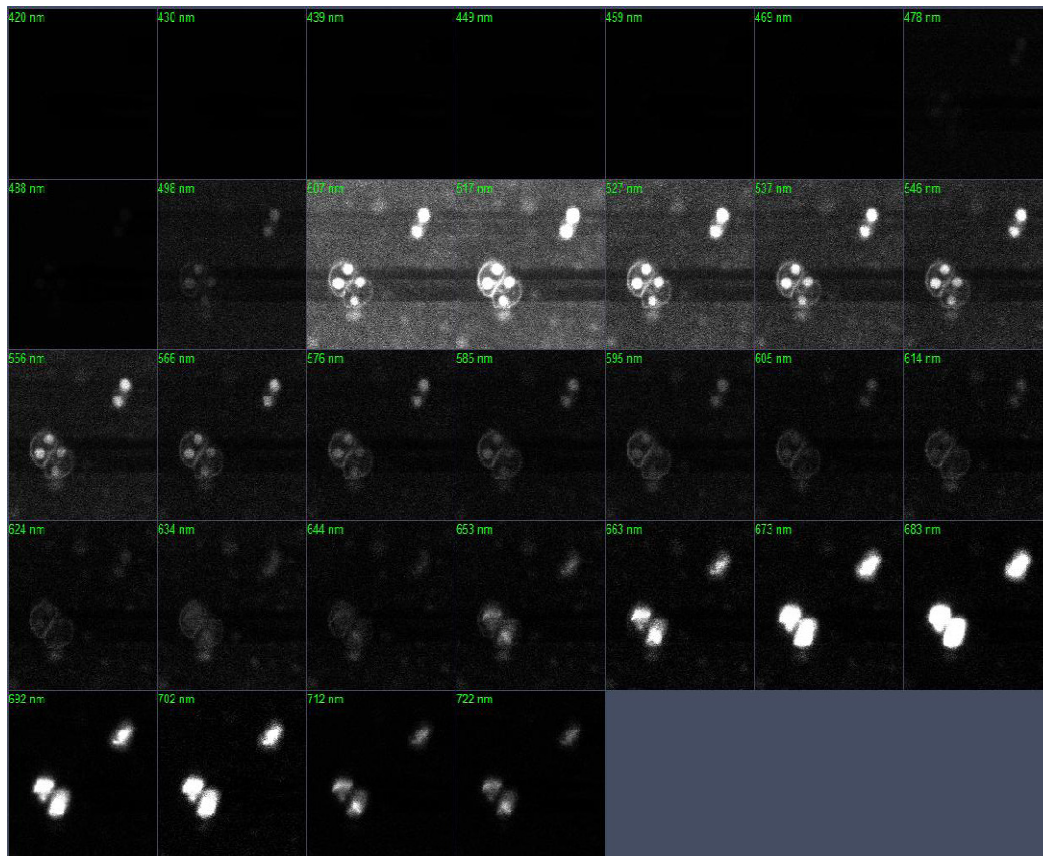


Figure 3.56. Wavelength scanning of fluorescence pattern observed in stressed *D. primolecta* cells subject to bodipy staining indicating lipidic and chlorophyll fluorescence at 517 and 617 nm, respectively.

Table 3.15. Confocal parameters of lipid detection in *D. primolecta*

Unstressed <i>D. primolecta</i>				
Confocal microscope setting	Digital parameters			
	Microscope image	Lambda stack and graphical representation		
Master gain	755	900		
Digital gain	1	1		
Digital offset	1	1		
Bit depth	8	8		
Pinhole	168.4 (1 AU) airy unit	178.4 (1 AU) airy unit		
Average number	2	2		
Frame size	512 x 512	512 x 512		
Stressed <i>D. primolecta</i>				
Confocal microscope setting	Digital parameters			
	Green channel	Red channel	*DIC	Lambda stack and graphical representation
Master gain	800	820	700	900
Digital gain	1	1	1	1
Digital offset	1	1	1	1
Bit depth	8	8	8	8
Pinhole	56.1 (1 AU)	60 (1 AU)	60 (1 AU)	56.1 (1 AU)
Average number	2	2	2	2
Frame size	512 x 512	512 x 512	512 x 512	512 x 512

CHAPTER FOUR

CONCLUSIONS

According to the literature, nutrient limitation or high light intensity is known to trigger triacylglycerol (TAG) accumulation (Tomabene *et al.*, 1983; Uriarte *et al.*, 1993; Gordillo *et al.*, 1998; Su *et al.*, 2003; Carvalho and Xavier Malcata, 2005; Weldy and Huesemann, 2007; Chen *et al.*, 2010). Spoehr and Milner (1949) initially reported the accumulation of lipidic bodies in algal cells when grown in nitrogen - deprived media. In the present study, the oil - hydrocarbon yields for *Chlorella vulgaris* and *Dunaliella primolecta*, in a nitrogen - deprived environment were 0.01 % and 0.02 % greater, respectively than when grown in conventional BG 11 medium (Appendix A). In spite of the relatively low increments when compared to literature, autotrophic propagation results in low oil yields as natural sunlight is the sole source of energy, coupled with CO₂ sequestration from air as the source of carbon. CO₂ supplementation may aid the evaluation of lipid production (Chinnasamy *et al.*, 2009; Khozin - Goldberg and Cohen, 2010). A block in starch biosynthesis yields also enhances formation of lipidic bodies and TAG. Starch biosynthesis is impaired in the *sta6* mutant of *Chlamydomonas reinhardtii* harbouring a mutation that leads to inactivation of ADP - glucose pyrophosphorylase. In this nitrogen - starved mutant, Khozin - Goldberg and Cohen (2010) reported a 30 - fold increase in the cellular content of lipid bodies thus, providing direct evidence that genetic interference of the starch biosynthesis pathway can stimulate lipid accumulation. A further study conducted by Li *et al.* (2010) revealed a 10 - fold increase in cellular TAG production when a starchless mutant of the *C. reinhardtii* was exposed to stressful conditions. Modification of fatty acid chain length and levels of saturation to produce monosaturated and saturated TAG, the ideal form of biodiesel, can be further accomplished via the silencing of desaturases and expression of thioesterases. These studies were made possible by understanding lipid metabolism in higher plants (Khozin - Goldberg and Cohen, 2010) and the success of manipulating lipid - biosynthesis pathways with molecular tools (Khozin - Goldberg and Cohen, 2010). Moreover, these strategies can be applied to algae which produce greater levels of TAG under stressful

conditions and are amendable to genetic manipulation. Another feasible approach, to modulate lipid metabolism, is the regulation of gene expression by transcription (Khozin - Goldberg and Cohen, 2010; Moellering and Benning, 2010).

The newly discovered major lipid droplet protein (MLDP) is considered rare and unique to green algae (Moellering and Benning, 2010). The expression of its gene is strictly limited to conditions favouring TAG biosynthesis thus, providing indirect evidence for a role of this protein in lipid droplet formation or maintenance. These properties could potentially yield MLDP a marker for lipid droplets and TAG accumulation. The ability of cells to accumulate polyunsaturated fatty acids (PUFAs) intrinsically is limited in most algae, since fatty acids are generally components of membranal lipids; whose content is strictly regulated (Bigogno *et al.*, 2002).

This study has shown:

- I. Lipid bodies accumulate in microalgae when grown in nitrogen - restricted BG 11 medium although biomass accumulation is impeded as also shown by Uriarte *et al.* (1993) in their studies involving *D. primolecta*.
- II. The hexane soluble oil - hydrocarbon fraction of *C. vulgaris* and *D. primolecta* cells contained acylglycerols, phospholipids, carotenoids and chlorophyll. TLC analyses and spectrophotometry gave a tentative identification of these components and their differing R_f and spectral properties in test and control cultures.
- III. Nile red differentiated fluorescence patterns of neutral lipids, phospholipids and chlorophyll. The ZEN software of the Zeiss LSM 710 confocal microscope generated graphical fluorescence plots against specific wavelengths to confirm the fluorescent components reported by similar published data. Fluorescent component addition was confirmed using the lambda stack facility which enabled sequential wavelength scanning and pseudo - colouring of each component. Bodipy fluorescence could only distinguish between the composite oil body and chlorophyll.
- IV. Protein analyses from the algal oil proved to be difficult as extraction procedures could have denatured protein components into subunit structure. In comparison with the data presented by Moellering and Benning (2010) where 259 proteins were estimated from the oil of *C. reinhardtii*, it is likely that a band smear will result if a similar protein mixture is separated by PAGE. This is especially true for protein mixtures where molecular

weights differ by small increments. The effect of protein extractants, urea and SDS, do affect protein quantitation from algal oil as determined using the Bio - Rad RC - DC quantitation kit. Nitrogen starvation correlated with lower protein content in the oil of *C. vulgaris* although *D. primolecta* oil showed similar yields of protein from test and control cultures, regardless of nitrogen supplementation or exclusion, respectively.

- V. The predominant fatty acid of all algae tested herein was the palmitic acid methyl ester especially in control nitrogen - starved cultures of *D. primolecta*. Nitrogen starvation also correlated with production of the C18 stearic acid fatty acid in both *D. primolecta* and *C. vulgaris*. In addition, only *D. primolecta* produced linolelaidic acid (C18:2n6t) under both test and control conditions. The longest fatty acid chain, namely, the C22:0 docosanoic acid fatty acid, was produced by *C. vulgaris* under test conditions involving nitrogen supplementation.

The current study has identified key components associated with oil of *Chlorella vulgaris* and *Dunaliella primolecta*, however their role and structural assembly within the oil droplet itself requires further study.

REFERENCES

Arad Malis, S., Cohen, E. and Ben - Amotz, A. (1993) Accumulation of canthaxanthin in *Chlorella emersonii*. *Physiologia Plantarum*, **87** (22): 232 - 236.

Azúa - Bustos, A., González - Silva, C., Salas, L., Palmer, R. E. and Vicuña, R. (2010) A novel subaerial *Dunaliella* species growing on cave spiderwebs in the Atacama Desert. *Extremophiles*, **14**: 443 - 452.

Barbosa, M.J.G.V. (2003) Microalgal photobioreactors: scale up and optimization, University of Wageningen, Netherlands (PhD thesis).

Belarbi, E.H., Molina, E. and Chisti, Y. (2000) A process for high yield and scaleable recovery of high purity eicosapentaenoic acid esters from microalgae and fish oil. *Enzyme Microbial Technology*, **26**, 516 - 29.

Ben - Amotz, A., Shaish, A. and Avron, M. (1989) Mode of action of the massively accumulated β - carotene of *Dunaliella bardawil* in protecting the alga against damage by excess irradiation. *Plant Physiology*, **91**, 1040 - 1043.

Ben - Amotz, A., (1999) Production of β - carotene from *Dunaliella*. *Chemicals from Microalgae*, **3**, 196 - 204.

Berkelman, T., Petersen, S., Sun, C. and Cater, S. (2009) Mini - PROTEAN TGX precast gel: A gel for SDS - PAGE with improved stability - comparison with standard Laemmli gels. *Bio - Rad Bulletin 5910 Rev B*, 1203 - 1210.

Bernart, M.W., Whatley, G.G. and Gerwick, W.H. (1993) Unprecedented oxylipins from the marine green alga *Acrosiphonia coalita*. *Journal of Natural Products*, **56**: 245 - 259.

Bigogno, C., Goldberg, I. K., Boussiba, S., Vonshak, A. and Cohen, Z. (2002) Lipid and fatty acid composition of the green oleaginous alga *Parietochloris incisa*, the richest plant source of arachidonic acid. *Phytochemistry*, **60**, 497 - 503.

Bleé, E. (2002) Impact of phyto-oxylipins in plant defense. *Trends in Plant Science*, **7**: 315 - 321.

Blumberg, L.M. and Klee, M.S. (2001) Quantitative comparison of performance of isothermal and temperature - programmed gas chromatography. *Journal of Chromatography A*, **933**, 13 - 26.

Böck, G., Recheis, H. and Wick, G. (1993) Anti-fading embedding media in confocal immunofluorescence microscopy. *Journal of Fluorescence*, **3**: 173 - 178.

Brdička, R. (1936) The kinetics of saponification of iodoacetic acid by sodium hydroxide and certain alkaline buffer solutions. *Journal of General Physiology*, **19**: 899 - 906.

Brennan, L., Blanco, F.A., Mostaert, A.S. and Owende, P. (2012) Enhancement of bodipy 505/515 lipid fluorescence method for application in biofuel - directed microalgae production. *Journal of Microbiological Methods*, **90** (2): 137 - 143.

Butcher, R. W. (1959) An introductory account of the smaller algae of British coastal waters. Part 1: Introduction and Chlorophyceae. Vol. ser. IV (Part 1) pp. 74. Great Britain: Minist. Agric. Fish. Fodd, Fish.

Carvalho, A. P. and Xavier Malcata, F. (2005) Optimization of ω - 3 fatty acid production by microalgae: crossover effects of CO₂ and light intensity under batch and continuous cultivation modes. *Marine Biotechnology*, **7**, 381 - 388.

Chen, W., Sommerfield, M. and Hu, Q. (2011) Microwave - assisted Nile red method for the *in vivo* quantitation of neutral lipids in microalgae. *Bioresource Technology*, **102**: 135 - 141.

Chen, M., Tanga, H., Maa, H., Holland, C.T., Simon, K.Y. and Salleya, O.S. (2010) Effect of nutrients on growth and lipid accumulation in the green algae *Dunaliella tertiolecta*. *Bioresource Technology*, **102**: 1649 - 1655.

Chen, W., Zhang, C., Song, L., Sommerfeld, M. and Hu, Q. (2009) A high throughput Nile red method for quantitative measurement of neutral lipids in microalgae. *Journal of Microbiological Methods*, **77**: 41 - 47.

Cheng, K.C. and Ogden, L.K. (2011) Algal Biofuels: The Research. *The American Institute of Chemical Engineers (AIChE)*, **43**, 134 - 138.

Chinnasamy, S., Ramakrishnan, B., Bhatnagar, A. and Das, K.C. (2009) Biomass production potential of a wastewater alga *Chlorella vulgaris* ARC 1 under elevated levels of CO₂ and temperature. *International Journal of Molecular Science*, **10**, 518 - 532.

Chirac, C., Casadevall, E., Largeau, C. and Metzger, P. (1985) Bacterial influence upon growth and hydrocarbon production of the green alga *Botryococcus braunii*. *Phycology*, **21**, 380 - 387.

Chisti, Y. (2007) Biodiesel from microalgae. *Biotechnology Advances*, **25**, 294 - 306.

Chisti, Y. (2008) Biodiesel from microalgae beats bioethanol. *Trends in Biotechnology* **26**, 126 - 130.

Cooper, M.S., Hardin, W.R., Petersen, T.W. and Cattolico, R.A. (2010) Visualizing "green oil" in live algal cells. *Journal of Bioscience and Bioengineering*, **109**: 198 - 201.

Dahlqvist, A., Stahl, U., Lenman, M., Banas, A., Lee, M., Sandager, L., Ronne, H. and Stymne, S. (2000) Phospholipid:diacylglycerol acyltransferase: an enzyme that catalyzes the acyl - CoA - independent formation of triacylglycerol in yeast and plants. *Proc. Natl Acad. Sci. USA*, **97**, 6487 - 6492.

Danks, S.M., Evans, E.H. and Whittaker, P.A. (1983) Photosynthetic systems: structure, function and assembly, John Wiley and Sons Limited, UK (<http://www.google.com>).

Davidi, L. and Pick, U. (2012) Oil globule proteins in oleaginous green microalgae. <http://www.weizmann.ac.il/conferences/brew2011/sites/Weizmann.ac.il>

Dayananda, C., Sarada, R., Kumar, V. and Ravishankar, G.A. (2007a) Isolation and characterization of hydrocarbon producing green alga *Botryococcus braunii* from Indian freshwater bodies. *Electronic Journal of Biotechnology*, **10**: 79 - 97.

Dayananda, C., Sarada, R., Usha Rani, M., Shamala, T.R. and Ravishankar, G.A. (2007b) Autotrophic cultivation of *Botryococcus braunii* for the production of hydrocarbons and exopolysaccharides in various media. *Biomass and Bioenergy*, **31**, 87 - 93.

De la Jara, A., Mendoza, H., Martel, A., Molina, C., Nordström, L., De la Rosa, V. and D'íaz, R. (2003) Flow cytometric determination of lipid content in a marine dinoflagellate, *Cryptothecodinium cohnii*. *Journal of Applied Phycology*, **15**, 433 - 438.

Demirbas, A. (2008) Biodiesel production via rapid transesterification. *Energy Sources Part A*, **30**, 1830 - 1840.

Don - Hee, P., Hwa - Won, R., Ki - Young, L., Choon - Hyoung, K., Tae - Ho, K., and Hyeon - Yong, L., (1998) The production of hydrocarbons from photoautotrophic growth of *Dunaliella salina* 1650. *Applied Biochemistry and Biotechnology*, **70**, 739 - 746.

Elsay, D., Jameson, D., Raleigh, B. and Cooney, M.J. (2007) Fluorescent measurement of microalgal neutral lipids. *Journal of Microbiological Methods*, **68**, 639 - 642.

Figueroa, F.L., Israel, A., Neori, A., Martínez, B., Malta, E.J., Put, A., Inken, S., Marquardt, R., Abdala, R. and Korbee, N. (2010) Effect of nutrient supply on photosynthesis and pigmentation to short - term stress (UV radiation) in *Gracilaria conferta* (Rhodophyta). *Marine Pollution Bulletin*, **10**, 1 - 11.

Fowler, S. D., Brown, W. J., Warfel, J. and Greenspan, P. (1987) Use of Nile red for the rapid *in situ* quantitation of lipids on thin layer chromatograms. *Journal of Lipid Research*, **28**, 1225 - 1232.

Fowler, S.D. and Greenspan, P. (1985) Application of Nile red, a fluorescent hydrophobic probe, for the detection of neutral lipid deposits in tissue sections: Comparison with oil red O. *Journal of Histochemistry and Cytochemistry*, **33** (8): 833 - 836.

Frandsen, G.I., Mundy, J. and Tzen, J.T.C. (2001) Oil bodies and their associated proteins, oleosin and caleosin. *Physiologia Plantarum*, **112**, 301 - 307.

Garcia - Gonzalez M., Manzano, J.C., Moreno, J. and Guerrero, M.G., (2000) Biotecnología del cultivo de *Dunaliella salina* en el litoral andaluz. Pesca y Acuicultura. Consejería de Agricultura y Pesca. Spain, **16**, 163.

Garcia, F., Freile - Pelegrin, Y. and Robledo, D. (2007) Physiological characterization of *Dunaliella* sp. (*Chlorophyta*, *Volvocales*) from Yucatan, Mexico. *Bioresource Technology*, **98**, 1359 - 1356.

Geider, R. J., LaRoche, J., Greene, R. M. and Olaizola, M. (1993) Response of the photosynthetic apparatus of *Phaeodactylum tricornutum* (Bacillariophyceae) to nitrate, phosphate or iron starvation. *Journal of Phycology*, **29**, 755 - 66.

Gibbs, N. and Duffus, C.M. (1976) Natural protoplast *Dunaliella* as a source of protein. *Applied Environmental Microbiology*, **31**, 602 - 604.

Goldberg, I.K. and Cohen, Z. (2006) The effect of phosphate starvation on lipid and fatty acid composition of the freshwater eustigmatophyte *Monodus subterraneus*. *Phytochemistry*, **67**, 696 - 701.

Golueke, C. and Oswald, W. (1968) Power from solar energy via algae - produced methane. *Solar Energy*, **7**: 86 - 92.

Gordillo, F.J.L., Goutx, M., Figueroa, F.L. and Niell, X.F. (1998) Effects of light intensity, CO₂ and nitrogen supply on lipid class composition of *Dunaliella viridis*. *Journal of Applied Phycology*, **10**, 135 - 144.

Govender, T., Ramanna, L., Rawat, I. And Bux, F. (2012) Bodipy staining, an alternative to the Nile red fluorescence method for the evaluation of intracellular lipids in microalgae. *Bioresource Technology*, **114**, 507 - 511.

Greenspan, P., Mayer E.P. and Fowler, S.D. (1985) Nile red: a selective fluorescent stain for intracellular lipid droplets. *Journal of Cell Biology*, **100**, 965 - 973.

Griffiths, M. J. and Harrison, S. T. L. (2009) Lipid productivity as a key characteristic for choosing algal species for biodiesel production. *Journal for Applied Phycology*, **21**, 493 - 507.

Gupthar, A. S. (2012) Personal Communication. UKZN, Dept. of Biochemistry, Durban, SA.

Gurr, M. I. and James, A. T. (1980) Lipid biochemistry, an introduction. Science Paperback, Great Britain.

Guschina, I. A. and Harwood, J. L. (2006) Oleosin articles: Lipids and lipid metabolism in eukaryotic algae. *Progress in Lipid Research*, **45**, 160 - 186.

Halim, R., Rupasinghe, T. W. T., Tull, D. L. and Webley, P. A. (2013) Mechanical disruption for lipid extraction from microalgal biomass. *Bioresource Technology*. **140**, 53 - 63.

Heftmann, E. (2004) Chromatography fundamentals and application of chromatographic and electrophoretic methods. *Journal of Chromatography Library*, **2**, 2.

Held, P. and Raymond, K. (2011) Determination of algal cell lipids using Nile red - using microplates to monitor neutral lipids in *Chlorella vulgaris*. *Biofuel Research*, **7**: 67 - 69.

Hsieh, K. and Huang, A.H.C. (2004) Endoplasmic reticulum, oleosins and oils in seeds and tapetum cells. *Plant Physiology*, **136**, 3427 - 3434.

Hu, Q., Sommerfeld, M., Jarvis, E., Ghirardi, M., Posewitz, M., Seibert, M. and Darzins, A. (2008) Microalgal triacylglycerols as feedstock for biofuel production: perspectives and advance. *Plant Journal*, **54**, 621 - 639.

Jian, Y.L. and Qin, G. (2005) Comparison of growth and lipid content in three *Botryococcus braunii* strains. *Journal of Applied Phycology*, **17**, 551 - 556.

Johnson, E.T. and Schmidt - Dannert, C. (2008) Light - energy conversion in engineered micro - organisms. *Trends in Biotechnology*, **26** (12): 682 - 689.

Johnson, M. B. and Wen, Z. (2009) Production of biofuel from the microalga *Schizochytrium limacinum* by direct transesterification of algal biomass. *Energy Fuels*, **23**, 5179 - 5183.

Katz, A., Carlos, J. and Uri, P. (1995) Isolation and characterization of a protein associated with carotene globules in the alga *Dunaliella badawii*. *Plant Physiology*, **108**, 1657 - 1664.

Kenyon, N.C. (1972) Fatty acid composition of unicellular strains of blue - green algae, *Journal of Bacteriology*. **109** (2): 827 - 834.

Khozin - Goldberg, I. and Cohen Z. (2010) Unraveling algal lipid metabolism: Recent advances in gene identification. *Biochemie*, **7**, 1 - 10.

Kim, M.K., Park, J.W., Park C.S., Kim, S.J., Jeune, K.H., Chang, M.U. and Acreman, J. (2007) Enhanced production of *Scenedesmus* spp. (green microalgae) using a new medium containing fermented swine wastewater. *Bioresource Technology*, **98**, 2220 - 2228.

Kimura, K., Yamaoka, M. and Kamisaka, Y. (2004) Rapid estimation of lipids in oleaginous fungi and yeasts using Nile red fluorescence. *Journal of Microbiological Methods*, **56**, 331 - 338.

Lang, I.D. (2007) New fatty acids, oxylipins and volatiles in microalgae, University of Göttingen, Germany (pHD Thesis).

LaRoche, J., Geider, R. J., Graziano, L. M., Murray, H. and Lewis, K. (1993) Induction of specific proteins in eukaryotic algae grown under iron, phosphorus, or nitrogen - deficient conditions. *Journal of Phycology*, **29**, 767 - 77.

Lee, S.J., Kim, S.B., Kim, J.E., Kwon, G.S., Yoon, B.D. and Oh, H.M. (1988) Effect of harvesting method and growth stage on the flocculation of the green alga *Botryococcus braunii*. *Journal of Applied Microbiology*, **27**: 14 - 18.

Li, Y. and Qin, J.G. (2005) Comparison of growth and lipid content in three *Botryococcus braunii* strains. *Journal of Applied Phycology*, **17**, 551 - 556.

Li, Y., Han, D., Hu, G., Dauvillee, D., Sommerfeld, M., Ball, S. and Hu, Q. (2010) *Chlamydomonas* starchless mutant defective in ADP - glucose pyrophosphorylase hyperaccumulates triacylglycerol. *Metabolic Engineering*, **12** (4): 387 - 391.

Lv, J.M., Cheng, L.H., Xu, X.H., Zhang, L. and Chen, H.L. (2010) Enhanced lipid production of *Chlorella vulgaris* by adjustment of cultivation conditions. *Bioresource Technology*, **101**, 6797 - 6804.

Miao, X. and Wu, Q. (2006) Biodiesel production from heterotrophic microalgal oil. *Bioresource Technology*, **97**, 841 - 846.

Mock, T. and Kroon, B.M.A. (2002) Photosynthetic energy conversion under extreme conditions - II: the significance of lipids under light limited growth in Antarctic sea ice diatoms. *Phytochemistry*, **61**, 53 - 60.

Moellering, E.R. and Benning, C. (2010) RNA interference silencing of a major lipid droplet protein affects lipid droplet size in *Chlamydomonas reinhardtii*. *Journal of Eukaryotic Cells*, **9**: 97 - 106.

Molina, E., Fernandez, J., Acie, F.G. and Chisti, Y. (2001) Tubular photobioreactor design for algal cultures. *Journal of Biotechnology*, **92**, 113 - 131.

Montes D'Oca, M. G., Viegas, C. V., Lemos, J. S., Miyasaki, E. K., Morón - Villarreyes, J. A., Primel, E. G. and Abreu, P. C. (2011) Production of FAMES from several microalgal lipidic extracts and direct transesterification of the *Chlorella pyrenoidosa*. *Biomass and Bioenergy*, **35**, 1533 - 1538.

Murphy, D.J. (2004) The roles of lipid bodies and lipid - body proteins in the assembly and trafficking of lipids in plant cells. Biotechnology unit, University of Glamorgan, United Kingdom.

Panday, B.P. (1994) A textbook of botany: algae. S. Chand and Company Limited, Ram Nagar, New Delhi.

Pinchetti, J.L.G., Fernández, E.C., Diez, P.M. and Reina, G.G. (2009) Nitrogen availability influences the biochemical composition and photosynthesis of tank - cultivated *Ulva rigida* (Chlorophyta). *Journal of Applied Phycology*, **10**: 383 - 389.

Pisal, S.D. and Lele, S.S. (2004) Carotenoid production from microalga, *Dunaliella salina*. *Indian Journal of Biotechnology*, **4**, 476 - 483.

Patil, V., Källqvist, T., Olsen, E., Vogt, G. and Gislerød, H. R. (2007) Fatty acid composition of 12 microalgae for possible use in aquaculture feed. *Aquaculture International*, **15**, 1 - 9.

Plummer, D.T. (1987) Practical Biochemistry 3rd edition. McGRAW - HILL. England.

Pollack, J.D., Clark, D.S. and Somerson, N.L. (1971) Four-directional-development thin layer chromatography of lipids using trimethyl borate. *Journal of Lipid Research*, **12**, 563 - 569.

Qin, J. (2005) Bio-Hydrocarbons from Algae: Impacts of temperature, light and salinity on algae growth; Rural Industries Research and Development Corporation (Report to the Australian government: <http://rirdc.infoservices.com.au/downloads/05-025.pdf>).

Ra, T. (2010) Observation and Lipid Production from Microalgae, University of Biotechnology, Myanmar (pHD Thesis).

Rabbani, S., Beyer, P., Von Lintig, J., Hugueney, P. and Kleinig, H., (1998) Induced beta - carotene synthesis driven by triacylglycerol deposition in the unicellular alga *Dunaliella bardawil*. *Plant Physiology*, **116**, 1239 - 1248.

Rao, A. R., Dayananda, C., Sarada, R., Shamala, T. R. and Ravishankar, G. A. (2007). Effect of salinity on growth of green alga *Botryococcus braunii* and its constituents. *Bioresource Technology*, **98**, 560 - 564.

Rubio - Rodríguez, N., Beltrán, S., Jaime, I., Diego, M., Sanz, M.T. and Carballido, J.R. (2010) Production of omega-3 polyunsaturated fatty acid concentrates: A review. *Innovative Food Science and Emerging Technologies*, **11**, 1 - 12.

Schneiter, R. and Daum, G. (2006) Analysis of Lipids. *Methods of Molecular Biology: Yeast Protocols: second edition*, **313**, 75 - 84.

Shimadzu. Biodiesel quality control, application book volume 4, Shimadzu Europa GmbH, Germany pp. 9 - 12.

Sigee, D.C. (2005) Freshwater Microbiology: Biodiversity and dynamic interactions of micro - organisms in the aquatic environment. John Wiley and Sons Ltd, England pp.141 - 142.

Singh, J. and Gu, S. (2010) Commercialization potential of microalgae for biofuels production. *Renewable and Sustainable Energy Reviews*, **14**, 2596 - 2610.

Spoehr, H.A. and Milner, H.W. (1949) The chemical composition of *Chlorella*; effect of environmental conditions. *Plant Physiology*, **24**, 120 - 149.

Su, W.W., Li, J. and Xu, N.S. (2003) State and parameter estimation of microalgal photobioreactor cultures based on local irradiance measurement. *Journal of Biotechnology*, **105**, 165 - 178.

Tornabene, T.G., Holzer, G. and Peterson, S. L. (1980) Lipid profile of the halophilic alga, *Dunaliella salina*. *Biochemical and Biophysical Research Communications*, **96**: 1349 - 1356.

Tornabene, T.G., Holzer, G., Lien, S. and Burris, N. (1983) Lipid composition of the nitrogen starved green alga *Neochloris oleoabundans*. *Enzyme and Microbial Technology*, **5**, 435 - 440.

Uriarte , A., Farias, A. J. S. and Hawkins B. L. (1993) Cell characteristics and biochemical composition of *Dunaliella primolecta* Butcher conditioned at different concentrations of dissolved nitrogen. *Journal of Applied Phycology*, **5**, 447 - 453.

UKZN Biochemistry 1992 undergraduate practical manual, p. 42.

Vázquez - Duhalt, R. and Arredondo-Vega, B.Q. (1990) Oil production from microalgae under saline stress. *Biomass for Energy and Industry*, **1**, 547 - 551.

Vechtel, B., Eichenberger, W. and Ruppel, H. G. (1992) Lipid bodies in *Eremosphaera viridis* De Bary (Chlorophyceae). *Plant Physiology*, **33**: 41 - 48.

Vieler, A., Wilhelm, C., Goss, R., Süß, R. and Schiller, J. (2007) The lipid composition of the unicellular green alga *Chlamydomonas reinhardtii* and the diatom *Cyclotella meneghiniana* investigated by MALDI-TOF MS and TLC. *Chemistry and Physics of Lipids*, **150**, 143 - 155.

Vladislav, C. and Jaromir, L. (1994) The effect of high radiances on growth, biosynthetic activities and the ultrastructure of the green alga *Botryococcus braunii* strain droop 1950/807 - 1. *Archiv für Hydrobiologie*, **10**, 115 - 131.

Volova, T.G., Kalacheva, G.S. and Zhila, N.O. (2003) Specificity of lipid composition in two *Botryococcus* strains, the producers of liquid hydrocarbons. *Russian Journal of Plant Physiology*, **50**: 627 - 633.

Voronova, E.N., Il'ash, L.V., Pogosyan, S.I., Ulanova, A.Y., Matorin, D.N., Cho, M. and Rubin, A.B. (1998) Intrapopulation heterogeneity of the fluorescence parameters of the marine plankton alga *Thalassiosira weissflogii* at various nitrogen levels. *Microbiology*, **78**: 419 - 427.

Vyas, A.P., Verma, J.L. and Subrahmanyam, N. (2010) A review on FAME production processes. *Fuel*, **89**, 1 - 9.

Wang, Z.T., Ulrich, N., Joo, S., Waffenschmidt, S. and Goodenough, U. (2009) Algal lipid bodies: stress induction, purification and biochemical characterization in wild - type and starchless *Chlamydomonas reinhardtii*. *Journal of Eukaryotic Cells*, **8**: 1856 - 1868.

Weldy, S. C. and Huesemann, M. (2007) Lipid production by *Dunaliella salina* in batch culture: Effects on nitrogen limitation and light intensity. *Energy Journal*, **7**, 115 - 122.

Woertz, I.C. (2007) Lipid productivity of algae grown on dairy wastewater as a possible feedstock for biodiesel, California Polytechnic University, San Luis Obispo (pHD thesis).

INTERNET REFERENCES

http://botany.natur.cuni.cz/algo/images/CAUP/H1998_1

Date accessed: 19/05/12

www.uky.edu/~dhild/biochem/20/fig10_20.png

Date accessed: 22/01/13

<http://www.dunaliella.org/dccbc/picturegallery.php>

Date accessed: 03/02/13

http://wikipedia_BODIPY

Date accessed: 05/02/13

<http://en.wikipedia.org/wiki/BODIPY>

Date accessed: 05/02/13

http://www.wikipedia/nile_red

Date accessed: 07/02/13

<http://www.microscopyu.com/tutorials/flash/spectralimaging.html>

Date accessed: 11/04/13

<http://www.wikipedia.org/wiki/Chlorella>

Date accessed: 14/04/13

<http://www.fao.org/docrep/003/w3732e/w3732e06.htm>

Date accessed: 19/04/13

<http://en.wikipedia.org/wiki/Dunaliella>

Date accessed: 10/06/13

<http://toolboxes.flexiblelearning.net.htm>

Date accessed: 05/07/13

<http://www.marine.csiro.au/microalgae/methods/Light%20Physical%20Units.htm>

Date accessed: 03/09/13

http://www.ccap.ac.uk/strain_info.php?.Strain_No=211/11B

Date accessed: 27/08/13

http://www.ccap.ac.uk/strain_info.php?Strain_No=11/34

Date accessed: 27/08/13

http://en.wikipedia.org/wiki/Nile_red

Date accessed: 08/10/13

APPENDIX A

Media and reagents

Media

i. Bovine serum albumin (BSA) commercial stock

This was prepared by adding 20 ml of sterile distilled water to BSA (Sigma Chemicals Co., USA) to attain a BSA stock of concentration 1.45 mg/ml. Of this, 0.1 ml was extracted and added to 9.9 ml distilled water for further use.

ii. BG11 medium (ATCC Medium 616) (1X)

The BG11 medium known as “Medium 616” by the American Type Culture Collection (ATCC) (Chinnasamy *et al.*, 2009) was used for the autotrophic growth of the experimental alga. In grams per litre, the medium was composed of 1.5 g NaNO₃ (Merck, FRG), 0.04 g K₂HPO₄ (Merck, FRG), 0.075 g MgSO₄.7H₂O (BDH. Ltd., England), 0.036 g CaCl₂.2H₂O (Merck, FRG), 0.006 g citric acid (Saarchem, SA), 0.006 g ferric ammonium citrate (Saarchem, SA), 0.02 g NaCO₃ (Merck, FRG) and 0.001 g EDTA (Saarchem, SA). Approximately 1 ml of Trace metal mix A5 was added, this comprised of the following (g/l); 2.86 g H₃BO₃ (Merck, FRG), 1.81 g MnCl₂.4H₂O (Merck, FRG), 0.222 g ZnSO₄.7H₂O (Merck, FRG), 0.39 g NaMoO₄.2H₂O (Fluka analytical, England), 0.079 g CuSO₄.5H₂O (Merck, FRG) and 0.049 g Co(NO₃)₂.6H₂O (Merck, FRG).

The medium was brought up to 1 litre with distilled water and the pH set to 7.4 before autoclaving at 121 °C for 20 minutes in a Hirayama autoclave (Hirayama, Japan).

iii. Control BG 11 medium for marine algae (1X)

The BG 11 control medium used was prepared using the same reagents of exact quantity as mentioned above. However, 1.5g NaNO₃ (Merck, FRG) and 0.049 g Co(NO₃)₂ (Merck, FRG) were excluded from the medium.

Reagents

i. DMSO - Nile red stock solutions

Of the stock DMSO (Merck, FRG) solution, 25 ml was mixed with 40 mg of Nile red (Sigma Chemicals Co., USA). The dye stock solution was stored in a foil - covered McCartney bottle to avert any possible effects of light on the dye.

ii. DMSO - Bodipy dye stock

Bodipy dye of 1 mg (Invitrogen, U.S.A) was added to 0.800 ml of DMSO in a McCartney bottle. The emulsion was shaken to enable an even distribution of the contents and was thereafter covered in foil to avert any possible effects of light on the dye.

iii. Thin layer chromatography standards

Standards used were: L - α - dioleoylphosphatidylethanolamine (DOPE) (Sigma Chemicals Co., USA), evening primrose oil (Vital, South Africa), salmon oil (Vital, South Africa), sunflower oil (Flora, South Africa) and olive oil (Santagata, South Africa). The DOPE standard was suspended in chloroform to obtain a final concentration of 10 $\mu\text{g}/\mu\text{l}$. Other oil standards were made up of 0.2% v/v in CHCl_3 .

iv. Protein sample buffer (SDS reducing buffer)

The sample buffer was made up of 1.2 ml of 0.5 M Tris - HCl (pH 6.8) (Sigma Chemicals Co., USA), 1.0 ml glycerol (Sigma Chemicals Co., USA), 2.0 ml of 10 % (w/v) SDS (Sigma Chemicals Co., USA), 0.5 ml of 0.1 % (w/v) bromophenol blue (Bio - Rad, USA) and 4.8 ml deionised water. Prior to use, 50 μl β - mercaptoethanol (Sigma Chemicals Co., USA) was added to 950 μl of buffer in an eppendorf tube which made up the SDS reducing sample buffer.

v. Electrode running buffer (10 X) (pH 8.3)

The running buffer was made up using 7.5 g Tris base, 36 g glycine and 2.5 g SDS which was brought up to a volume of 250 ml with deionised water. All the aforementioned reagents were purchased from Sigma Chemicals Co., (USA). For the electrophoresis run, 50 ml of the buffer was diluted with 450 ml deionised water.

vi. Coomassie blue R - 250 staining solution (0.1 %)

The staining solution comprised 0.1 g of coomassie blue R - 250 (Bio - Rad, USA) dissolved in 500 ml deionised water, 10 % acetic acid (Sigma Chemicals Co., USA) and 40 % methanol (Sigma Chemicals Co., USA). Destaining of the gels was achieved using the same solution minus the dye.

vii. Silver staining solution

Fixative: 10 % acetic acid (Sigma Chemicals Co., USA), 40 % ml methanol (Sigma Chemicals Co., USA), 50 % water

Wash solution: 30 % ethanol (Merck, FRG) in deionised water

Reductant solution: 50 mg sodium thiosulphate (Sigma Chemicals Co., USA) in 250 ml deionised water

Silver stain: 0.5 g silver stain (Bio - Rad, USA), 50 µl formaldehyde (Sigma Chemicals Co., USA), 250 ml deionised water

Stop solution: 5 % acetic acid (Sigma Chemicals Co., USA) in deionised water

Gels were immersed in the fixative solution prior to being washed three times in the wash solution. These were then placed in the reductant solution and followed by the wash step being repeated. The silver staining solution was then used for the staining of the gels and bands were developed in 7.5 g sodium carbonate, 1.25 mg sodium thiosulphate, 125 µl formaldehyde and 250 ml deionised water. The final step involved the gels being washed three times followed by immersion into the stop solution.

Appendix B

Other Technical Information

i. Use of a haemocytometer

A haemocytometer is a specialized slide that has a counting chamber with a known volume of liquid.

- The haemocytometer consists of a heavy glass slide with two counting chambers, each of which is divided into nine large 1 mm squares, on an etched and silvered surface separated by a trough.
- A coverslip sits on top of the raised supports of the 'H' shaped troughs enclosing both chambers. There is a 'V' or notch at either end where the cell suspension is loaded into the haemocytometer. When loaded with the cell suspension it contains a defined volume of liquid.
- The engraved grid on the surface of the counting chamber ensures that the number of particles in a defined volume of liquid is counted.
- The haemocytometer is placed on the microscope stage and the cell suspension is counted.

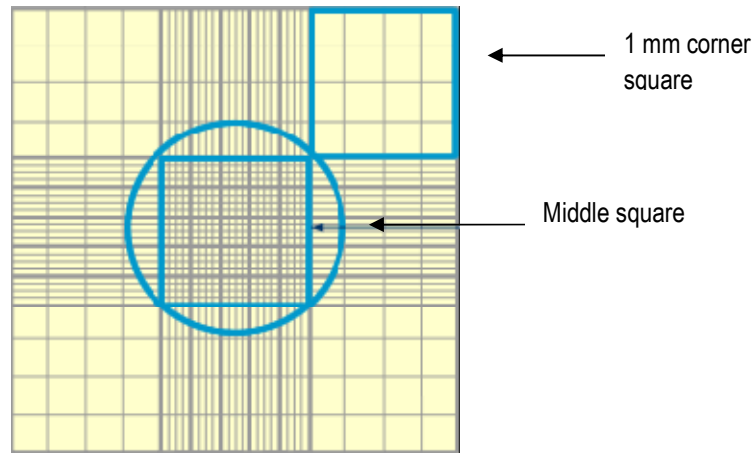


Figure B1. Diagram of a hemocytometer chamber (<http://toolboxes.flexiblelearning.net.htm>).

The entire chamber has nine 1.0 mm × 1.0 mm large squares separated from one another by the triple lines. The area of each is 1 mm².

The central 1 mm² area is divided into 25 small squares, each 0.04 mm² and marked into a further 16 squares.

Magnification:

Using 40X magnification, a 16 block grid can be visualized; however 6 of the 16 blocks are in the field focus when viewed under a 100X magnification. The area of each block of 0.05 × 0.05mm is 2.5×10^{-3} mm².

Therefore, the volume is calculated as follows:

$$\begin{aligned} \text{Volume} &= \text{area of block} \times h \\ &= (0.05 \text{ mm} \times 0.05 \text{ mm}) \times 0.1 \text{ mm} \\ &= 2.5 \times 10^{-4} \text{ mm}^3 \end{aligned}$$

Bearing in mind that 1cm³ = 1ml = 1000mm³, calculating cell number / ml :

Eg. Assuming 4 algal cells were counted per block, the cell number / ml was established as follows:

$$\rightarrow 4 \text{ algal cells per } 2.5 \times 10^{-3} \text{ mm}^2$$

$$\rightarrow 4 \text{ algal cells per } 2.5 \times 10^{-3} \text{ mm}^2 \times 0.1 \text{ mm}$$

$$\rightarrow 4 \text{ cells} / 2.5 \times 10^{-4} \text{ mm}^3$$

Hence: 4 cells $2.5 \times 10^{-4} \text{ mm}^3$

X 1000 mm^3

Where $X = 4000 / 2.5 \times 10^{-4}$

= 1.6×10^7 cells / ml

ii. Standard curves

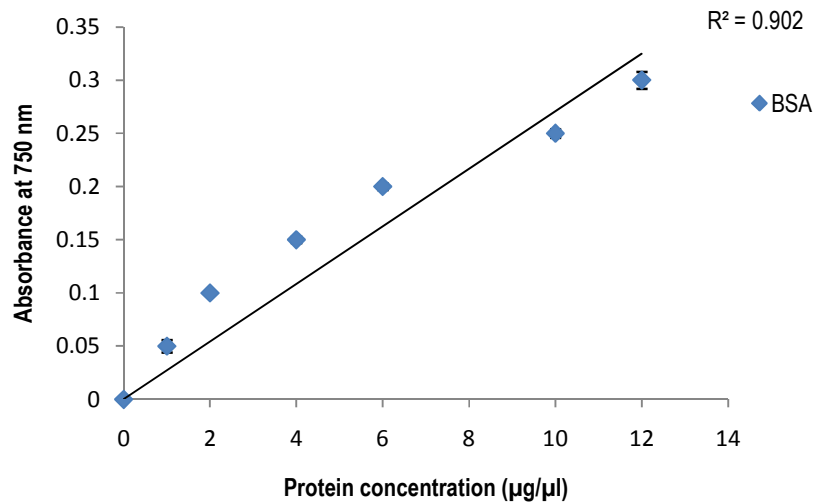


Figure B2. Standard curve of BSA versus absorbance using the Bio - Rad RC - DC kit.

Deviation bars were too small for insertion as these located within the shading of each point.

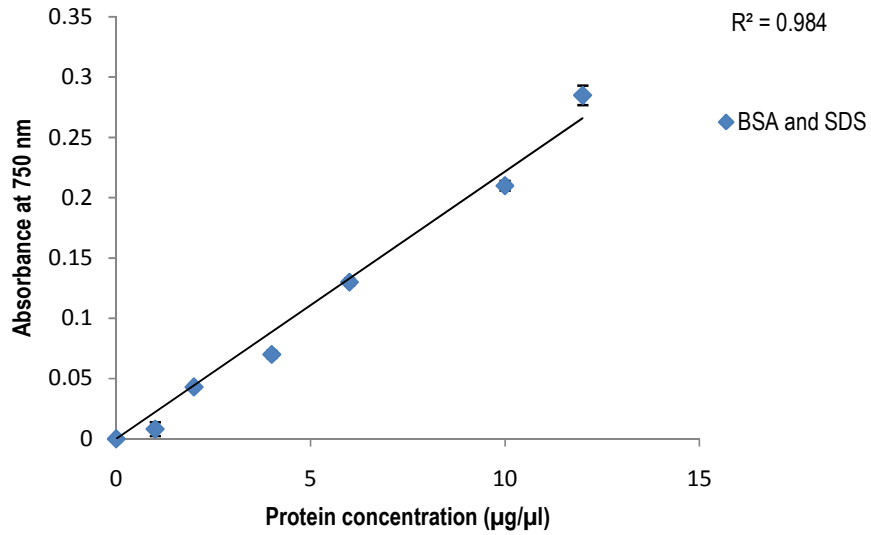


Figure B3. Standard curve of SDS treated BSA and standards versus absorbance using the Bio - Rad RC - DC kit.

Deviation bars were too small for insertion as these located within the shading of each point.

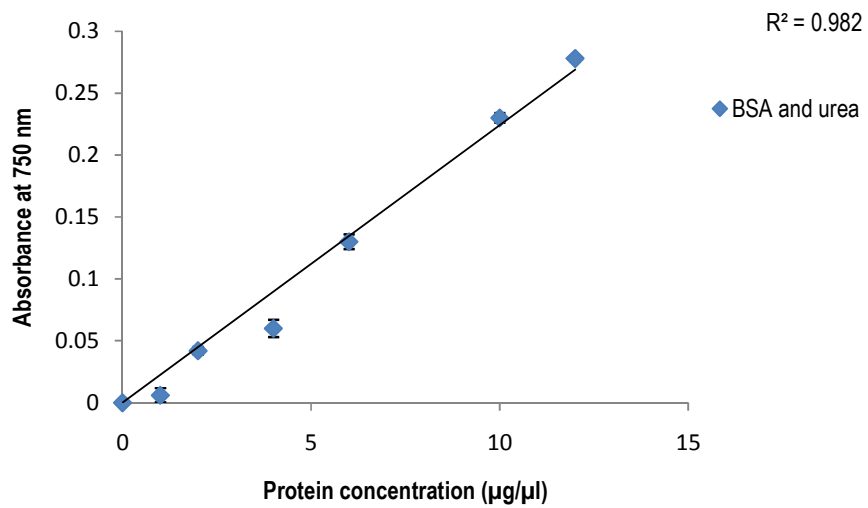


Figure B4. Standard curve of urea treated BSA versus absorbance using the Bio - Rad RC - DC kit.

Deviation bars were too small for insertion as these located within the shading of each point.

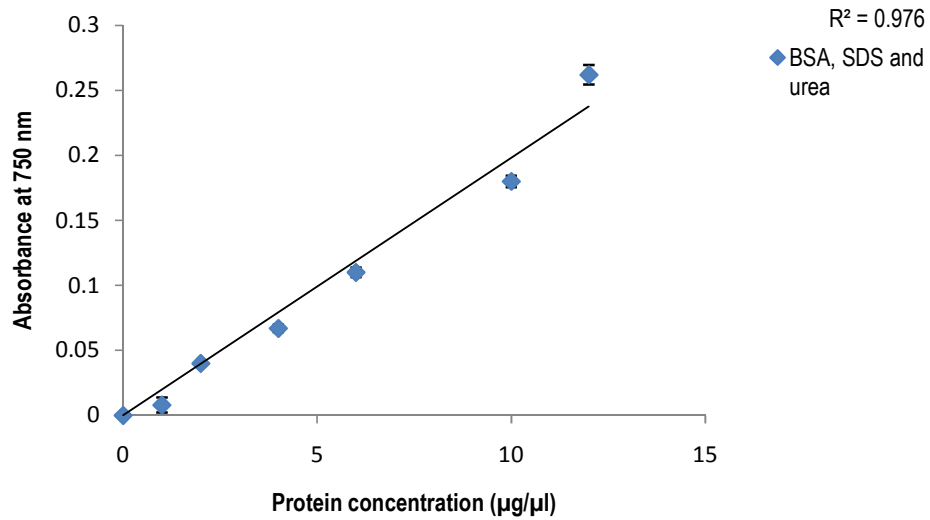


Figure B5. Standard curve of SDS and urea treated BSA versus absorbance using the Bio - Rad RC - DC kit.

Deviation bars were too small for insertion as these located within the shading of each point.

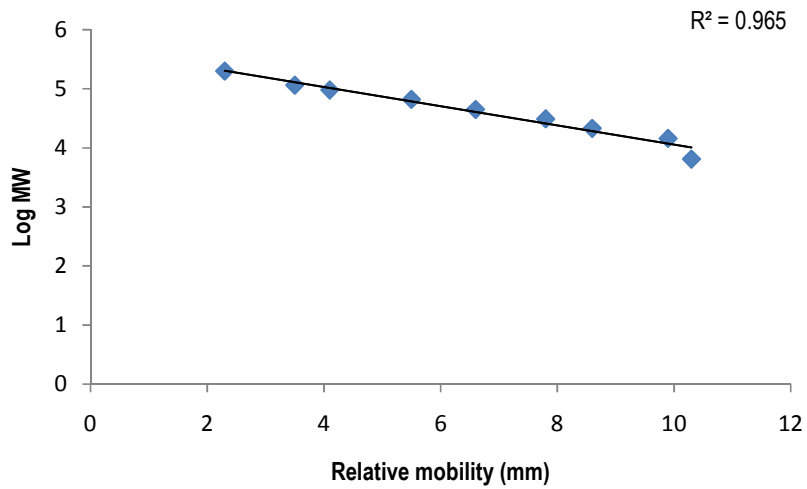


Figure B6. Standard curve of log of the molecular weight of the broad range protein standards versus the relative mobility.

iii. G Force conversion

- a. The equation (Eppendorf centrifuge handbook 2005) for G force conversion from rpm settings, using an Eppendorf rotor FA-45-24-11 without adaptor, in an Eppendorf 5424 microfuge, is

$$\text{RCF (G force)} = 1.118 \cdot 10^{-5} \cdot n^2 \cdot r_{\max}$$

where n = speed in rpm and r_{\max} = maximum centrifugal radius in cm.

- b. For the JA 10 rotor and Beckman Avanti J-26 XPI centrifuge, rpm conversion is facilitated automatically on scale setting in the console of the machine.